HEAVY QUARK SYMMETRY AND HADRONIC MODELS

by

SINIŠA VESELI

A dissertation submitted in partial fulfillment of the

requirements for the degree of

Doctor of Philosophy

(Physics)

at the

UNIVERSITY OF WISCONSIN — MADISON

1996

Abstract

The decays of heavy-light mesons are described by form factors which cannot be calculated from first principles. In this thesis we address the problem of extracting these form factors from given bound state models. We present a simple and straightforward method for relating the form factors, as defined within the covariant trace formalism of the heavy quark effective theory, to the overlaps of the rest frame wave functions of the light degrees of freedom. We also advocate an analysis which uses Regge structure, and the Bjorken and Voloshin sum rules in the heavy quark limit, to restrict the choice of parameters of a given relativistic quark model. Using this approach we examine several hadronic models in the heavy quark limit. Within the framework of the heavy quark effective theory, we also investigate semileptonic and radiative rare B meson decays.

Acknowledgments

I wish to take this opportunity to thank many people who helped me to get through graduate school. In particular, I'd like to acknowledge my fellow students John Beacom, Hassan Chehime, Donko Donjerković, and Zoran Škoda, for many enlightening conversations about physics, math, computers, and other topics unrelated to science. John Beacom deserves my special thanks for the hours he spent helping me understand the intricacies of UNIX, and for many helpful comments he made after reading my thesis.

I would also like to thank UW professors Baha Balantekin, Randy Durand, Francis Halzen, Martin Olsson, and Dieter Zeppenfeld, who always found time in their busy schedule to answer many physics questions I had.

Special thanks goes to my thesis advisor and very dear friend, Martin Olsson, for all his guidance and encouragement during the last few years, and for countless *the*'s and *a*'s he has corrected in our papers.

Most of all, I'd like to thank my wife Kornelija, who is always there for me, and who brought the most beautiful little girl into this world, my daughter Iva. To the two of them this thesis is dedicated.

Contents

List of Figures

List of Tables

Chapter 1

Introduction and History

The standard model [1] provides a very successful description of the physics currently accessible with particle accelerators. However, in spite of its success, many questions remain unanswered. In particular, the flavor sector of the theory contains a large number of undetermined parameters. These are the quark masses, as well as the four parameters of the Cabbibo-Kobayashi-Maskawa (CKM) matrix, which describes the mixing of the mass eigenstates of the quarks under the weak interactions. Precise determination of these parameters depends crucially on an understanding of the connection between quark and hadronic properties. Unfortunately, the nonperturbative long-distance forces, responsible for the confinement of quarks into hadrons, belong to the part of the strong interaction physics which is the least understood.

Indeed, there are very few cases in which it is possible using analytic methods to make systematic predictions based on quantum chromodynamics (QCD) in the low-energy, nonperturbative regime. All such predictions are based not on dynamical calculations, but on symmetries.

A well-known example is chiral symmetry [2], which arises since the current

masses of the light quarks[1] are small compared to Λ_{QCD}, the intrinsic mass scale of the strong interactions. In the limiting case of n_f massless quarks, the QCD Lagrangian has an $SU_L(n_f) \times SU_R(n_f)$ chiral symmetry. Although spontaneously broken in nature, the existence of this underlying symmetry allows the systematic expansion within chiral perturbation theory, in which many of the low-energy properties of QCD are related to a few reduced matrix elements.

Over the last few years it has become clear that a similar situation arises in systems containing a single heavy quark [3]. This symmetry arises because once a quark becomes sufficiently heavy, its mass and spin become irrelevant to the nonperturbative dynamics of the light degrees of freedom (LDF) of QCD.[2] As an extreme example, consider two very heavy quarks of masses one and ten kilograms. Even though these quarks are surrounded by the "brown muck" of the LDF, they will hardly notice it, and their motion will fluctuate only slightly about that of a free heavy quark. Given that such quarks can define with great precision their own center-of-mass, they act as a static source of color localized at the origin. QCD field equations in the neighborhood of such an isolated heavy quark are therefore those of the LDF, subject to the boundary condition that there is a static triplet source of color-electric field at the origin. Since this boundary condition is the same for both of our hypothetical heavy quarks, the solutions for the configuration of the LDF in their presence will be the same, even though the heavy quark masses are different. Furthermore, since the

[1] The quarks of the standard model fall naturally into two classes: u, d, and s are light quarks, whereas c, b and t quarks are heavy.

[2] By the light degrees of freedom we mean the light quarks and antiquarks, and the gluons.

spin of the heavy quark decouples from the spin of the LDF as $1/m_Q$, it also becomes irrelevant for the configuration of the LDF in the limit where the heavy quark mass goes to infinity. Therefore, hadronic systems containing a single heavy quark admit an additional symmetry which is not present in the full QCD Lagrangian, the heavy quark symmetry (HQS). For N_h heavy quarks the static HQS is actually an $SU(2N_h)$ spin-flavor symmetry, since both the spin and the flavor of the heavy quark are irrelevant.

In much the same way as the chiral symmetry of light quarks, HQS also endows us with predictive power. The most important predictions are for semileptonic B meson decay form factors, which are expected to play an important role in the accurate determination of the CKM matrix elements V_{cb} and V_{ub} from the experimental data.

Nevertheless, the discovery of HQS has not eliminated the need for models. It has rather provided a solid foundation for model building, and also redefined the role models should play. Among other things, they should complement HQS by providing predictions for the various universal form factors. Because of that, it is important to have reliable hadronic models in the heavy quark limit. One of the goals of this thesis is an attempt to provide some insight into that subject.

While the present burst of interest in the field stems from the work of Isgur and Wise [3], the main ingredients of their work had been in the literature for some time. Even before the discovery of the charm quark, De Rújula, Georgi and Glashow considered a model that incorporated the observation that the

spin of the heavy quark decouples in the heavy-light system [4]. They estimated the mass difference of D and D^* mesons to be of the order of the pion mass, which turned out to be about right. The concept of a new flavor symmetry for hadrons containing a heavy quark was introduced as early as 1980 by Shuryak [5], who later studied many properties of heavy mesons and baryons in the context of QCD sum rules [6]. The infinite quark mass limit in QCD was used by Eichten and Feinberg to study the heavy quark-antiquark potential [7]. Almost ten years later, Eichten [8], and Lepage and Thacker [9], suggested applying the same techniques to heavy-light systems, thus opening the way towards an effective theory with explicit spin symmetries. Motivated by experimental progress in the measurement of semileptonic decays of B mesons, several theoretical calculations of the rates for these decays appeared in the mid 1980s [10–17]. In [13] and [14] it was also pointed out that matrix element for $B \to De\nu_e$ was most reliably calculated at the kinematic point where the D meson does not recoil in the rest frame of the B meson. Furthermore, Nussinov and Wetzel gave a physical explanation which was close in spirit to the modern argument of HQS that the state of the LDF in heavy-light meson is independent of the mass of the heavy quark [14] . The work of Voloshin and Shifman [18] was also important to the formulation of HQS. They proposed a theoretical limit $m_c \to m_b$ (now called the Shifman-Voloshin limit), in which the matrix element for $B \to De\nu_e$ is exactly calculable. The last element used by Isgur and Wise comes from the work of Voloshin and Shifman [19], and of Politzer and Wise [20], who extracted violations to the flavor symmetry predictions in the form of logarithms of the ratio of heavy quark masses. These

arise from the short-distance physics related to hard gluons probing the quantum numbers (i.e., spin, flavor, and velocity) of heavy quarks. Politzer and Wise later attempted to reproduce these calculations working directly within the context of an effective theory [21].

Even though there is no doubt that HQS is a large step forward in our understanding of QCD, it is also certainly true that there is only so much one can learn from the symmetry arguments. The most obvious examples are the unknown form factors for semileptonic B meson decays. In order to calculate them, one still has to rely on some model of strong interactions. It is therefore important to have a formalism, consistent with HQS and its effective theory (HQET), which can be used to extract these form factors from a given model. The aim of this thesis is to make progress towards accomplishing this task.

By using the Bjorken [22,23] and the Voloshin [24] sum rules, we also present an attempt to shed some light onto description of meson dynamics in terms of the bound state models. The purpose here is not to say whether a particular model of quark confinement is right or wrong, but instead to establish whether or not it is self-consistent in the heavy quark limit.

The remainder of the thesis is organized as follows: Chapter 2 presents an overview of HQS and HQET. There is a vast literature on this subject and many excellent reviews already exist [25–28]. The purpose of this chapter is to introduce the basic ideas and formalism which will be used in subsequent chapters. The heart of the thesis is Chapter 3 where the formalism for extracting form factors from a given bound state model is developed. Several models in the heavy quark limit are described, and their self-consistency in

terms of the sum rules of HQET is investigated in Chapter 4. These models are used for the analysis of semileptonic B meson decays in Chapter 5, as the most important application of HQET, together with the formalism developed in Chapter 3. As another example, radiative rare B meson decays are examined in Chapter 6. Our conclusions are summarized in Chapter 7. Appendix A contains a brief description of the numerical methods used to deal with the different bound state models considered in this thesis.

Chapter 2

Heavy Quark Symmetry

2.1 Introduction

The existence of heavy quark symmetry (HQS) in hadrons composed of one heavy quark and any number of light quarks is by now a well-established fact. In the rest frame of the heavy hadron, the heavy quark is practically at rest. It effectively acts as a static source of color localized at the origin, and therefore its mass doesn't matter as far as the light degrees of freedom (LDF) are concerned. Furthermore, since the spin-spin interaction involves an explicit factor of g_s/m_Q, where g_s is the strong coupling constant, the spin of the heavy quark decouples in the limit $m_Q \to \infty$. Therefore, the properties of heavy hadrons are independent of the spin and mass of the heavy source of color. This is the basic idea of HQS. The heavy quark effective theory (HQET) is nothing more than a method for giving these observations a formal basis.

There are many excellent reviews on HQS and HQET [25–28], and this chapter is not intended to be yet another one. Instead, its purpose is to introduce the basic ideas and methods of HQET which are necessary for understanding of the rest of this thesis. Because of that, many important topics

in HQET will not be covered here, and some of them, such as renormalization, will be only briefly described, without going through the actual calculations in detail.

2.2 The Effective Lagrangian and Its Symmetries

In a physical situation where a heavy quark Q is interacting with the light degrees of freedom (LDF) carrying four-momenta much smaller than the heavy quark mass m_Q, it is appropriate to go over to an effective theory, in which $m_Q \to \infty$ with its four-velocity v^μ fixed. For a heavy quark field we can then write [29]

$$Q = e^{-im_Q v\cdot x} h_v^{(Q)} \ . \tag{2.1}$$

The field $h_v^{(Q)}$ is constrained to satisfy[1]

$$\not{v}\, h_v^{(Q)} = h_v^{(Q)} \ . \tag{2.2}$$

It destroys a heavy quark of four-velocity v^μ, but it does not create an antiquark, since in the effective theory pair creation is not present, and the field for the antiquark is an independent degree of freedom. Putting (2.1) into the part of the QCD Lagrangian density involving the heavy quark field Q,

$$\mathcal{L} = \bar{Q}(i\not{D} - m_Q)Q \ , \tag{2.3}$$

and using the constraint (2.2), we find

$$\mathcal{L}_v^{eff} = \bar{h}_v^{(Q)} i\not{D} h_v^{(Q)} \ . \tag{2.4}$$

[1] As usual, the slash indicates contraction with γ^μ.

Since $\frac{1}{2}(1+\not{v})h_v^{(Q)} = h_v^{(Q)}$, this can be further simplified to

$$\mathcal{L}_v^{eff} = \bar{h}_v^{(Q)} iv \cdot D h_v^{(Q)} \ . \tag{2.5}$$

In the above D^μ is the covariant derivative, $D^\mu = \partial^\mu - ig_s T_a A_a^\mu$, where A_a^μ are the gluon fields, and T_a are the generators of color $SU(3)$, normalized to $\mathrm{Tr}(T_a T_b) = \frac{1}{2}\delta_{ab}$. Note that a derivative acting on $h_v^{(Q)}$ produces a factor of the residual momentum k^μ, because the large part ($m_Q v^\mu$) of heavy quark momentum ($p_Q^\mu = m_Q v^\mu + k^\mu$), was scaled out of the field.

Since there are no Dirac matrices in the effective Lagrangian (2.5), interactions of the heavy quark with gluons leave its spin unchanged. Associated with this is an $SU(2)$ symmetry group under which $\mathcal{L}_v^{eff}$ is invariant. In the rest frame of the heavy quark we can choose the generators S^i of this group to be

$$S^i = \frac{1}{2}\gamma_5 \gamma^0 \gamma^i \ , \tag{2.6}$$

where the γ-matrices in the standard representation are given by

$$\gamma^0 = \begin{pmatrix} 1 & 0 \\ 0 & -1 \end{pmatrix} \ , \ \gamma^i = \begin{pmatrix} 0 & \sigma^i \\ -\sigma^i & 0 \end{pmatrix} \ , \ \gamma^5 = \begin{pmatrix} 0 & 1 \\ 1 & 0 \end{pmatrix} \ . \tag{2.7}$$

In the above σ^i are the Pauli matrices,

$$\sigma^1 = \begin{pmatrix} 0 & 1 \\ 1 & 0 \end{pmatrix} \ , \ \sigma^2 = \begin{pmatrix} 0 & -i \\ i & 0 \end{pmatrix} \ , \ \sigma^3 = \begin{pmatrix} 1 & 0 \\ 0 & -1 \end{pmatrix} \ . \tag{2.8}$$

In a general frame, we first define a set of three orthonormal polarization vectors ε^i, such that $\varepsilon^i \cdot v = 0$, and then take the generators of the spin $SU(2)$ group to be

$$S^i = \frac{1}{2}\gamma_5 \not{v} \not{\varepsilon}^i \ . \tag{2.9}$$

Defined in this way, the generators S^i satisfy $SU(2)$ commutation relations,

$$[S^i, S^j] = i\epsilon^{ijk} S^k \ , \tag{2.10}$$

and also commute with $\not{v}$, i.e., $[\not{v}, S^i] = 0$. It can be easily shown that an infinitesimal $SU(2)$ transformation,

$$h_v^{(Q)} \to (1 + i\boldsymbol{\epsilon} \cdot \boldsymbol{S}) h_v^{(Q)} \ , \tag{2.11}$$

leaves $\mathcal{L}_v^{eff}$ invariant, and also preserves the on-shell condition (2.2) for $h_v^{(Q)}$.

In the effective Lagrangian the mass of the heavy quark does not appear. For N_h heavy quarks moving with the same velocity v^μ (2.5) becomes

$$\mathcal{L}_v^{eff} = \sum_{i=1}^{N_h} \bar{h}_v^{(Q_i)} iv \cdot D h_v^{(Q_i)} \ , \tag{2.12}$$

which is clearly invariant under rotations in flavor space. Therefore, in such a situation an $SU(2)$ spin symmetry becomes an $SU(2N_h)$ heavy quark spin-flavor symmetry [3].

From (2.5) it is straightforward to obtain Feynman rules. In particular, the heavy quark propagator in the effective theory becomes

$$\frac{i}{v \cdot k} \ , \tag{2.13}$$

while the vertex for gluon-heavy quark interactions takes the form

$$ig_s T^a v^\mu \ . \tag{2.14}$$

These can also be obtained from the corresponding Feynman rules in the full theory of QCD, by using $p_Q^\mu = m_Q v^\mu + k^\mu$, and the property $\not{v}\, u_Q = u_Q$ of the on-shell heavy quark spinors.

2.3 Spectroscopic Implications

The most direct consequences of the HQS concern the spectroscopy of states containing one heavy quark [30]. In the $m_Q \to \infty$ limit the total angular momentum j of the LDF decouples from the spin of the heavy quark, and both are separately conserved by the strong interaction. Therefore, j is a good quantum number, so that states can be labeled as J_j^P. The spin symmetry predicts that for each j there are two degenerate heavy-light states with total angular momentum $J = j \pm \frac{1}{2}$ (unless $j = 0$, in which case a single $J = 1/2$ state is obtained). The flavor symmetry ensures that the spectrum is identical for each heavy quark Q up to an overall constant mass shift associated with the heavy quark mass.

As an example, consider ground-state mesons containing a heavy quark. There, the LDF have the quantum numbers of a light antiquark, and the degenerate states are pseudoscalar ($J_j^P = 0^-_{1/2}$), and vector ($J_j^P = 1^-_{1/2}$) mesons. In the charm and bottom systems we have [31]

$$\begin{aligned} m_{D^*} - m_D &\approx 141\ MeV\ , \\ m_{D_s^*} - m_{D_s} &\approx 141\ MeV\ , \\ m_{B^*} - m_B &\approx 46\ MeV\ , \\ m_{B_s^*} - m_{B_s} &\approx 46\ MeV\ . \end{aligned} \tag{2.15}$$

Even though these mass splitting are reasonably small, one can make even more accurate predictions. At order $1/m_Q$ one expects hyperfine corrections to resolve the degeneracy, e.g. $m_{D^*} - m_D \propto 1/m_c$. This leads to stronger statements $m_{B^*}^2 - m_B^2 \approx m_{D^*}^2 - m_D^2 \approx const.$, and similarly for the strange mesons $m_{B_s^*}^2 - m_{B_s}^2 \approx m_{D_s^*}^2 - m_{D_s}^2 \approx const.$ These two constants can in principle

be different, since the flavor quantum numbers of the light degrees of freedom are different for the strange and non-strange states. However, from experiment we know that [31]

$$\begin{aligned} m^2_{D^*} - m^2_D &\approx 0.55\ GeV^2\ , \\ m^2_{B^*} - m^2_B &\approx 0.49\ GeV^2\ , \end{aligned} \tag{2.16}$$

and also

$$\begin{aligned} m^2_{D^*_s} - m^2_{D_s} &\approx 0.58\ GeV^2\ , \\ m^2_{B^*_s} - m^2_{B_s} &\approx 0.51\ GeV^2\ , \end{aligned} \tag{2.17}$$

which indicates that to first approximation hyperfine corrections are independent of the flavor of the LDF.

Excited meson states (i.e., those in which the LDF carry orbital angular momentum) can also be studied using HQS. For example, if one interprets $D_1(2420)$ and $D^*_2(2460)$ as members of the $j = 3/2$ P-wave doublet $(1^+_{3/2}, 2^+_{3/2})$, one then expects

$$m^2_{B^*_2} - m^2_{B_1} \approx m^2_{D^*_2} - m^2_{D_1} \approx 0.17\ GeV^2\ . \tag{2.18}$$

This splitting is much smaller than corresponding ones for the S-wave mesons. The reason is that wave function of the LDF in a P-wave state vanishes at the origin, so that hyperfine corrections are strongly suppressed.

Another typical prediction of the flavor symmetry is that spectra built on different heavy quarks are identical up to an overall constant mass shift associated with the heavy quark mass. Thus, we expect relations such as $m_{B_s} - m_B \approx m_{D_s} - m_D$, or $m_{B_1} - m_B \approx m_{D_1} - m_D$, to hold. Indeed, the first

relation is nicely confirmed by experiment which gives [31]

$$\begin{aligned} m_{D_s} - m_D &\approx 99\ MeV\ , \\ m_{B_s} - m_B &\approx 96\ MeV\ . \end{aligned} \tag{2.19}$$

Since the heavy quark flavor symmetry applies not only to mass splittings, but also to all other properties of hadrons containing a single heavy quark, it has many more applications to the strong interactions of those hadrons. For instance, one can find relations between the decay amplitudes describing the emission of light quanta such as π, ρ, or $\pi\pi$, from a heavy hadron [30].

2.4 Transition Matrix Elements and Covariant Trace Formalism

In this section we consider matrix elements of operators in HQET. For the sake of clarity, we focus on the well-known example of the semileptonic decays of a B meson to D or D^* mesons. These decays play an important role in determining the CKM matrix element V_{cb}.

In order to extract this angle from experiment, the theory has to provide the six unknown form factors for $B \to D$ and $B \to D^*$ transitions. The standard definition of these form factors is

$$\langle D(p')|V^\mu|B(p)\rangle = f_+(q^2)(p+p')^\mu + f_-(q^2)(p-p')^\mu\ , \tag{2.20}$$

$$\begin{aligned} \langle D^*(p',\varepsilon')|A^\mu|B(p)\rangle &= f(q^2)\varepsilon'^{*\mu} + a_+(q^2)(\varepsilon'^*\cdot p)(p+p')^\mu \\ &+ a_-(q^2)(\varepsilon'^*\cdot p)(p-p')^\mu\ , \end{aligned} \tag{2.21}$$

$$\langle D^*(p',\varepsilon')|V^\mu|B(p)\rangle = ig(q^2)\epsilon^{\mu\nu\alpha\beta}\varepsilon'^*_\nu(p+p')_\alpha(p-p')_\beta\ , \tag{2.22}$$

where $V^\mu = \bar{c}\gamma^\mu b$ and $A^\mu = \bar{c}\gamma^\mu\gamma^5 b$ are the vector and the axial-vector currents, respectively, and $q^2 = (p - p')^2$ is momentum transfer. Meson states in the above expressions have the conventional relativistic normalization,

$$\langle M(p', \varepsilon')|M(p, \varepsilon)\rangle = 2p^0\delta_{\varepsilon\varepsilon'}\delta^{(3)}(\boldsymbol{p} - \boldsymbol{p'}) \ . \tag{2.23}$$

Several methods of estimating the above form factors can be found in the literature. A frequently used method consists of estimating the form factor at one value of momentum transfer $q^2 = q_0^2$ (e.g., using the nonrelativistic constituent quark model), and then introducing the functional dependence on q^2 in some reasonable, but completely arbitrary way.

However, HQET gives the form factor at the maximum momentum transfer, $q^2 = q^2_{max} = (m_B - m_D)^2$, the point at which the resulting D or D^* meson does not recoil in the rest frame of the decaying B meson. Furthermore, even though the functional dependence of form factors on q^2 is a nonperturbative problem, in the heavy quark limit not all of the form factors in (2.20)-(2.22) are independent. In fact, one of the most important applications of HQET is providing relations between different form factors which describe decays of heavy-light mesons. For $B \to D$ and $B \to D^*$ transitions these relations have been first derived by Isgur and Wise [3]. Nevertheless, the covariant trace formalism (CTF), formulated in [16,32,33] and generalized to excited states in [34], is the most convenient method for extracting the consequences of the spin and flavor symmetries of HQET, i.e., for keeping track of the relevant Clebsch-Gordan (CG) coefficients.

For heavy quark systems it is a more natural to use meson velocity instead of momentum. Instead of (2.23), meson states in HQET are normalized to

$2v^0 = 2p^0/m_M$, i.e.,

$$\langle M(v',\varepsilon')|M(v,\varepsilon)\rangle = 2v^0\delta_{\varepsilon\varepsilon'}\delta^{(3)}(\boldsymbol{v}-\boldsymbol{v}') \ . \tag{2.24}$$

In the $m_Q \to \infty$ limit, the states $|M(v,\varepsilon)\rangle$ are completely characterized by the configuration of the LDF. The wave function for these states is defined as

$$M(v,\varepsilon) \propto \langle 0|h_v^{(Q)}\bar{q}|M(v,\varepsilon)\rangle \ . \tag{2.25}$$

Now, let us denote wave functions for pseudoscalar and vector states as $C(v)$ and $C^*(v,\varepsilon)$, respectively.[2] For these mesons (2.25) will be a product of the form $u_Q\bar{v}_{\bar{q}}$, where u_Q is a heavy quark spinor satisfying $\not{v}\, u_Q = u_Q$, and $\bar{v}_{\bar{q}} = v_{\bar{q}}^\dagger\gamma^0$ is an anti-spinor representing the LDF with $j = 1/2$. Such a product is a superposition of states with $J = 0$ and $J = 1$. The easiest way to identify $C(v)$ and $C^*(v,\varepsilon)$, is to form appropriate combinations of the spin-up and spin-down spinors in the rest frame, where $v^\mu = (1,\mathbf{0})$. The result can then be generalized to arbitrary v^μ by boosting.

In the standard (Dirac) representation, the spinor basis $u_\alpha^{(1)} \propto \delta_{1\alpha}$ and $u_\alpha^{(2)} \propto \delta_{2\alpha}$ corresponds to spin up and spin down, while the anti-spinor basis $v_\alpha^{(1)} \propto -\delta_{3\alpha}$ and $v_\alpha^{(2)} \propto \delta_{4\alpha}$ corresponds to spin down and spin up. In order to have meson states normalized according to (2.24), we normalize heavy quark spinors to 2, i.e., $\bar{u}_Q^{(s')}u_Q^{(s)} = 2\delta_{ss'}$, and for anti-spinors describing the LDF we use $\bar{v}_{\bar{q}}^{(s')}v_{\bar{q}}^{(s)} = -\delta_{ss'}$. With these definitions we can use ordinary CG coefficients to form the desired states. The pseudoscalar state in the rest frame is given

[2] $M(v,\varepsilon)$ will be used for a generic heavy-light meson matrix wave function.

by

$$C(v) = \frac{1}{\sqrt{2}}(u_Q^{(1)}\bar{v}_{\bar{q}}^{(1)} - u_Q^{(2)}\bar{v}_{\bar{q}}^{(2)}) = \begin{pmatrix} 0 & 1 \\ 0 & 0 \end{pmatrix} = \frac{1+\gamma^0}{2}\gamma^5 \ . \tag{2.26}$$

Similarly, the three vector states are

$$C^*(\varepsilon^{(+)}) = u_Q^{(1)}\bar{v}_{\bar{q}}^{(2)} = \frac{-1}{\sqrt{2}} \begin{pmatrix} 0 & \sigma^1 + i\sigma^2 \\ 0 & 0 \end{pmatrix} = \frac{1+\gamma^0}{2} \not{\varepsilon}^{(+)} \ , \tag{2.27}$$

$$C^*(\varepsilon^{(0)}) = \frac{1}{\sqrt{2}}(u_Q^{(1)}\bar{v}_{\bar{q}}^{(1)} + u_Q^{(2)}\bar{v}_{\bar{q}}^{(2)}) = \begin{pmatrix} 0 & \sigma^3 \\ 0 & 0 \end{pmatrix} = \frac{1+\gamma^0}{2} \not{\varepsilon}^{(0)} \ , \tag{2.28}$$

$$C^*(\varepsilon^{(-)}) = u_Q^{(2)}\bar{v}_{\bar{q}}^{(1)} = \frac{1}{\sqrt{2}} \begin{pmatrix} 0 & \sigma^1 - i\sigma^2 \\ 0 & 0 \end{pmatrix} = \frac{1+\gamma^0}{2} \not{\varepsilon}^{(-)} \ . \tag{2.29}$$

Here, polarization vectors are the usual ones,

$$\varepsilon^{(\pm)} = \mp\frac{1}{\sqrt{2}}(0, 1, \pm i, 0) \ , \tag{2.30}$$

$$\varepsilon^{(0)} = (0, 0, 0, 1) \ . \tag{2.31}$$

Using $\boldsymbol{S} = \frac{1}{2}\gamma^5\gamma^0\boldsymbol{\gamma}$, and $\boldsymbol{S}(u\bar{v}) = [\boldsymbol{S}, u\bar{v}]$, one can check that (2.26) has spin zero, while (2.27), (2.28), and (2.29), have spin one, with third component 1, 0, and -1, respectively. It is straightforward to generalize the above results to arbitrary velocity. Replacing $\gamma^0 v^0 \to \not{v}$, we find

$$C(v) = \frac{1+\not{v}}{2}\gamma^5 \ , \tag{2.32}$$

$$C^*(v, \varepsilon) = \frac{1+\not{v}}{2} \not{\varepsilon} \ . \tag{2.33}$$

As expected, $\not{v}\, C(v) = C(v)$ and $\not{v}\, C^*(v, \varepsilon) = C^*(v, \varepsilon)$. By construction, the spin symmetry acts on this representation only on the first index of matrices $C(v)$ and $C^*(v, \varepsilon)$.

Consider now the matrix elements of heavy quark currents which are relevant for the semileptonic $B \to D$ and $B \to D^*$ decays. The heavy quark spin indices must be contracted in order to ensure $SU(2)$ invariance, and we must form a trace over the remaining Dirac indices, together with all possible terms constructed of $\not{v}$, $\not{v}'$, etc. It turns out that $f_1 + f_2 \not{v}' + f_3 \not{v}$, where f_i are the Lorentz scalar functions of $\omega = v \cdot v'$, is the most general form consistent with Lorentz covariance and parity conservation of the strong interactions. Therefore, we have

$$\langle D(v')|\bar{h}^{(c)}_{v'}\Gamma h^{(b)}_v|B(v)\rangle = \mathrm{Tr}\left[\bar{C}(v')\Gamma C(v)(f_1 + f_2 \not{v}' + f_3 \not{v})\right] , \qquad (2.34)$$

$$\langle D^*(v',\varepsilon')|\bar{h}^{(c)}_{v'}\Gamma h^{(b)}_v|B(v)\rangle = \mathrm{Tr}\left[\bar{C}^*(v',\varepsilon')\Gamma C(v)(f_1 + f_2 \not{v}' + f_3 \not{v})\right] , \qquad (2.35)$$

where $\bar{M} = \gamma^0 M^\dagger \gamma^0$. One might think that f_i's are all independent functions, but since $\not{v} M(v,\varepsilon) = M(v,\varepsilon)$, it is straightforward to see that the combination $\xi_C = f_1 - f_2 - f_3$ in the trace has the same effect as $f_1 + f_2 \not{v}' + f_3 \not{v}$. Hence, (2.34) and (2.35) become

$$\langle D(v')|\bar{h}^{(c)}_{v'}\Gamma h^{(b)}_v|B(v)\rangle = \mathrm{Tr}\left[\bar{C}(v')\Gamma C(v)\right]\xi_C(\omega) , \qquad (2.36)$$

$$\langle D^*(v',\varepsilon')|\bar{h}^{(c)}_{v'}\Gamma h^{(b)}_v|B(v)\rangle = \mathrm{Tr}\left[\bar{C}^*(v',\varepsilon')\Gamma C(v)\right]\xi_C(\omega) . \qquad (2.37)$$

As one can see, the six form factors in (2.20)-(2.22), which parametrize semileptonic $B \to D$ and $B \to D^*$ decays, are in the heavy quark limit reduced to a single universal function $\xi_C(\omega)$. This is the famous Isgur-Wise (IW) function [3].

The flavor symmetry also implies that the form factor for the matrix element of the B-current between B meson states, is given by the same reduced

matrix element as (2.36), i.e.,

$$\langle B(v')|\bar{h}^{(b)}_{v'}\Gamma h^{(b)}_{v}|B(v)\rangle = \mathrm{Tr}\left[\bar{C}(v')\Gamma C(v)\right]\xi_C(\omega)\ . \tag{2.38}$$

Using $\Gamma = \gamma^0$, and recalling that B number is conserved, one finds that ξ_C is fixed at $v' = v$. Normalization of states (2.24) then gives

$$\xi_C(1) = 1\ . \tag{2.39}$$

The IW function is truly universal, since it doesn't depend on the heavy quark's mass or spin, nor does it depend on the current which causes the $Q_i \to Q_j$ transition. It is remarkable that ξ_C describes both timelike form factors (as in $B \to Dl\bar{\nu}_l$) and spacelike form factors (as in $B \to B$). Of course, in both cases it actually describes transitions between infinitely heavy sources at fixed velocity transfer $(v - v')^2$.

Using properties of spin-$(n+1/2)$ Rarita-Schwinger tensor spinors [35], one can find covariant representations, analogous to (2.32) and (2.33), for heavy-light states with non-zero orbital angular momentum [34]. The eight lowest lying states form four doublets, and we denote them as follows: (C, C^*) is the $L = 0$ doublet, (E, E^*) and (F, F^*) are the two $L = 1$ doublets, and (G, G^*) is the $L = 2$ doublet. Spin zero states are characterized only by their four-velocity v^μ. In addition to v^μ, spin one states are characterized with a polarization vector ε^μ (satisfying $\varepsilon\cdot v = 0$), while spin two objects are described with a symmetric tensor $\varepsilon^{\mu\nu}$ ($\varepsilon^{\mu\nu} = \varepsilon^{\nu\mu}$, $\varepsilon^{\mu\nu}v_\nu = 0$, $\varepsilon^{\mu}_{\ \mu} = 0$). For the future

reference we summarize now the expressions for these states [34]:

$$\begin{aligned}
C(v) &= \tfrac{1}{2}(\not{v}+1)\gamma_5 \ , & J_j^P &= 0^-_{1/2} \ , \\
C^*(v,\varepsilon) &= \tfrac{1}{2}(\not{v}+1)\ \not{\varepsilon} \ , & J_j^P &= 1^-_{1/2} \ , \\
E(v) &= \tfrac{1}{2}(\not{v}+1) \ , & J_j^P &= 0^+_{1/2} \ , \\
E^*(v,\varepsilon) &= \tfrac{1}{2}(\not{v}+1)\gamma_5\ \not{\varepsilon} \ , & J_j^P &= 1^+_{1/2} \ , \\
F(v,\varepsilon) &= \tfrac{1}{2}\sqrt{\tfrac{3}{2}}(\not{v}+1)\gamma_5[\varepsilon^\mu - \tfrac{1}{3}\ \not{\varepsilon}(\gamma^\mu - v^\mu)] \ , & J_j^P &= 1^+_{3/2} \ , \\
F^*(v,\varepsilon) &= \tfrac{1}{2}(\not{v}+1)\gamma_\nu \varepsilon^{\mu\nu} \ , & J_j^P &= 2^+_{3/2} \ , \\
G(v,\varepsilon) &= \tfrac{1}{2}\sqrt{\tfrac{3}{2}}(\not{v}+1)[\varepsilon^\mu - \tfrac{1}{3}\ \not{\varepsilon}(\gamma^\mu + v^\mu)] \ , & J_j^P &= 1^-_{3/2} \ , \\
G^*(v,\varepsilon) &= \tfrac{1}{2}(\not{v}+1)\gamma_5\gamma_\nu \varepsilon^{\mu\nu} \ , & J_j^P &= 2^-_{3/2} \ .
\end{aligned} \tag{2.40}$$

Matrix elements of a heavy quark current between the physical meson states are calculated by taking the trace ($\omega = v\cdot v'$),

$$\langle M'(v',\varepsilon')|\bar{h}^{(Q')}_{v'}\Gamma h^{(Q)}_v|M(v,\varepsilon)\rangle = \mathrm{Tr}[\bar{M}'(v',\varepsilon')\Gamma M(v,\varepsilon)]\mathcal{M}_l(\omega) \ , \tag{2.41}$$

where M' and M denote appropriate matrices from (2.40), and $\bar{M} = \gamma^0 M^\dagger \gamma^0$. In order to restore to the standard normalization of states, the trace in (2.41) has to be multiplied by $\sqrt{m_M m_{M'}}$. The unknown function $\mathcal{M}_l(\omega)$ represents the LDF. For the transitions of a $0^-_{1/2}$ ground state into an excited state it is defined as [34]

$$\mathcal{M}_l(\omega) = \begin{cases} \xi_C(\omega) \ , & C \to (C, C^*) \ , \\ \xi_E(\omega) \ , & C \to (E, E^*) \ , \\ \xi_F(\omega) v_\mu \ , & C \to (F, F^*) \ , \\ \xi_G(\omega) v_\mu \ , & C \to (G, G^*) \ . \end{cases} \tag{2.42}$$

The vector index in the last two definitions will be contracted with the one in the representations of $j = 3/2$ excited states in (2.40). Let us also mention that

heavy-light baryon states, which correspond to integral j, were also studied in [34]. However, those states will not be considered here.

2.5 Sum Rules

The IW function $\xi_C(\omega)$, or the elastic form factor, plays a central role in the description of the weak decays $B \to D$ and $B \to D^*$. It contains the long distance physics associated with the strong interactions of the LDF, and cannot be calculated from first principles. Nevertheless, some of its properties can be deduced on general grounds. As we have already seen in (2.39), one such property is its normalization at $\omega = 1$. Also of a particular interest is behavior of the IW function close to $\omega = 1$, since a reliable extrapolation of experimental data to zero recoil point can be used for measuring V_{cb} [36]. Near zero recoil, behavior of $\xi_C(\omega)$ is determined by its slope $\xi_C'(1)$, i.e.,

$$\xi_C(\omega) \simeq 1 + \xi_C'(1)(\omega - 1) + \mathcal{O}[(\omega - 1)^2] \ . \tag{2.43}$$

Since the kinematic region accessible in semileptonic $B \to D$ and $B \to D^*$ decays is small ($1 \leq \omega \leq 1.6$), a precise knowledge of the slope parameter would basically determine the IW function in the physical region.

Bjorken has shown [22,23] that a sum rule relates $\xi_C'(1)$ to the zero recoil inelastic form factors $\xi_E(1)$ and $\xi_F(1)$, which describe transitions $C \to (E, E^*)$ and $C \to (F, F^*)$, respectively. Consider the quantity[3]

$$h_\Gamma^{X_c}(\omega) = \sum_{\varepsilon'} \langle B(v)|\bar{h}_v^{(b)}\bar{\Gamma}h_{v'}^{(c)}|X_c(v',\varepsilon')\rangle\langle X_c(v',\varepsilon')|\bar{h}_{v'}^{(c)}\Gamma h_v^{(b)}|B\rangle \ . \tag{2.44}$$

[3]Here we ignore renormalization subtleties.

If one sums over final states X_c, then it seems reasonable that this inclusive quantity can be calculated as a heavy quark transition. In other words, using $\sum_{X_c} |X_c\rangle\langle X_c| = 1$, and $\sum_s u_Q^{(s)}(v)\bar{u}_Q^{(s)}(v) = \not{v} + 1$, one finds

$$\frac{1}{2}\mathrm{Tr}\left[(\not{v}+1)\bar{\Gamma}(\not{v}'+1)\Gamma\right] = \sum_{X_c} h_\Gamma^{X_c}(\omega) \ . \tag{2.45}$$

On the other hand, the contribution of any charmed state to the right-hand side of (2.45) can be be evaluated by (2.41). The sum over X_c polarizations can be performed using standard expressions. For spin one states we have

$$\sum_{\varepsilon'} \varepsilon'^*_\mu \varepsilon'_\nu = -g_{\mu\nu} + v'_\mu v'_\nu \ , \tag{2.46}$$

while for spin two states we use

$$\begin{aligned} \sum_{\varepsilon'} \varepsilon'^*_{\mu\nu}\varepsilon'_{\alpha\beta} &= -\frac{1}{3}(g_{\mu\nu} - v'_\mu v'_\nu)(g_{\alpha\beta} - v'_\alpha v'_\beta) + \frac{1}{2}(g_{\mu\alpha} - v'_\mu v'_\alpha)(g_{\nu\beta} - v'_\nu v'_\beta) \\ &+ \frac{1}{2}(g_{\mu\beta} - v'_\mu v'_\beta)(g_{\nu\alpha} - v'_\nu v'_\alpha) \ . \end{aligned} \tag{2.47}$$

Including all charm states with $j^P = 1/2^-, 1/2^+$, and $3/2^+$ (i.e., all S and P-waves), and using (2.40)-(2.42), (2.45) becomes[4]

$$\begin{aligned} 1 &= \frac{1}{2}(\omega+1)\sum_n \left|\xi_C^{(n)}(\omega)\right|^2 \\ &+ (\omega-1)\left[\frac{1}{2}\sum_i \left|\xi_E^{(i)}(\omega)\right|^2 + \frac{1}{3}(\omega+1)^2\sum_j \left|\xi_F^{(j)}(\omega)\right|^2\right] + \ldots \ . \end{aligned} \tag{2.48}$$

In the above n, i, and j label the radial excitations of states with the same quantum numbers. We adopt convention that $\xi_C^{(1)} \equiv \xi_C$, the IW function for

[4]Since (2.45) does not depend on the choice of Γ, the simplest way to prove (2.48) is to choose $\Gamma = 1$, in which case the matrix elements (2.41) are zero for $C \to C^*$, $C \to E$, and for $C \to F^*$ transitions.

semileptonic $B \to D, D^*$ transitions. The ellipsis denote contributions from systems with quantum numbers for the LDF other than $j^P = 1/2^-, 1/2^+$, and $3/2^+$. Also, the sums in (2.48) are understood in a generalized sense as sums over discrete states and integrals over continuum states. Since the radially excited S-waves are orthogonal to the ground state B meson, the form factors $\xi_C^{(n)}$, where $n > 1$, all vanish as $\omega \to 1$. Therefore, the number of states contributing in (2.48) can be drastically reduced by expanding in a power series about $\omega = 1$. Using (2.43), and keeping terms up to linear order in $(\omega - 1)$, (2.48) gives $\xi_C(1) = 1$, and also the Bjorken sum rule relating the slope $\xi_C'(1)$ to the inelastic form factors at zero recoil,

$$-\xi_C'(1) = \frac{1}{4} + \frac{1}{4}\sum_i \left|\xi_E^{(i)}(1)\right|^2 + \frac{2}{3}\sum_j \left|\xi_F^{(j)}(1)\right|^2 \ . \tag{2.49}$$

This sum rule provides the well-known upper bound on $\xi_C'(1)$,

$$-\xi_C'(1) \geq \frac{1}{4} \ . \tag{2.50}$$

Similar considerations lead to another, less well-known sum rule, which also involves the inelastic form factors, first derived by Voloshin [24]. The Voloshin sum rule is the analog of the "optical" sum rule for the dipole scattering of light in atomic physics. It can be written in the form

$$\frac{1}{2} = \frac{1}{4}\sum_i (\frac{E_E^{(i)}}{E_C} - 1)\left|\xi_E^{(i)}(1)\right|^2 + \frac{2}{3}\sum_j (\frac{E_F^{(j)}}{E_C} - 1)\left|\xi_F^{(j)}(1)\right|^2 \equiv \Delta \ . \tag{2.51}$$

In the above expression $E_E^{(i)}$ and $E_F^{(j)}$ denote energies of the LDF in the i-th excited state with quantum numbers of the (E, E^*) doublet, and j-th excited state with quantum numbers of the (F, F^*) doublet, respectively. E_C is the LDF energy in the lowest (C, C^*) doublet (corresponding to (D, D^*) mesons

in semileptonic B decays). Note that the energy of the LDF in any heavy-light state is defined as the state mass minus the heavy quark mass.

Clearly, contributions of all P-wave states (including continuum) to the right-hand sides of (2.49) and (2.51) are positive, and therefore the total contributions of meson states only, should be smaller than $-\xi_C'(1)$ and $1/2$ for the Bjorken and Voloshin sum rules, respectively. This argument will be later used for constraining parameters of bound state models.

2.6 Renormalization

The effective Lagrangian (2.5) was constructed in such a way that Green functions calculated from it agreed, at tree level and to leading order in heavy quark mass, with corresponding Green functions in QCD. In other words, the effective theory correctly reproduces the long-distance (low-energy) physics of the full theory. Since the heavy quark participates in strong interactions through its coupling with gluons, whose virtual momenta can be large (of the order of the heavy quark mass), the effective theory and the full theory will differ at short distances (high energies). However, the short-distance effects can be calculated within perturbation theory.

In order to clarify the above statements, consider matrix elements of the vector current $V^\mu_{ji} = \bar{Q}_j \gamma^\mu Q_i$. In QCD this current is conserved, and doesn't need renormalization [37]. Its matrix elements are free of ultraviolet divergences, but can have logarithmic dependence on m_{Q_i} and m_{Q_j}, coming from the exchange of hard gluons with virtual momenta comparable to the heavy

quark masses. In the effective theory where heavy quark masses go to infinity, these logarithms diverge. Therefore, the vector current in the effective theory does require renormalization [20,21]. Its matrix elements depend on an arbitrary renormalization scale μ, which separates the regions of short and long-distance physics. If μ is chosen such that $\Lambda_{QCD} \ll \mu \ll m_{Q_j} \ll m_{Q_i}$, the effective coupling constant α_s in the region between μ and m_{Q_i} is small, and perturbation theory can be used for calculation of the short-distance corrections. These corrections have to be added to matrix elements of the effective theory, which contain only the long-distance physics below the scale μ. Schematically, the relation between matrix elements in the full and in the effective theory is given by

$$\langle V_{ji}^{\mu} \rangle_{QCD} = C_{ji}(\mu) \langle V_{ji}^{\mu}(\mu) \rangle_{HQET} + \mathcal{O}(1/m_Q) + \mathcal{O}(\alpha_s) \; . \tag{2.52}$$

The short-distance, or Wilson coefficients $C_{ji}(\mu)$ are defined by this relation, and are calculated order by order in perturbation theory from comparison of the matrix elements in both theories. This procedure is called "matching", and is independent on any long-distance physics. It is only at high energies where the two theories differ, and these differences are corrected by Wilson coefficients.

Calculation of these coefficients in perturbation theory uses renormalization group methods. It is in principle straightforward, but in practice rather tedious. We shall not discuss these calculations in details because of their complexity. Instead, we quote the result [32,38] for the case of the vector current

$V^\mu = \bar{c}\gamma^\mu b$, where

$$C_{cb}(\mu) = \left[\frac{\alpha_s(m_b)}{\alpha_s(m_c)}\right]^{-6/25} \left[\frac{\alpha_s(m_c)}{\alpha_s(\mu)}\right]^{8[\omega r(\omega)-1]/27} , \tag{2.53}$$

with

$$r(\omega) = \frac{\ln\left(\omega + \sqrt{\omega^2-1}\right)}{\sqrt{\omega^2-1}} . \tag{2.54}$$

An identical expression is also obtained in the case of the axial-vector current $A^\mu = \bar{c}\gamma^\mu\gamma^5 b$.

The above result can be combined with those of Section 2.4 to give hadronic matrix elements relevant for the semileptonic $B \to D$ and $B \to D^*$ decays. Using (2.36) and (2.37) gives

$$\langle D(v')|\bar{c}\gamma^\mu b|B(v)\rangle = \sqrt{m_B m_D}\, C_{cb}\xi_C(\omega)(v+v')^\mu , \tag{2.55}$$

$$\langle D^*(v',\varepsilon')|\bar{c}\gamma^\mu\gamma^5 b|B(v)\rangle = \sqrt{m_B m_{D^*}}\, C_{cb}\xi_C(\omega)[(1+\omega)\varepsilon'^{*\mu} - (\varepsilon'^*\cdot v)v'^\mu] , \tag{2.56}$$

$$\langle D^*(v',\varepsilon')|\bar{c}\gamma^\mu b|B(v)\rangle = \sqrt{m_B m_{D^*}}\, C_{cb}\xi_C(\omega) i\epsilon^{\mu\nu\alpha\beta}\varepsilon'^*_\nu v'_\alpha v_\beta . \tag{2.57}$$

The scale dependence of ξ_C must cancel that of the Wilson coefficient C_{cb}. At zero recoil we still have $\xi_C(1) = 1$.

2.7 Power Corrections

The ultimate utility of the ideas presented so far will depend largely on the size of Λ_{QCD}/m_Q corrections. We end this brief review of HQS and corresponding effective theory by briefly describing the physical effects of these corrections.

Since the heavy quark is not precisely on shell as it propagates, it is appropriate to introduce "large" and "small" component fields $h_v^{(Q)}$ and $H_v^{(Q)}$

by

$$h_v^{(Q)} = e^{im_Q v\cdot x}\frac{1}{2}(1+\not{v})Q \ , \tag{2.58}$$

$$H_v^{(Q)} = e^{im_Q v\cdot x}\frac{1}{2}(1-\not{v})Q \ . \tag{2.59}$$

These fields satisfy $\not{v}\, h_v^{(Q)} = h_v^{(Q)}$ and $\not{v}\, H_v^{(Q)} = -H_v^{(Q)}$. In the rest frame of the heavy quark $h_v^{(Q)}$ corresponds to the upper two components of Q, while $H_v^{(Q)}$ corresponds to the lower two. Instead of (2.1) we then have

$$Q = e^{-im_Q v\cdot x}[h_v^{(Q)} + H_v^{(Q)}] \ , \tag{2.60}$$

In terms of the new fields, the QCD Lagrangian for heavy quarks given in (2.3) becomes

$$\begin{aligned}\mathcal{L} &= \bar{h}_v^{(Q)} iv\cdot D h_v^{(Q)} - \bar{H}_v^{(Q)}(iv\cdot D + 2m_Q)H_v^{(Q)} \\ &+ \bar{h}_v^{(Q)} i\not{D}_\perp H_v^{(Q)} + \bar{H}_v^{(Q)} i\not{D}_\perp h_v^{(Q)} \ ,\end{aligned} \tag{2.61}$$

where $D^\mu = \partial^\mu - ig_s T_a A_a^\mu$ is covariant derivative, and

$$D_\perp = D^\mu - (v\cdot D)v^\mu \ . \tag{2.62}$$

On a classical level, the heavy degrees of freedom $H_v^{(Q)}$ can be eliminated using the equations of motion. Putting (2.60) into $(i\not{D} - m_Q)Q = 0$ yields

$$i\not{D} h_v^{(Q)} + (i\not{D} - 2m_Q)H_v^{(Q)} = 0 \ . \tag{2.63}$$

Multiplying this by $\frac{1}{2}(1\pm\not{v})$ we obtain the two equations,

$$-iv\cdot D h_v^{(Q)} = i\not{D}_\perp H_v^{(Q)} \ , \tag{2.64}$$

$$(iv\cdot D + 2m_Q)H_v^{(Q)} = i\not{D}_\perp h_v^{(Q)} \ , \tag{2.65}$$

and the second one implies

$$H_v^{(Q)} = \frac{1}{iv\cdot D + 2m_Q - i\epsilon} i\not{D}_\perp h_v^{(Q)} \ . \tag{2.66}$$

This shows that the small component field $H_v^{(Q)}$ is indeed of order $1/m_Q$. Expression for $H_v^{(Q)}$ can now be inserted in (2.64) to obtain the equation of motion for $h_v^{(Q)}$. It is not hard to see that (2.66) follows from the effective Lagrangian

$$\mathcal{L}_v^{eff} = \bar{h}_v^{(Q)} iv\cdot D h_v^{(Q)} + \bar{h}_v^{(Q)} i\not{D}_\perp \frac{1}{iv\cdot D + 2m_Q - i\epsilon} i\not{D}_\perp h_v^{(Q)} \ , \tag{2.67}$$

which is generalization of (2.5) for a large but finite heavy quark mass.

The second term in (2.67) can be expanded in powers of iD/m_Q. Taking into account that $\not{v} h_v^{(Q)} = h_v^{(Q)}$, and using the identity

$$\frac{1+\not{v}}{2} i\not{D}_\perp i\not{D}_\perp \frac{1+\not{v}}{2} = \frac{1+\not{v}}{2}\left[(iD_\perp)^2 + \frac{g_s}{2}\sigma_{\alpha\beta}G^{\alpha\beta}\right]\frac{1+\not{v}}{2} \ , \tag{2.68}$$

where $\sigma^{\alpha\beta} = \frac{i}{2}[\gamma^\alpha, \gamma^\beta]$, and $G^{\alpha\beta}$ is the gluon field strength tensor,

$$[iD^\alpha, iD^\beta] = ig_s G^{\alpha\beta} = ig_s T_a G_a^{\alpha\beta} \ , \tag{2.69}$$

we find the effective Lagrangian at order Λ_{QCD}/m_Q [39,40]. Explicitly,

$$\begin{aligned} \mathcal{L}_v^{eff} &= \bar{h}_v^{(Q)} iv\cdot D h_v^{(Q)} + \frac{1}{2m_Q}\bar{h}_v^{(Q)}(iD_\perp)^2 h_v^{(Q)} \\ &+ \frac{g_s}{4m_Q}\bar{h}_v^{(Q)}\sigma_{\alpha\beta}G^{\alpha\beta}h_v^{(Q)} + \mathcal{O}(1/m_Q^2) \ . \end{aligned} \tag{2.70}$$

The leading term coincides with (2.5). The new operators arising at order $1/m_Q$ can be identified in the rest frame of the heavy quark, where

$$\mathcal{O}_{kin} = \frac{1}{2m_Q}\bar{h}_v^{(Q)}(iD_\perp)^2 h_v^{(Q)} \to -\frac{1}{2m_Q}\bar{h}_v^{(Q)}(i\boldsymbol{D})^2 h_v^{(Q)} \ , \tag{2.71}$$

$$\mathcal{O}_{mag} = \frac{g_s}{4m_Q}\bar{h}_v^{(Q)}\sigma_{\alpha\beta}G^{\alpha\beta}h_v^{(Q)} \to -\frac{g_s}{m_Q}\bar{h}_v^{(Q)}\boldsymbol{S}\cdot\boldsymbol{B}_c h_v^{(Q)} \ . \tag{2.72}$$

In the above, the spin operator is $S^i = \frac{1}{2}\gamma^5\gamma^0\gamma^i$ as before, and $B_c^i = -\frac{1}{2}\epsilon^{ijk}G^{jk}$ are components of the color-magnetic gluon field. $\mathcal{O}_{kin}$ is just the gauge covariant extension of the kinetic energy which arises from the off-shell residual motion of the heavy quark. $\mathcal{O}_{mag}$ is the chromo-magnetic "hyperfine" interaction, which is a relativistic effect, and vanishes as $m_Q \to \infty$. This is the origin of the heavy quark spin symmetry. Both $\mathcal{O}_{kin}$ and $\mathcal{O}_{mag}$ should be treated as perturbations in the computation of S-matrix elements.

2.8 Conclusion

With this brief illustration of the physical effects which arise because heavy quark masses are not infinite, we completed our short overview of heavy quark symmetry and heavy quark effective theory. This is certainly a vast subject and a very active area of research, where new papers appear almost every day. Because of that, it is impossible to fully cover (or even just touch upon) all of its parts in only a few pages. We do hope though that this chapter served its purpose of describing the basic ideas and techniques, which will be used in subsequent parts of this thesis.

Chapter 3

Modelling Form Factors

3.1 Introduction

As we have seen in Chapter 2, in the heavy quark limit the various form factors which parametrize semileptonic B decays, can be expressed in terms of a single unknown function. Nevertheless, the remaining universal function cannot be calculated from the first principles. In order to estimate it, one still has to rely on some model of strong interactions. In general, the unknown IW function for a particular decay will be related to the overlap of the wave functions of the LDF in mesons before and after the decay. However, one has to be careful in identifying the form factor directly with the overlap. Depending on the definition of a particular form factor, there may be a kinematic factor involved. If this factor is not taken into account, significantly incorrect results can be obtained, no matter which model for wave functions of the LDF one uses.

In [41] Zalewski observed that the heavy quark limit implies a simple formula for the wave function of any particle containing one heavy quark. Based on this, in this chapter we develop a straightforward method [42] for relating

the form factors, as defined within the framework of the CTF [16,32–34], to overlaps of the rest frame wave functions of the LDF before and after the decay. Even though we are interested here only in mesons, it is obvious that an analogous calculation can also be done for baryons.

3.2 Defining IW Functions

As pointed out in [41], the assumption of the heavy quark limit implies a simple formula for the wave function of any particle containing one very heavy quark (with total angular momentum J and its projection λ),

$$\Psi^{(n)}_{J\lambda}(v) = \sum_{\lambda_j,\lambda_Q} \langle j,\lambda_j;\frac{1}{2},\lambda_Q|J\lambda\rangle \Phi^{(n)}_{j\lambda_j}(v) u_{\lambda_Q}(v) \ . \tag{3.1}$$

In this formula n refers to radial and all other quantum numbers of the meson, $u_{\lambda_Q}(v)$ is the free Dirac bispinor describing a heavy quark with spin $\frac{1}{2}$, helicity λ_Q, and velocity v (and normalized to $\bar{u}u = 2$). $\Phi^{(n)}_{j\lambda_j}(v)$ is the wave function of the LDF in a meson moving with a velocity v (normalized to one), with total angular momentum j (in the rest frame of the particle), and its projection λ_j. For a meson, this is the wave function of the light antiquark.

From (3.1) it can be immediately seen that matrix elements of the heavy quark currents $\bar{Q}'\Gamma Q$, are linear combinations of matrix elements

$$\langle \Phi'_{j'\lambda'_j}(v')|\Phi_{j\lambda_j}(v)\rangle \bar{u}'_{\lambda'_Q}(v')\Gamma u_{\lambda_Q}(v) \ . \tag{3.2}$$

For a given Γ, $\bar{u}'\Gamma u$ is a product of known matrices, and therefore all the unknown dynamics is contained in the overlaps of the LDF wave functions $\langle\Phi'|\Phi\rangle$. We choose the spin projection axis (z) as the velocity direction of

meson M' as seen in the rest frame of meson M. From the independence of the overlap on the direction of the x-axis we then have

$$\langle \Phi'_{j'\lambda'_j} | \Phi_{j\lambda_j} \rangle = 0 \ , \ \text{if} \ \lambda'_j \neq \lambda_j \ . \tag{3.3}$$

Similarly, from the independence of the overlap on the orientation of the y axis,

$$\langle \Phi'_{j'\lambda'_j} | \Phi_{j\lambda_j} \rangle = \eta\eta'(-1)^{j'-j} \langle \Phi'_{j',-\lambda'_j} | \Phi_{j,-\lambda_j} \rangle \ , \tag{3.4}$$

where η and η' are the orbital parities of the initial and final state of the LDF. In the case of interest to us, for the change of the orbital angular momentum from L to L', $\eta\eta' = (-1)^{L+L'}$. Equations (3.3) and (3.4) have been first discussed by Politzer [43].

In order to show how one can relate universal functions, defined within the CTF, to the overlaps of the LDF wave functions, we choose the $0^-_{1/2} \to 0^+_{1/2}$ transitions, and axial-vector current ($\Gamma = \gamma^\mu\gamma^5$), as an illustrative example. From (3.1) we have

$$\Psi_0^{(\pm)} = \frac{1}{\sqrt{2}} [\Phi^{(\pm)}_{\frac{1}{2},\frac{1}{2}} u_{-\frac{1}{2}} - \Phi^{(\pm)}_{\frac{1}{2},-\frac{1}{2}} u_{\frac{1}{2}}] \ , \tag{3.5}$$

where $+$ and $-$ refer to $0^+_{1/2}$ and $0^-_{1/2}$ states, respectively. Also, from (3.3) and (3.4) one can see that

$$\langle \Phi'^{(+)}_{\frac{1}{2},-\frac{1}{2}}(v') | \Phi^{(-)}_{\frac{1}{2},-\frac{1}{2}}(v) \rangle = -\langle \Phi'^{(+)}_{\frac{1}{2},\frac{1}{2}}(v') | \Phi^{(-)}_{\frac{1}{2},\frac{1}{2}}(v) \rangle \ , \tag{3.6}$$

and all other overlaps are zero. Therefore, it immediately follows that

$$\langle 0^+_{1/2}(v') | \bar{Q}'\Gamma Q | 0^-_{1/2}(v) \rangle = \frac{1}{2} [\bar{u}'_{-\frac{1}{2}} \Gamma u_{-\frac{1}{2}} - \bar{u}'_{\frac{1}{2}} \Gamma u_{\frac{1}{2}}] \langle \Phi'^{(+)}_{\frac{1}{2},\frac{1}{2}}(v') | \Phi^{(-)}_{\frac{1}{2},\frac{1}{2}}(v) \rangle \ . \tag{3.7}$$

Now, choosing $\Gamma = \gamma^3\gamma^5$ and evaluating (3.7) in the rest frame of $0^-_{1/2}$ meson, where $v^\mu = (1,0,0,0)$ and $v'^\mu = (\omega, 0, 0, \sqrt{\omega^2-1})$, one obtains

$$\langle 0^+_{1/2}(v')|\bar{Q}'\gamma^3\gamma^5 Q|0^-_{1/2}(v)\rangle = -\sqrt{2}\sqrt{\omega+1}\langle \Phi'^{(+)}_{\frac{1}{2},\frac{1}{2}}(v')|\Phi^{(-)}_{\frac{1}{2},\frac{1}{2}}(v)\rangle \ . \tag{3.8}$$

On the other hand, using (2.41) and (2.42), together with matrix wave functions $C(v)$ and $E(v')$ given in (2.40), one finds

$$\langle 0^+_{1/2}(v')|\bar{Q}'\gamma^\mu\gamma^5 Q|0^-_{1/2}(v)\rangle = (-v^\mu + v'^\mu)\xi_E(\omega) \ , \tag{3.9}$$

which specialized to the rest frame of $0^-_{1/2}$ state yields

$$\langle 0^+_{1/2}(v')|\bar{Q}'\gamma^3\gamma^5 Q|0^-_{1/2}(v)\rangle = \sqrt{\omega^2-1}\xi_E(\omega) \ . \tag{3.10}$$

Comparing (3.8) and (3.10) we obtain (apart from the irrelevant overall sign)

$$\xi_E(\omega) = \sqrt{\frac{2}{\omega-1}}\langle \Phi'^{(+)}_{\frac{1}{2},\frac{1}{2}}(v')|\Phi^{(-)}_{\frac{1}{2},\frac{1}{2}}(v)\rangle \ . \tag{3.11}$$

Because of the heavy quark spin symmetry, the particular choice of the third component of the axial-vector current is not important. The same result for ξ_E (and with the same overall sign), can be obtained from any component of $\gamma^\mu\gamma^5$ current, or any other current, which gives a non-vanishing matrix element. For the same reason, instead of $0^-_{1/2} \to 0^+_{1/2}$ transitions, we can choose, for instance, $0^-_{1/2} \to 1^+_{1/2}$ transitions, and specialize to any of the three possible polarizations of the $1^+_{1/2}$ state. Since IW functions are Lorentz invariant, the particular choice of the reference frame also doesn't matter. Any convenient reference frame should yield the same result.

Let us now summarize the results obtained following the simple proceedure outlined above for several cases of interest. We emphasize that all the

results given here were explicitly verified for all possible choices of Γ (i.e., $\Gamma = 1, \gamma^5, \gamma^\mu, \gamma^\mu\gamma^5$, and $\gamma^\mu\gamma^\nu$), and also in two convenient reference frames: besides the rest frame of the $0^-_{1/2}$ meson, we have also used the Breit frame ($\mathbf{v} = -\mathbf{v}'$), in which $v^\mu = (\sqrt{\frac{\omega+1}{2}}, 0, 0, -\sqrt{\frac{\omega-1}{2}})$ and $v'^\mu = (\sqrt{\frac{\omega+1}{2}}, 0, 0, \sqrt{\frac{\omega-1}{2}})$. Polarization vectors describing spin one states ($\epsilon \cdot v' = 0$) were the standard ones, $\epsilon^{(\pm)} = \mp\frac{1}{\sqrt{2}}(0, 1, \pm i, 0)$ in both frames, $\epsilon^{(0)} = (\sqrt{\omega^2-1}, 0, 0, \omega)$ in the rest frame of $0^-_{1/2}$, and $\epsilon^{(0)} = (\sqrt{\frac{\omega-1}{2}}, 0, 0, \sqrt{\frac{\omega+1}{2}})$ in the Breit frame. Let us also, for the sake of simplicity, define

$$\langle \Phi' | \Phi \rangle \equiv \langle \Phi'^{(n')}_{j', \frac{1}{2}}(v') | \Phi^{(n)}_{\frac{1}{2}, \frac{1}{2}}(v) \rangle \ , \tag{3.12}$$

and state our results in terms of this overlap:

$$\xi_C(\omega) = \sqrt{\frac{2}{\omega+1}} \langle \Phi' | \Phi \rangle \ , \tag{3.13}$$

$$\xi_E(\omega) = \sqrt{\frac{2}{\omega-1}} \langle \Phi' | \Phi \rangle \ , \tag{3.14}$$

$$\xi_F(\omega) = \sqrt{\frac{3}{\omega-1}} \frac{1}{\omega+1} \langle \Phi' | \Phi \rangle \ , \tag{3.15}$$

$$\xi_G(\omega) = \sqrt{\frac{3}{\omega+1}} \frac{1}{\omega-1} \langle \Phi' | \Phi \rangle \ . \tag{3.16}$$

The definition (3.13) for ξ_C agrees with the one given in [44,45]. As one can see, different IW functions are related to overlaps of the LDF wave functions through different kinematic factors. These factors are the reason why, for instance, the inelastic form factors ξ_E, ξ_F and ξ_G do not vanish at zero recoil point.

3.3 Evaluating LDF Overlaps

In expressions (3.13)-(3.16), $\langle\Phi'|\Phi\rangle$ involve wave functions of the LDF in mesons moving with velocities v and v'. Usually hadronic models provide us with the wave functions in the meson rest frame. Because of that, it is convenient to express the overlaps $\langle\Phi'|\Phi\rangle$ in terms of the wave functions describing the LDF in the rest frame of the particle. Following [45,46], in the valence quark approximation we write for the rest frame LDF wave function

$$\Phi^{(0)}(x) = \phi^{(0)}(\boldsymbol{x})e^{-iE_M t} \ , \tag{3.17}$$

where E_M denotes the energy of the LDF in meson M. The LDF wave function of the same meson moving with (ordinary) velocity $\boldsymbol{\beta}$ along the z axis (laboratory frame), is then given by

$$\Phi(x') = S(\boldsymbol{\beta})\Phi^{(0)}(x) \ , \tag{3.18}$$

with $x' = \Lambda^{-1}(\boldsymbol{\beta})x$ being the laboratory frame, x the rest frame of the meson, and $S(\boldsymbol{\beta})$ the wave function Lorentz boost.

Because IW functions are Lorentz invariant quantities, they can be calculated in any frame. Particularly convenient is the Breit frame, in which the two mesons move with equal and opposite velocities. As noted in [45], the wave functions relevant for the overlap $\langle\Phi'|\Phi\rangle$ are at $t' = 0$ in the Breit frame. Therefore, denoting the three-velocity of the final meson as $\boldsymbol{\beta}$, by the use of (3.18) we have

$$\begin{aligned}
\langle\Phi'(v')|\Phi(v)\rangle &= \int d^3x' \Phi'^{\dagger}(x')\Phi(x')|_{t'=0} \\
&= \int d^3x' \Phi'^{(0)\dagger}(x_+)S^{\dagger}(\boldsymbol{\beta})S(-\boldsymbol{\beta})\Phi^{(0)}(x_-)|_{t'=0}
\end{aligned}$$

$$= \int d^3x' \Phi'^{(0)\dagger}(x_+)\Phi^{(0)}(x_-)|_{t'=0} \ . \tag{3.19}$$

In this expression x_+ and x_- denote the rest frames of the final (moving in the $+z$ direction) and initial meson (moving in the $-z$ direction), respectively. To obtain the last equation we have used the fact that Lorentz boosts satisfy $S^\dagger(\boldsymbol{\beta}) = S(\boldsymbol{\beta}) = S^{-1}(-\boldsymbol{\beta})$, so that boost factors cancel out. Also, we have ($\beta = |\boldsymbol{\beta}|$)

$$x_\pm|_{t'=0} = \Lambda(\pm\boldsymbol{\beta})x'|_{t'=0} = (\mp\gamma\beta z', x', y', \gamma z') \ , \tag{3.20}$$

where, in terms of ω,

$$\gamma = \sqrt{\frac{\omega+1}{2}} \ , \tag{3.21}$$

$$\beta = \sqrt{\frac{\omega-1}{\omega+1}} \ . \tag{3.22}$$

Using (3.17) and (3.20) in (3.19) we find

$$\langle \Phi'(v')|\Phi(v)\rangle = \int d^3x' \phi'^{(0)\dagger}(x', y', \gamma z')\phi^{(0)}(x', y', \gamma z')e^{-i(E_M+E_{M'})\gamma\beta z'} \ . \tag{3.23}$$

After rescaling the z' coordinate ($z' \to \frac{1}{\gamma}z'$), renaming integration variables, and using kinematical identities (3.21) and (3.22), we obtain

$$\langle \Phi'(v')|\Phi(v)\rangle = \sqrt{\frac{2}{\omega+1}} \int d^3x \phi'^{(0)\dagger}(\boldsymbol{x})\phi^{(0)}(\boldsymbol{x})e^{-iaz} \ , \tag{3.24}$$

where

$$a = (E_M + E_{M'})\sqrt{\frac{\omega-1}{\omega+1}} \ . \tag{3.25}$$

This formula was first obtained in [45] for the semileptonic $B \to D$ ($C \to C'$) and $B \to D^*$ ($C \to C^*$) decays (where $E_{M'} = E_M = E_C$). To illustrate the use of the results obtained in this section, we next consider the spinless constituent quark model as one simple example.

3.4 Spinless Constituent Quark Models

Assuming that we can describe heavy-light mesons using a particular spinless constituent quark model, the rest frame LDF wave functions (with angular momentum j and its projection λ_j), can be written as

$$\phi^{(nL)}_{j\lambda_j}(\boldsymbol{x}) = \sum_{m_L,m_s} R_{nL}(r) Y_{Lm_L}(\Omega)\chi_{m_s}\langle L, m_L; \frac{1}{2}, m_s | j, \lambda_j; L, \frac{1}{2}\rangle \ . \tag{3.26}$$

In the above expression χ_{m_s} represent the rest frame spinors normalized to one, $\chi^\dagger_{m'_s}\chi_{m_s} = \delta_{m'_s,m_s}$, $R_{nL}(r)$ is the radial wave function, and Y_{Lm_L} are the usual spherical harmonics. Explicitly, taking into account relevant CG coefficients, the states that we need are

$$\phi^{(n0)}_{\frac{1}{2}\frac{1}{2}}(\boldsymbol{x}) = R_{n0}(r)Y_{00}(\Omega)\chi_{\frac{1}{2}} \ , \tag{3.27}$$

$$\phi^{(n1)}_{\frac{1}{2}\frac{1}{2}}(\boldsymbol{x}) = R_{n1}(r)[\sqrt{\frac{2}{3}}Y_{11}(\Omega)\chi_{-\frac{1}{2}} - \sqrt{\frac{1}{3}}Y_{10}(\Omega)\chi_{\frac{1}{2}}] \ , \tag{3.28}$$

$$\phi^{(n1)}_{\frac{3}{2}\frac{1}{2}}(\boldsymbol{x}) = R_{n1}(r)[\sqrt{\frac{1}{3}}Y_{11}(\Omega)\chi_{-\frac{1}{2}} + \sqrt{\frac{2}{3}}Y_{10}(\Omega)\chi_{\frac{1}{2}}] \ , \tag{3.29}$$

$$\phi^{(n2)}_{\frac{3}{2}\frac{1}{2}}(\boldsymbol{x}) = R_{n2}(r)[\sqrt{\frac{3}{5}}Y_{21}(\Omega)\chi_{-\frac{1}{2}} - \sqrt{\frac{2}{5}}Y_{20}(\Omega)\chi_{\frac{1}{2}}] \ . \tag{3.30}$$

Now, using the well known expansion of a plane wave e^{-ikz} in terms of spherical Bessel functions $j_l(kr)$,

$$e^{-ikz} = \sum_{l=0}^{\infty}(2l+1)(-i)^l j_l(kr)\sqrt{\frac{4\pi}{2l+1}}Y_{l0} \ , \tag{3.31}$$

together with the wave functions given above, the overlap (3.24) gives[1]

$$\langle \Phi^{n'0}_{\frac{1}{2}\frac{1}{2}}(v')|\Phi^{n0}_{\frac{1}{2}\frac{1}{2}}(v)\rangle = \sqrt{\frac{2}{\omega+1}}\langle j_0(ar)\rangle^{n'n}_{00} \ , \tag{3.32}$$

[1]Using states analogous to (3.27)-(3.30), but for $\lambda_j = -\frac{1}{2}$, one can indeed verify that all overlaps indeed satisfy (3.3) and (3.4).

$$\langle \Phi^{n'1}_{\frac{1}{2}\frac{1}{2}}(v')|\Phi^{n0}_{\frac{1}{2}\frac{1}{2}}(v)\rangle = i\sqrt{\frac{2}{\omega+1}}\langle j_1(ar)\rangle^{n'n}_{10} , \tag{3.33}$$

$$\langle \Phi^{n'1}_{\frac{3}{2}\frac{1}{2}}(v')|\Phi^{n0}_{\frac{1}{2}\frac{1}{2}}(v)\rangle = -i\sqrt{2}\sqrt{\frac{2}{\omega+1}}\langle j_1(ar)\rangle^{n'n}_{10} , \tag{3.34}$$

$$\langle \Phi^{n'2}_{\frac{3}{2}\frac{1}{2}}(v')|\Phi^{n0}_{\frac{1}{2}\frac{1}{2}}(v)\rangle = \sqrt{2}\sqrt{\frac{2}{\omega+1}}\langle j_2(ar)\rangle^{n'n}_{20} , \tag{3.35}$$

where

$$\langle F(r)\rangle^{n'n}_{L'L} = \int r^2 dr R^*_{n'L'}(r) R_{nL}(r) F(r) . \tag{3.36}$$

At this point, one can readily obtain expressions for the IW functions (3.13)-(3.16) in terms of the radial wave functions and energies of the LDF. One can also find form factors and their derivatives at the zero recoil point. Let us summarize here the results [42] (ignoring irrelevant phase factors and suppressing quantum numbers n' and n):

- $0^-_{1/2} \to 0^-_{1/2}, 1^-_{1/2}$ $(C \to C, C^*)$ transitions.

$$\xi_C(\omega) = \frac{2}{\omega+1}\langle j_0(ar)\rangle_{00} , \text{ with } a = (E_C + E_{C'})\sqrt{\frac{\omega-1}{\omega+1}} , \tag{3.37}$$

$$\xi_C(1) = \langle 1\rangle_{00} , \tag{3.38}$$

$$\xi'_C(1) = -\left[\frac{1}{2} + \frac{1}{12}(E_C + E_{C'})^2\langle r^2\rangle_{00}\right] . \tag{3.39}$$

- $0^-_{1/2} \to 0^+_{1/2}, 1^+_{1/2}$ $(C \to E, E^*)$ transitions.

$$\xi_E(\omega) = \frac{2}{\sqrt{\omega^2-1}}\langle j_1(ar)\rangle_{10} , \text{ with } a = (E_C + E_E)\sqrt{\frac{\omega-1}{\omega+1}} , \tag{3.40}$$

$$\xi_E(1) = \frac{1}{3}(E_C + E_E)\langle r\rangle_{10} , \tag{3.41}$$

$$\xi'_E(1) = -\left[\frac{1}{6}(E_C + E_E)\langle r\rangle_{10} + \frac{1}{60}(E_C + E_E)^3\langle r^3\rangle_{10}\right] . \tag{3.42}$$

- $0^-_{1/2} \to 1^+_{3/2}, 2^+_{3/2}$ $(C \to F, F^*)$ transitions.

$$\xi_F(\omega) = \sqrt{\frac{3}{\omega^2-1}}\frac{2}{\omega+1}\langle j_1(ar)\rangle_{10} \text{ , with } a = (E_C+E_F)\sqrt{\frac{\omega-1}{\omega+1}} \ , \quad (3.43)$$

$$\xi_F(1) = \frac{1}{2\sqrt{3}}(E_C+E_F)\langle r\rangle_{10} \ , \quad (3.44)$$

$$\xi'_F(1) = -\left[\frac{1}{2\sqrt{3}}(E_C+E_F)\langle r\rangle_{10} + \frac{1}{40\sqrt{3}}(E_C+E_F)^3\langle r^3\rangle_{10}\right] \ . \quad (3.45)$$

- $0^-_{1/2} \to 1^-_{3/2}, 2^-_{3/2}$ $(C \to G, G^*)$ transitions.

$$\xi_G(\omega) = \frac{2\sqrt{3}}{\omega^2-1}\langle j_2(ar)\rangle_{20} \ , \text{ with } a = (E_C+E_G)\sqrt{\frac{\omega-1}{\omega+1}} \ , \quad (3.46)$$

$$\xi_G(1) = \frac{1}{10\sqrt{3}}(E_C+E_G)^2\langle r^2\rangle_{20} \ , \quad (3.47)$$

$$\xi'_G(1) = -\left[\frac{1}{10\sqrt{3}}(E_C+E_G)^2\langle r^2\rangle_{20} + \frac{1}{280\sqrt{3}}(E_C+E_G)^4\langle r^4\rangle_{20}\right] \ . \quad (3.48)$$

Note that these expressions include transitions from the ground state into radially excited states. If the two C states are the same, $\xi_C(1)$ is normalized to one and $E_{C'} = E_C$. Otherwise, $\xi_C(1)$ vanishes because excited states are orthogonal to the ground state. From (3.39) we reobtain the bound $-\xi'_C(1) \geq 1/2$ [45], which is lower than the bound obtained from the Bjorken sum rule (2.49) $(-\xi'_C(1) \geq 1/4)$ [22,23]. Both upper bounds follow from the basic principles and are not inconsistent. From (3.41) and (3.44) one can see that the P-wave form factors ξ_E and ξ_F do not vanish at zero recoil point, which is consistent with sum rules (2.49) and (2.51). Furthermore, since spinless models do not distinguish between the two P-wave doublets ($E_E = E_F$ and wave functions are the same), from (3.40) and (3.43) we find

$$\xi_E(\omega) = \frac{\omega+1}{\sqrt{3}}\xi_F(\omega) \ , \quad (3.49)$$

and in particular

$$\xi_E(1) = \frac{2}{\sqrt{3}}\xi_F(1) \ . \tag{3.50}$$

Equations (3.37)-(3.48) are among the principal results of this thesis.

3.5 Models Based on Dirac Equation

Important class of models, especially in the heavy-light limit, are those based on the Dirac equation. Our results from the previous section [42] can be generalized to any model involving the Dirac equation with a spherically symmetric potential. There, the wave function has the form

$$\phi^{(nk)}_{j\lambda_j}(\boldsymbol{x}) = \begin{pmatrix} f^k_{nj}(r)\mathcal{Y}^k_{j\lambda_j}(\Omega) \\ ig^k_{nj}(r)\mathcal{Y}^{-k}_{j\lambda_j}(\Omega) \end{pmatrix} \ , \tag{3.51}$$

where $\mathcal{Y}^k_{j\lambda_j}$ are the spherical spinors, $k = l$ ($l = j + \frac{1}{2}$) or $k = -l-1$ ($l = j - \frac{1}{2}$), and n again denotes all other quantum numbers. Using (3.51) it can be shown that all the expressions (3.32)-(3.35) and (3.37)-(3.48) are unchanged, except that the expectation value (3.36) is replaced by [42]

$$\langle F(r)\rangle^{n'n}_{L'L} \to \langle F(r)\rangle^{n'n}_{j'j} = \int r^2 dr[f^{*k'}_{n'j'}(r)f^k_{nj}(r) + g^{*k'}_{n'j'}(r)g^k_{nj}(r)]F(r) \ . \tag{3.52}$$

It is important to realize that now (E, E^*) and (F, F^*) doublets are no longer degenerate, so that we do not have relation between ξ_E and ξ_F, such is (3.49).

3.6 Comparison with Literature

We have already mentioned that kinematic factors in definitions of IW functions have to be taken correctly into account. Otherwise, significantly wrong

results for the heavy-light meson decays can be obtained. One such example is approach developed by Ali et al. [47] (AOM), and later used in [48–51]. There, apart from irrelevant phase factors, different IW functions are identified directly as overlaps of the wave functions of the initial and the final state of the LDF in the rest frame of the initial meson. Explicitly (putting a tilde over the AOM form factors to avoid confusion),

$$\tilde{\xi}_C(\omega) = \langle j_0(\tilde{a}r)\rangle_{00} \ , \ \text{with } \tilde{a} = E_{C'}\sqrt{\omega^2-1} \ , \tag{3.53}$$

$$\tilde{\xi}_E(\omega) = \sqrt{3}\langle j_1(\tilde{a}r)\rangle_{10} \ , \ \text{with } \tilde{a} = E_{E'}\sqrt{\omega^2-1} \ , \tag{3.54}$$

$$\tilde{\xi}_F(\omega) = \sqrt{3}\langle j_1(\tilde{a}r)\rangle_{10} \ , \ \text{with } \tilde{a} = E_{F'}\sqrt{\omega^2-1} \ , \tag{3.55}$$

$$\tilde{\xi}_G(\omega) = \sqrt{5}\langle j_2(\tilde{a}r)\rangle_{20} \ , \ \text{with } \tilde{a} = E_{G'}\sqrt{\omega^2-1} \ . \tag{3.56}$$

As pointed out in [42], this formulation has several difficulties. For example, the zero recoil slope of the IW function ξ_C for semileptonic $B \to D, D^*$ decays doesn't necessarily obey the Bjorken sum rule bound. The easiest way to see that is to use harmonic oscillator (HO) wave functions as wave functions of the LDF.[2] It is straightforward to show that the $1S$ HO wave function, $R_{1S}(r) = 2\beta^{3/2}\exp\left[-\beta^2 r^2/2\right]/\pi^{1/4}$, where β is variational parameter, gives

$$\tilde{\xi}'_C(1) = -\frac{E^2_{C'}}{2\beta^2} \ . \tag{3.57}$$

For some choices of $E_{C'}$ and β this clearly can violate the Bjorken bound of $\xi'_C \leq -1/4$. Using values from the ISGW model [17], $\beta \approx 0.40\ GeV$ and

[2]This approach was advocated by Isgur et al. [17] (within the ISGW model), and widely followed in the literature. However, there is no justification whatsoever for description of meson states with a single HO wave function. We use it here for purpose of illustration only, and not for any real calculation.

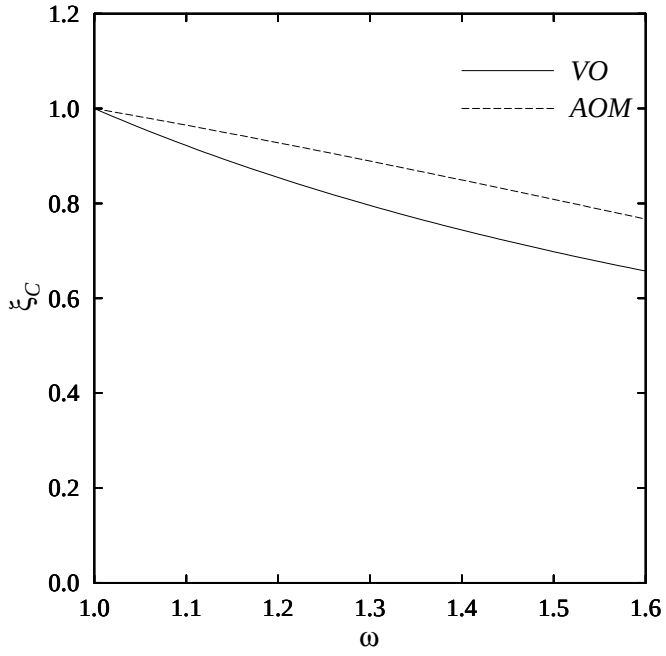

Figure 3.1: The elastic form factor ξ_C for semileptonic $B \to D, D^*$ decays, obtained using $1S$ HO wave function, with $\beta = 0.40\ GeV$. Our result (full line) is obtained from (3.37), while the AOM result (dashed line) follows from (3.53). We assumed $E_{C'} = E_C = 330\ MeV$.

$E_{C'} \approx 330\ MeV$, one gets

$$\tilde{\xi}'_C(1) \approx -0.34\ , \tag{3.58}$$

which is too large [52]. On the other hand, the same wave function used in (3.39) gives ($E_C = E_{C'} \approx 330\ MeV$)

$$\xi'_C(1) \approx -0.84\ , \tag{3.59}$$

a result which is in much better agreement with the data [52]. Furthermore, from (3.53)-(3.56) one can see that all form factors (except for $\tilde{\xi}_C$) vanish at the zero recoil point, which is not consistent with sum rules (2.49) and (2.51).

In order to further illustrate differences between our form factors and the ones of Ali et al. [47], in Figure 3.1 we show results for the elastic form

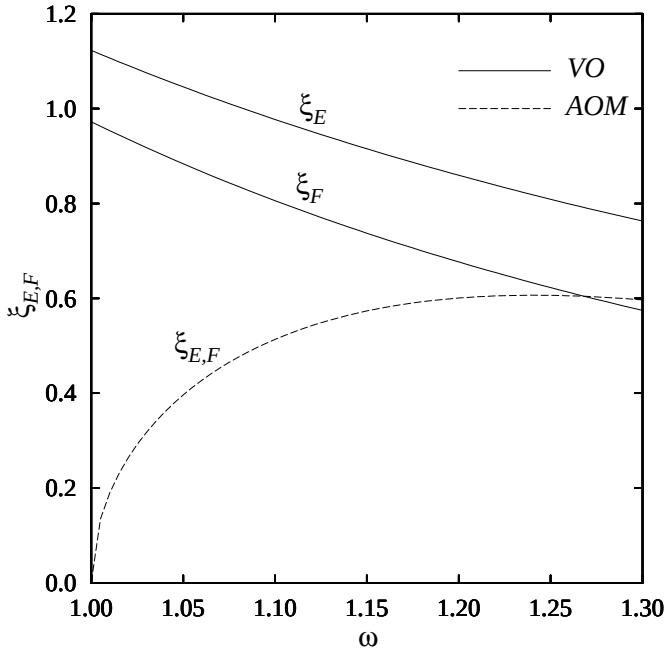

Figure 3.2: The inelastic form factors ξ_E and ξ_F describing S to P-wave transitions for semileptonic B decays, obtained using $1S$ and $1P$ HO wave functions, with $\beta = 0.40\ GeV$. Our results (full lines) are obtained from (3.40) and (3.43), while the AOM result (dashed line) follows from (3.54) ($\xi_E = \xi_F$). We assumed $E_C = 330\ MeV$ and $E_{E,F} = 770\ MeV$.

factor ξ_C for semileptonic $B \to D, D^*$ decays,[3] obtained with $1S$ HO wave function ($\beta = 0.40\ GeV$). Our result (VO) [42], shown with the full line, is obtained from (3.37). The AOM result [47] (dashed line) follows from (3.53). We assumed $E_{C'} = E_C = 330\ MeV$. As expected on the basis of slope estimates (3.58) and (3.59), the AOM form factor is much flatter than ours, which leads to higher branching ratios for these decays. In Figure 3.2 we show inelastic P-wave form factors ξ_E and ξ_F for semileptonic B decays.[4] For

[3]The kinematic limit for $B \to D$ decays is $\omega_{max} \simeq 1.6$, while for $B \to D^*$ decays it is $\omega_{max} \simeq 1.5$.

[4]For these decays the kinematic limit is $\omega_{max} \simeq 1.3$.

the LDF energies we assumed $E_C = 330\ MeV$ and $E_{E,F} = 770\ MeV$,[5] and for the LDF wave functions we used $1S$ and $1P$ HO basis states ($R_{1P}(r) = \sqrt{8/3}\beta^{5/2} r \exp[-\beta^2 r^2/2]/\pi^{1/4}$), with $\beta = 0.40\ GeV$. From that figure it is clear that our form factors qualitatively differ from the AOM result.

3.7 Conclusion

In this chapter we have presented a simple method for relating form factors, defined within the covariant trace formalism [16,32–34], to the explicit overlaps of the rest frame wave functions describing the initial and the final states of the light degrees of freedom [42]. We have obtained explicit formulae for several transitions of interest (from the ground state $0^-_{1/2}$ into a few lowest excited states), and have shown how one can apply these expressions in the spinless constituent quark models, and in models involving the Dirac equation with spherically symmetric potentials. These results are central to this thesis.

Expression (3.37) has already been used in several hadronic models for calculation of ξ_C (which describes semileptonic $B \to D, D^*$ decays). For instance, the bag model was employed in [45], while the Dirac equation with color electric potential was used in [46]. In [53] ξ_C was obtained from the Dirac equation with scalar confinement, and also from the Salpeter equation with vector confinement. Predictions of the relativistic flux tube model based on the Salpeter

[5] Assuming that the lowest (E, E^*) doublet in D-systems has spin-averaged energy of $\sim 2350\ MeV$, then experimental masses of D_1 nd D_2^* mesons lead to spin-averaged energy of $\sim 2414\ MeV$ for the lowest $1P$ state. Since the spin-averaged mass of D and D^* mesons is 1974 MeV, the $1P$ LDF energy should be $\sim 440\ MeV$ higher than the $1S$ LDF energy. Therefore, $E_C = 330\ MeV$ leads to $E_{E,F} = 770\ MeV$.

equation are given in [54]. As far as spinless calculations are concerned, in [55] ξ_C was obtained from the spinless relativistic flux tube model, while authors of [56] used the $1S$ lattice QCD heavy-light wave function from Duncan et al. [57], together with experimental data on semileptonic $B \to D, D^*$ decays [52], in order to extract information on the energy of the light degrees of freedom in $1S$ heavy-light states.

We have also pointed out several inconsistencies in form factor definitions present in the approach of Ali et al. [47]. Because of those inconsistencies, in [47] significantly incorrect results were obtained for branching fractions of radiative rare B decays into higher K-resonances. We shall leave a full account of the radiative rare B decays within HQET framework [58] for Chapter 6.

Chapter 4

Hadronic Models in the Heavy Quark Limit

4.1 Introduction

We have seen in previous chapters that heavy quark symmetry (HQS) significantly reduces the number of independent form factors describing decays of heavy-light mesons. Nevertheless, the remaining form factors cannot be calculated from first principles. In order to estimate them, we have to rely on some model of strong interactions. In Chapter 3 we have found precise form factor definitions in the valence quark approximation [42], which are consistent with the covariant trace formalism [16,32–34]. The task of this chapter is to provide reliable and self-consistent hadronic models in the heavy-light limit, which can be used for the calculation of these form factors.

It is a well known fact that almost any relativistic quark model which involves a reasonable quark-antiquark potential will adequately reproduce the spin-averaged spectrum of the heavy-heavy and heavy-light states. Almost all successful potentials are based on some variant of a one-gluon-exchange

(Coulomb) part plus a confining part expected from QCD. However, the specific choice of parameters of the model is usually based only on their ability to reproduce data. That and the fact that parameters of the model are correlated as far as meson spectrum is concerned,[1] is the main reason why one can find nearly as many different sets of parameters for the same model, as there are papers using that particular model.

Here we advocate an analysis which uses the linear Regge structure of a given relativistic quark model [59–64], together with sum rules [22–24] of the heavy quark effective theory (HQET), in order to constrain confining parameters of that model. To determine other parameters, appropriate for the heavy-light limit, we use spin-averaged heavy-light meson spectrum. We shall present this analysis in more details using the simplest and widely used generalization of the nonrelativistic Schrödinger equation, the so-called spinless Salpeter (SSEQ), or the square root equation. We shall then use the same analysis to investigate several other models in the heavy-light limit: spinless relativistic flux tube model (RFTM), Salpeter equation with vector confinement (SEVC), flux tube model based on the Salpeter equation (SFTM), Salpeter equation with half-half mixture of vector and scalar confinement (SVSC), and Dirac equation with pure scalar confinement (DESC). We must emphasize that the goal of the analysis, which will be described in the next section, is not to say whether a particular model is right or wrong in terms of the type of confinement, or the particular potential it uses. Instead, its purpose is to show how

[1] By this we mean that changing one parameter in the model inevitably leads to changes in other parameters. For example, it is much easier to determine the difference between b and c quark mass from the meson spectrum, than it is to determine either mass.

one can construct a model which yields not only a good description of the spin-averaged meson spectrum (in our case it is the heavy-light spectrum), but is also consistent with experiment in terms of its Regge structure, and self-consistent with respect to the sum rules in the heavy-light limit.

There are at least two good reasons for investigating so many different models in this chapter. On one hand, by trying to constrain parameters of a particular model, we can shed some light on a model itself. On the other hand, by using many qualitatively different hadronic models we can estimate the model dependence of the unknown form factors and branching ratios describing decays of heavy-light mesons. This will be useful in Chapter 5, for investigation of semileptonic B decays.

4.2 Spinless Salpeter Equation (SSEQ)

4.2.1 Description of the Model

In the meson rest frame, Hamiltonian of the SSEQ is given by [65–69][2]

$$H = \sqrt{m_{\bar{q}}^2 + p^2} + \sqrt{m_Q^2 + p^2} + V(r) \ , \tag{4.1}$$

where $p^2 = p_r^2 + L^2/r^2$, while $m_{\bar{q}}$ and m_Q are the constituent quark masses. The potential interaction $V(r)$ usually contains the one-gluon-exchange and the confining part, i.e., $V(r) = V_{conf}(r) + V_{oge}(r)$. We take

$$V_{oge}(r) \ = \ -\frac{4}{3}\frac{\alpha_s}{r} \ , \tag{4.2}$$

[2]Numerical methods for solving SSEQ, and all other models investigated in this chapter, are briefly described in Appendix A.

$$V_{conf}(r) \;=\; br + c \;. \tag{4.3}$$

The necessity of adding a (negative) constant to the usual linear confining potential was shown in [70], from the nonrelativistic limit of the Bethe-Salpeter equation. There it was emphasized that c is a parameter which is as fundamental and indispensable as the quark masses, slope of the linear potential b, and the strong coupling constant α_s.[3]

One can find many papers[4] in the literature which use the above model with or without relativistic corrections (e.g., the spin-orbit and color hyperfine interaction), which are completely specified in terms of quark masses and parameters of $V_{conf}(r)$ and $V_{oge}(r)$, with the fixed effective or with some sort of running coupling constant. For the sake of simplicity, we use an effective short range coupling constant.

As one can see from (4.1), (4.2) and (4.3), in order to completely specify the model, which in our case should be able to reproduce spin-averaged heavy-light meson states, we need seven parameters:[5] four constituent quark masses, i.e., $m_{u,d}, m_s, m_c$ and m_b, strong coupling constant α_s, and two parameters specifying the confining part of the potential, b and c. There is little one can say about quark masses or α_s, since these are expected to run as one goes from the light-light to the heavy-light and heavy-heavy systems. These parameters are usually determined from the spectrum of states which one needs. However,

[3]Under additional assumptions an even stronger result $c \simeq -2\sqrt{b}\exp(-\gamma_E + 1/2)$ was obtained in [70]. We shall, however, consider c as an independent parameter.

[4]References [65–69,71–74] are just a few of them. Probably the most ambitious and the most sophisticated version of the model is due to Godfrey and Isgur [68].

[5]We assume that the u and d quarks have the same mass.

we can try to constrain the confining part of the potential so that the model is at least self-consistent in the light-light and the heavy-light limits.

4.2.2 Regge Structure

Let us first consider the effective string tension b. It is a well known experimental fact that all light-quark hadrons lie upon linear Regge trajectories with a universal slope [75]. While it may have been already pointed out in the past [59–64] we would like to reemphasize here the relation between linear trajectories, linear confinement, and relativistic dynamics. It seems inescapable that massless quarks bound by a linear confinement potential generate a family of parallel linear Regge trajectories, whose slopes depend on the Lorentz nature and other properties of the interaction.

The leading Regge slope follows from the correspondence (classical) limit. The lowest energy state of (4.1) for a given large angular momentum results for circular orbits at large r and p. The minimal energy condition $\frac{\partial H}{\partial r}\Big|_L \equiv 0$ implies that $(p_r \to 0,\ p \to L/r)$

$$Lp(\frac{1}{E_{\bar{q}}} + \frac{1}{E_Q}) = br^2 \ , \tag{4.4}$$

where $E_{\bar{q}} = \sqrt{p^2 + m_{\bar{q}}^2}$ and $E_Q = \sqrt{p^2 + m_Q^2}$. For a light-light meson $m_{\bar{q},Q} \to 0$, $E_{\bar{q},Q} \to p$, and hence (4.4) gives $2L = br^2$. This, together with $H \to 2L/r + br$, implies that the Regge slope is given by [64]

$$\alpha'_{LL} = \frac{L}{H^2} = \frac{1}{8b} \ . \tag{4.5}$$

Combining (4.5) with the observed slope of the leading ρ trajectory [31,75],

$$\alpha'^{exp}_{LL} = 0.88\ GeV^{-2} \ , \tag{4.6}$$

Table 4.1: Parameters of the confining part of the potential used in several papers which employed the relativistic generalization of the Schrödinger equation (SSEQ) given in (4.1), with the same type of the confining potential (4.3). The one-gluon-exchange potentials used in these papers are not necessarily the same as (4.2). Reference [72] used two different values for c for description of D and B mesons. To obtain the universal Regge slope SSEQ requires $b = 0.142\ GeV^2$, while the range of the c values for which this model is consistent with HQET sum rules depends on other parameters and assumptions of the model.

Author(s)	Reference	$b\ [GeV^2]$	$-c\ [MeV]$
Durand and Durand (1984)	[67]	0.180	0
Godfrey and Isgur (1985)	[68]	0.180	253
Jacobs et al. (1986)	[69]	0.192	0
Lucha et al. (1992)	[71]	0.211	850
Fulcher et al. (1993)	[72]	0.191	246 (214)
Fulcher (1994)	[73]	0.219	175
Hwang and Kim (1996)	[74]	0.183	0

we see that, in order for the model to be consistent with experiment in the light-light limit, we have to require

$$b = 0.142\ GeV^2\ . \tag{4.7}$$

This requirement is often overlooked in the literature,[6] and b is usually fixed to be about $0.18\ GeV^2$ (or slightly larger, see Table 4.1 for a few examples), which is a value suitable for models with the Nambu string slope of $\alpha'_{LL} = 1/(2\pi b)$ (e.g., flux tube models [76–78]).

A similar result for the effective string tension b can also be obtained from

[6] A most recent example is Ref. [74]. There (4.1) was used with several different potentials, and they were all inconsistent with the Regge structure of the model in the light-light limit.

the Regge behavior of the model in the heavy-light limit, since it is expected that the Regge slope for the energy of the light degrees of freedom is twice the slope for the light-light case [64], i.e., $\alpha'_{HL} = 2\alpha'_{LL}$. Indeed, in our case for a heavy-light meson we have $E_Q \to m_Q \to \infty$ and $E_{\bar{q}} \to p$ ($m_{\bar{q}} \to 0$), and hence (4.4) gives $L = br^2$. Together with $H \to m_Q + L/r + br$, this yields

$$\alpha'_{HL} = \frac{L}{(H - m_Q)^2} = \frac{1}{4b} \ . \tag{4.8}$$

We should also note that the results (4.6) and (4.8) depend on the nature of the confining potential used with (4.1), and that the above arguments cannot be used with models which do not exhibit linear Regge behavior (e.g., nonrelativistic quark model).

4.2.3 HQET Sum Rules

Let us now consider the heavy-light limit of (4.1),

$$H \stackrel{m_Q \to \infty}{\longrightarrow} m_Q + \sqrt{m_{\bar{q}}^2 + p^2} + V(r) \ . \tag{4.9}$$

It is clear that in this case the constant c can be absorbed into the heavy quark mass by $m_Q \to m_Q - c$, and that the heavy-light spin-averaged meson spectrum by itself does not contain enough information to determine c. However, additional constraints on the value of c can be obtained from the Bjorken [22,23] and Voloshin [24] sum rules.

These two sum rules involve inelastic form factors ξ_E and ξ_F for the semileptonic S to P-wave B (or B_s) decays, and are given in (2.49) and (2.51), respectively. As already mentioned in Chapter 2, the sums in these two equations are to be understood in a generalized sense, as sums over discrete states and

integrals over continuum states. Since bound state models we are considering cannot say anything about continuum contributions to the Bjorken and Voloshin sum rules, and since all contributions to the sums of (2.49) and (2.51) are positive definite, one can argue that resonant contributions to the right-hand sides of (2.49) and (2.51) should be smaller than the direct model calculation of $-\xi_C'(1)$, and $1/2$, respectively, if a given model is to be consistent with these two sum rules. This is in fact the key argument of the sum rule part of the model analysis.

In Chapter 3 we have found, in the valence quark approximation, precise definitions of the form factors which appear in (2.49) and (2.51). These are given in terms of the wave functions and energies of the LDF [42]. The relevant expressions are for $\xi_C'(1)$, $\xi_E(1)$ and $\xi_F(1)$, and are given in (3.39), (3.41) and (3.44), respectively. Since the model we are considering is spinless, the E and F doublets are degenerate and relation (3.50) holds. Using (3.41) and (3.44), one can simplify the expressions for both sum rules. The Bjorken sum rule (2.49) in the spinless case becomes

$$-\xi_C'(1) \geq \frac{1}{4} + \frac{1}{12}\sum_i \left[(E_C + E_{E,F}^{(i)})\langle r\rangle_{10}^{(i)}\right]^2 \ , \tag{4.10}$$

while the Voloshin sum rule (2.51) is given by

$$\frac{1}{2} \geq \frac{1}{12}\sum_i (\frac{E_{E,F}^{(i)}}{E_C} - 1)\left[(E_C + E_{E,F}^{(i)})\langle r\rangle_{10}^{(i)}\right]^2 \equiv \Delta \ . \tag{4.11}$$

In these two equations the sums are only over resonances, since we are neglecting continuum contributions.

To understand the essence of the sum rule constraint, we first consider a slightly oversimplified example. Assuming that non-resonant contributions are

small, the equality sign holds in (4.10) and (4.11). If we also assume that the sums in these two equations are saturated by the lowest P-wave doublets, then (4.10) and (4.11) imply

$$-\xi_C' \simeq \frac{1}{4} + \frac{1}{12}(2E_C + \Delta E)^2 \langle r \rangle_{10}^2 \ , \tag{4.12}$$

$$\frac{1}{2} \simeq \frac{1}{12}\frac{\Delta E}{E_C}(2E_C + \Delta E)^2 \langle r \rangle_{10}^2 \ . \tag{4.13}$$

In the above equations we have written $E_{E,F}^{(1)} = E_C + \Delta E$, where ΔE is just the difference between the spin-averaged masses of the S-wave and the lowest P-wave doublet.[7] From (4.13) one obtains

$$(2E_C + \Delta E)^2 \langle r \rangle_{10}^2 \simeq 6\frac{E_C}{\Delta E} \ . \tag{4.14}$$

Using the above expression in (4.12), together with the bound $-\xi_C'(1) \geq 1/2$ from (3.39), we find

$$E_C \geq \frac{1}{2}\Delta E \ . \tag{4.15}$$

This implies that energy of the LDF in the lowest S-wave mesons cannot be smaller than one half of the difference between spin-averaged masses of the lowest P-wave and the S-wave. In particular, this would also set a lower bound on the constant c, which is usually assumed to be negative, or an upper bound on the constituent heavy quark masses, since the energy of the LDF is defined as the state mass minus the heavy quark mass.

We now go back to the model analysis of (4.10) and (4.11). As already mentioned, for the description of heavy-light mesons we need seven parameters.

[7] If one assumes that the spin-averaged mass of the lowest (E, E^*) doublet in the D systems (corresponding to D_0 and D_1 mesons), is about 2350 MeV, then this difference is about 440 MeV.

We have already determined the effective string tension b from the consistency of the model with the experimental Regge slopes of light-light mesons. In order to determine all other parameters except c, we can use the observed heavy-light spectrum. Any change in c effectively just changes the constituent heavy quark masses by the same amount, and an equivalent description of the spectrum is obtained. It is also evident that the heavy-light wave functions are not affected by this change. However, changing c does affect the energies of the LDF in the heavy-light mesons. This in turn affects the form factors predicted by the model. The idea is that by examining the model predictions for the right-hand sides of (4.10) and (4.11), one can determine physically acceptable values of c, and other parameters of the model. As explained earlier, the main requirement here is self-consistency of the model in the sense that its predictions for the right-hand sides of (4.10) and (4.11) yield results which are smaller than its direct calculation of $-\xi_C'(1)$, and $1/2$, respectively. However, in order to account for all possible uncertainties in our calculations (e.g., effects of spin-averaging of meson masses, assumption of the unknown P-wave masses, etc.), we shall relax these constraints by 5%. This means that the sum rule calculation of Δ should yield result smaller than 0.525 (instead of 0.5), and that the sum rule calculation of $-\xi_C'(1)$ should yield result which is at most 5% larger than the result obtained from the direct calculation. In this way a more conservative bounds on c will be obtained.

In order to illustrate the above ideas, we consider two sets of parameters:

- Set 1: we fix $c = 0$ and $m_{u,d} = 350\ MeV$, and a fit to the spin-averaged heavy-light meson spectrum yields $m_s = 542\ MeV$, $m_c = 1366\ MeV$,

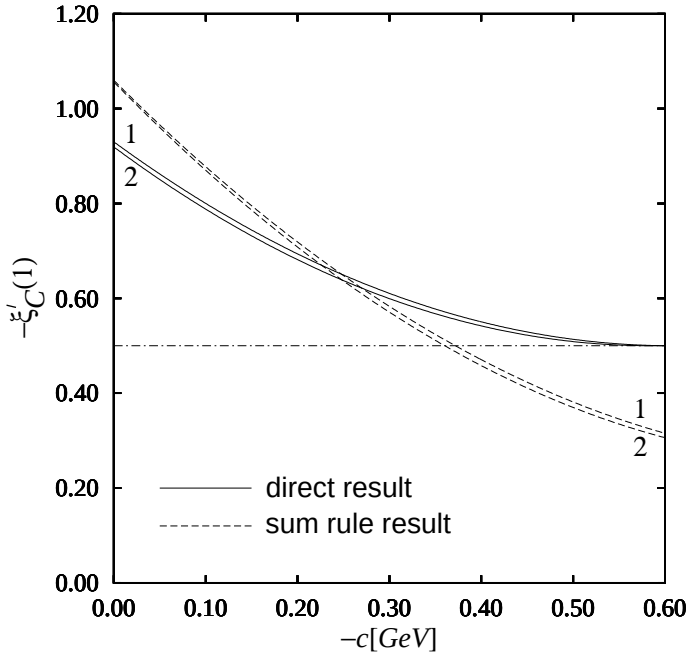

Figure 4.1: Comparison of the SSEQ direct calculation of $-\xi'_C(1)$ (full lines) with the Bjorken sum rule result, obtained with 15 lowest P-wave states (dashed lines). 1 and 2 denote the two different sets of parameters, as explained in the text. The dotted line is the bound $-\xi'_C(1) \geq \frac{1}{2}$ coming from (3.39). The results shown are for $B \to D, D^*$ semileptonic decays.

$m_b = 4703\ MeV$, and $\alpha_s = 0.390$.

- Set 2: we fix $c = 0$ and $m_{u,d} = 300\ MeV$, and from the fit to the heavy-light data we obtain $m_s = 503\ MeV$, $m_c = 1390\ MeV$, $m_b = 4726\ MeV$, and $\alpha_s = 0.390$.

For both of these two sets we used $b = 0.142\ GeV^2$ from (4.7), and both of them yield an excellent description of the known heavy-light (spin-averaged) meson masses, with errors less than $5\ MeV$.[8] Using the parameters which

[8]We have assumed that the D_0 ($0^+_{1/2}$ state) and D_1 ($1^+_{1/2}$ state) mesons have a spin-averaged mass of $2350\ MeV$, which together with the known P-waves $D_1(2425)$ and

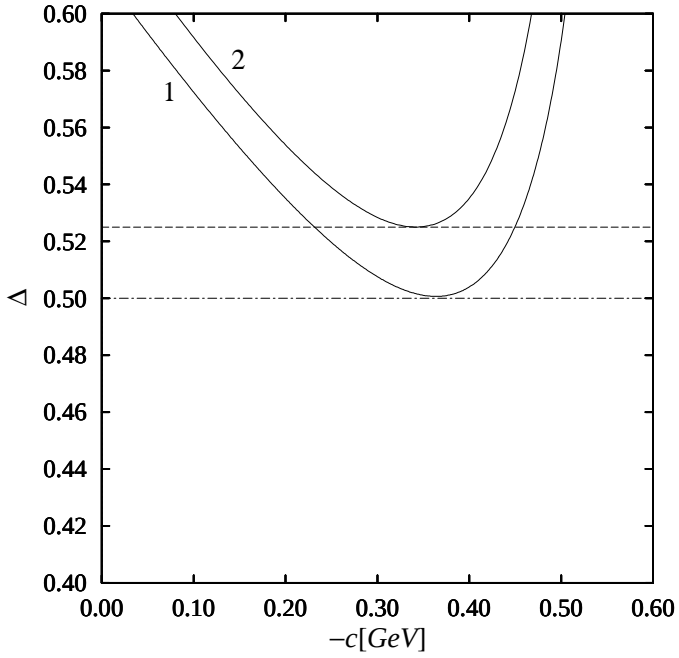

Figure 4.2: SSEQ Voloshin sum rule calculation of Δ with 15 lowest P-wave states (full lines), for the two different sets of parameters 1 and 2. The expected upper bound of 0.5, and the 5% relaxed bound of 0.525 are shown with the dotted and dashed line, respectively. These results are for $B \to D, D^*$ semileptonic decays.

reproduce spin-averaged data, and also an effective string tension consistent with experiment, gives us confidence that the unknown spin-averaged meson masses for radial excitations are reproduced reasonably well.

For both of these two sets, and for c ranging from 0 to $-600\ MeV$, we have evaluated $-\xi'_C$ directly using (3.39). Using 15 lowest P-waves we have also evaluated the right-hand sides of (4.10) and (4.11). The results of our calculations (for $B \to D, D^*$ semileptonic decays) are shown in Figures 4.1

$D_2^*(2459)$ leads to the spin-averaged mass of 2414 MeV for the lowest P-wave in the D systems. Heavy quark symmetry arguments then imply a spin-averaged mass of 2523 MeV for the corresponding lowest P-wave in the D_s systems.

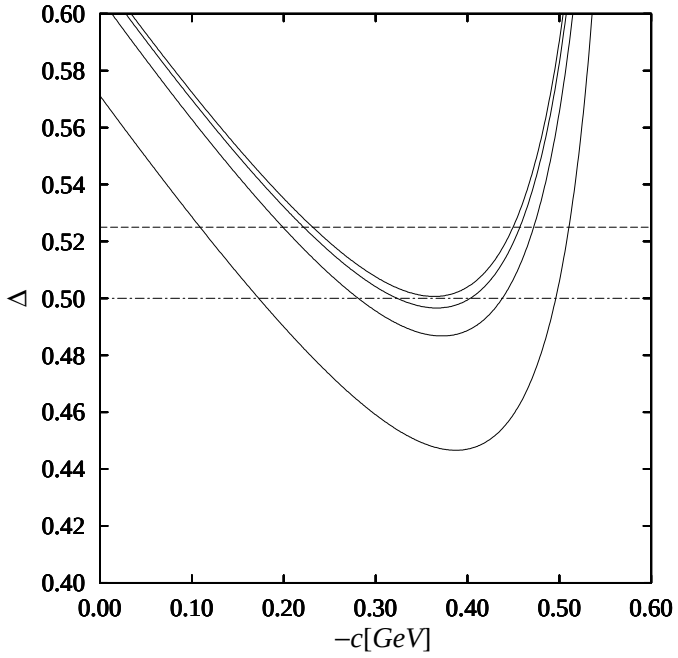

Figure 4.3: Convergence of the SSEQ Voloshin sum rule evaluation of Δ (for $B \to D, D^*$ semileptonic decays). Plotted with full lines are calculations done with 1, 5, 10, and with 15 lowest P-wave states, for parameter set 1. The expected upper bound of 0.5, and the 5% relaxed bound of 0.525 are shown with the dotted and dashed line, respectively.

(for the Bjorken sum rule) and 4.2 (for the Voloshin sum rule). As one can see in Figure 4.1, both sets of parameters can satisfy the Bjorken sum rule in the sense that the direct calculation of $-\xi'_C(1)$ yields larger result than the sum rule approach. Imposing weaker requirement, i.e., that the sum rule result is at most 5% larger than the direct result, for both sets we find $c \leq -185\ MeV$. We also note that for this value of c, $-\xi'_C(1) \simeq 0.71$ (for set 1) and $-\xi'_C(1) \simeq 0.70$ (for set 2). With the Voloshin sum rule (Figure 4.2) the situation is completely different. The minimum of $\Delta(c)$ for the parameter set 2 is slightly larger than 0.525 for $c = -0.342$, so that parameters from this set cannot satisfy even the weaker constraint $\Delta \leq 0.525$. On the other hand, for the set 1

minimum of $\Delta(c)$ is 0.501, and it occurs for $c = -364\ MeV$.[9] Imposing the requirement $\Delta \leq 0.525$ we find $235\ MeV \leq -c \leq 445\ MeV$. In order to illustrate convergence of the two sum rules, in Figure 4.3 we show SSEQ Voloshin sum rule calculations of Δ done with parameter set 1, which included 1, 5, 10, and 15 P-wave resonances.[10]

Therefore, in the two cases considered, we found the Voloshin sum rule being more restrictive than the Bjorken sum rule. Imposing the weaker constraint $\Delta \leq 0.525$, we also found that model is self-consistent with parameter set 1, with

$$235\ MeV \leq -c \leq 445\ MeV\ . \tag{4.16}$$

These values of c imply $1601\ MeV \leq m_c \leq 1811\ MeV$, and $4938\ MeV \leq m_b \leq 5148\ MeV$.

We have also repeated the sum rule calculations for the $B_s \to D_s, D_s^*$ semileptonic decays with the same sets of parameters (the difference is basically only the light quark mass), and found that these decays are much less restrictive than $B \to D, D^*$ decays. The same happens for all models investigated in this chapter.

For the SSEQ calculation of semileptonic B decays in Chapter 5 we choose

[9]It is also interesting to observe that the minimum of the function $\Delta(c)$ always occurs close to the point at which Bjorken sum rule approach yields $-\xi_C'(1) = 1/2$. This can be shown analytically from (4.12) and (4.13), and can be seen from Figures 4.1 and 4.2. However, this is not necessarily the case with models based on the Dirac (or Salpeter) equation.

[10]Due to factors involving energies of the LDF in (4.11), the Voloshin sum rule converges slower than the Bjorken sum rule. This can be clearly seen in Table 4.2.

Table 4.2: Sum rule contributions of different P-wave states to $-\xi_c'(1)$ (R_ξ) and Δ (R_Δ). E and F denote the ground state P-wave, E_2 and F_2 the first radial excitation, etc. SSEQ parameters are given in (4.17). Expected results are $-\xi_C'(1) = 0.590$ and $\Delta = 0.5$, while the sum rule results (using 15 P-wave states) are $-\xi_C'(1) = 0.547$ and $\Delta = 0.503$.

State	$M_{E,F}$ $[MeV]$	$\xi_E(1)$	$\xi_F(1)$	R_ξ [%]	R_Δ [%]
E, F	2416	0.616	0.534	90.68	90.52
E_2, F_2	2750	0.072	0.062	0.64	2.16
E_3, F_3	3028	0.078	0.067	0.78	3.44
E_4, F_4	3269	0.037	0.032	0.17	0.94
E_5, F_5	3485	0.034	0.030	0.15	0.96
E_6, F_6	3682	0.024	0.020	0.07	0.50
E_7, F_7	3864	0.021	0.019	0.05	0.48
E_8, F_8	4034	0.017	0.015	0.03	0.32
E_9, F_9	4194	0.015	0.013	0.03	0.28
E_{10}, F_{10}	4346	0.013	0.011	0.02	0.18
E_{11}, F_{11}	4491	0.012	0.010	0.02	0.20
E_{12}, F_{12}	4629	0.011	0.009	0.01	0.16
E_{13}, F_{13}	4762	0.010	0.009	0.01	0.14
E_{14}, F_{14}	4890	0.009	0.008	0.01	0.12
E_{15}, F_{15}	5013	0.008	0.007	0.00	0.12
			total	92.67	100.52

parameters corresponding to $c = -330\ MeV$, which are given as

$$\begin{aligned} m_{u,d} &= 0.350\ GeV\ , \\ m_s &= 0.542\ GeV\ , \\ m_c &= 1.696\ GeV\ , \\ m_b &= 5.033\ GeV\ , \\ \alpha_s &= 0.390\ , \\ b &= 0.142\ GeV^2\ , \\ c &= -0.330\ GeV\ . \end{aligned} \tag{4.17}$$

The chosen value for c is well within the range given in (4.16) and close to the minimum of $\Delta(c)$. Model with the above parameters yields the zero-recoil slope of $\xi'_C \simeq -0.59$.[11] In Table 4.2 we show sum rule contributions of different P-wave states to $-\xi'_c(1)$ and Δ. SSEQ predictions for the spin-averaged heavy-light masses, obtained with parameters given in (4.17), can be found in Table 4.3. Note that the energy of the LDF in the S-wave (C, C^*) heavy-light meson corresponding to the above value of c is about $280\ MeV$, which is within the allowed range of values for E_C obtained in [56] from the analysis of recent data on semileptonic B decays, and using the $1S$ lattice QCD heavy-light wave function from [57].[12]

The most serious concern which one might have about our sum rule analysis of SSEQ, is the issue of degeneracy of the two P-wave doublets, which is due to the spinless nature of this particular model.[13] While it is certainly true that

[11] Experimental result for the form factor $\hat{\xi}_C$ (which in the absence of the symmetry breaking corrections would be the Isgur-Wise function ξ_C), is $-\hat{\xi}'_C(1) = 0.84 \pm 0.12 \pm 0.08$ [52].

[12] In [56] it was found that $266\ MeV \leq E_C \leq 346\ MeV$.

[13] For models based on the Dirac or Salpeter equation this issue vanishes, since these

the uncertainties introduced in this way should partly cancel out (due to spin-averaging, contributions of some states to sum rules will be overestimated, and for other states they will be underestimated), we have still tried to account for possible theoretical errors by relaxing the sum rule constraints by 5%. Also note that including more radially excited states would yield more strict bounds on the acceptable values of c, than is the one we quote for the parameter set 1. Given all that, we believe that (4.16) represents reasonably conservative estimate. This conclusion is also supported by the comparison of the values for E_C obtained here with the ones obtained in [56].

4.3 Relativistic Flux Tube Model (RFTM)

The relativistic flux tube model is in essence a description of dynamical confinement. Its basic assumption of is that the QCD dynamical ground state for large quark separation consists of a rigid, straight, tubelike color flux configuration connecting the quarks. The classical Lagrangian and the corresponding equations of motion have been known for a long time [76], but quantum-mechanical version of the model has been developed only recently [77,78]. It should also be mentioned that spinless RFTM follows directly from the QCD Lagrangian, with natural approximations to the Wilson action [79,80].

In the heavy-light limit, the RFTM Hamiltonian is given by [78]

$$H = m_Q + \frac{1}{2}\{W_r, \gamma_\perp\} + \frac{b}{2}\{r, \frac{\arcsin v_\perp}{v_\perp}\} + c + V_{oge}(r) \ . \qquad (4.18)$$

models distinguish between (E, E^*) and (F, F^*) doublets. Because of that, sum rule analysis of these models should be more reliable than the one appropriate for the spinless models.

In the above we defined $\{A, B\} = AB + BA$, and

$$W_r = \sqrt{p_r^2 + m_{\bar{q}}^2} \, , \tag{4.19}$$

$$p_r^2 = -\frac{1}{r}\frac{\partial^2}{\partial r^2} r \, , \tag{4.20}$$

$$\gamma_\perp = \frac{1}{\sqrt{1 - v_\perp^2}} \, . \tag{4.21}$$

The one-gluon-exchange interaction is given in (4.2). For a state with orbital angular momentum L, the unknown operator $v_\perp$ can be determined by solving the corresponding quantized angular momentum equation [78]

$$\frac{\sqrt{L(L+1)}}{r} = \frac{1}{2}\left\{W_r, \gamma_\perp v_\perp\right\} + b\left\{r, f(v_\perp)\right\} \, , \tag{4.22}$$

where

$$f(v_\perp) = \frac{1}{4v_\perp}\left(\frac{\arcsin v_\perp}{v_\perp} - \frac{1}{\gamma_\perp}\right) \, . \tag{4.23}$$

We note that the short distance interaction (expected from QCD) and the constant c in (4.18) are not part of the flux tube configuration, and are added phenomenologically [78].

In [55] RFTM has already been used for calculation of the IW function for semileptonic $B \to D, D^*$ decays. However, constant c from (4.18) was in that paper simply absorbed into the heavy quark mass. Here we perform the analysis analogous to the one described in Section 4.2, in order to determine the allowed range for c.

It is not hard to show [78] that RFTM exhibits linear Regge behavior with the slope

$$\alpha'_{HL} = \frac{1}{\pi b} \, , \tag{4.24}$$

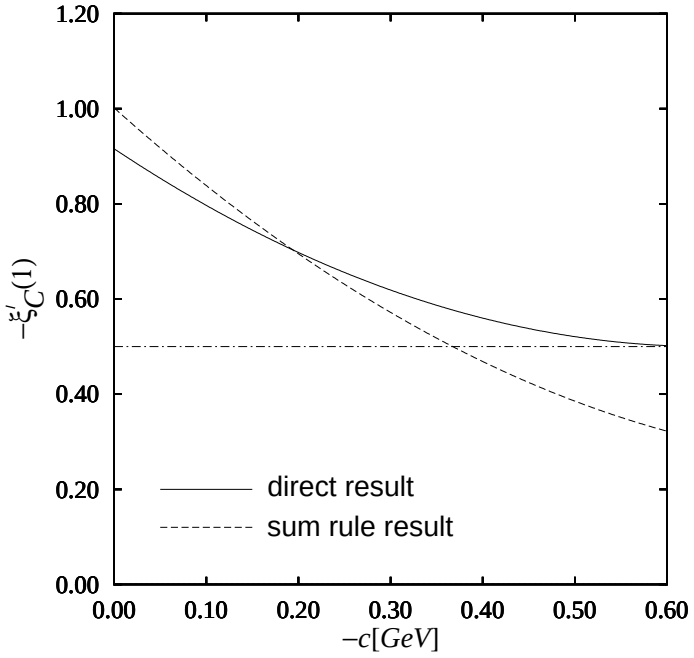

Figure 4.4: RFTM calculation of $-\xi'_C(1)$ (full line) for $B \to D, D^*$ semileptonic decays. Bjorken sum rule result is shown with the dashed line. The dotted line is the bound $-\xi'_C(1) \geq \frac{1}{2}$ coming from (3.39).

which is exactly twice the slope obtained from the model in the light-light limit. When combined with (4.6), the above equation implies

$$b = 0.181 \ GeV^2 \ . \tag{4.25}$$

Fixing the string tension to 0.181 GeV^2, and choosing $m_{u,d} = 300 \ MeV$, we find that in order to reproduce the spin-averaged heavy-light spectrum[14] we need (with $c = 0$) $m_s = 507 \ MeV$, $m_c = 1332 \ MeV$, $m_b = 4668 \ MeV$, and $\alpha_s = 0.390$. With these parameters, we have evaluated $-\xi'_C$ for semileptonic $B \to D$ and $B \to D^*$ decays directly, using (3.39). As before, we have also

[14] As in the case of SSEQ, we assumed that D_0 ($0^+_{1/2}$ state) and D_1 ($1^+_{1/2}$ state) have spin-averaged mass of 2350 MeV.

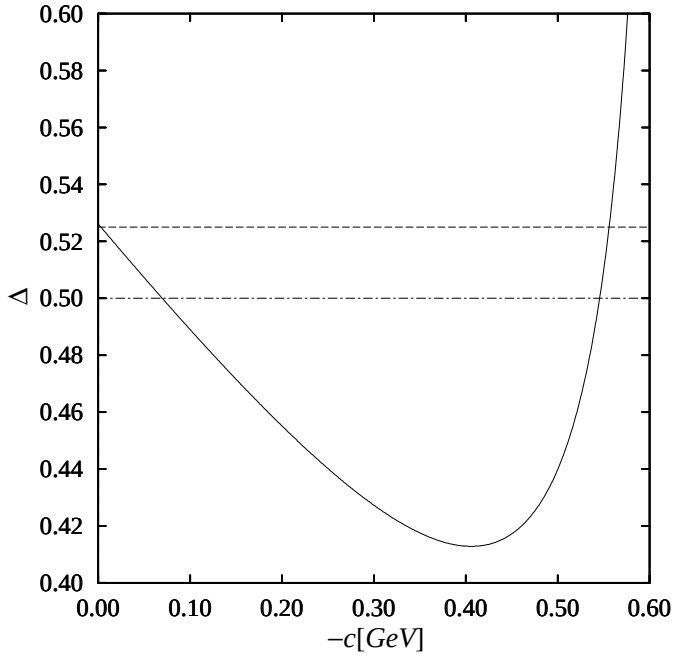

Figure 4.5: RFTM Voloshin sum rule calculation of Δ (full line) for $B \to D, D^*$ semileptonic decays. The expected upper bound of 0.5, and the 5% relaxed bound of 0.525 are shown with the dotted and dashed line, respectively.

evaluated the right-hand side of the Bjorken sum rule (4.10), with the lowest 15 P-wave resonances (Figure 4.4). If we impose the weaker requirement that the sum rule result can be at most 5% larger than the one obtained from the direct calculation, then we find that c has to be smaller than $-110\ MeV$. On the other hand, calculation of Δ from the Voloshin sum rule (4.11) (shown in Figure 4.5) yields $5\ MeV \leq -c \leq 555\ MeV$ as the allowed range for c (with the 5% weaker constraint). One should observe though that this model can easily satisfy the strong requirements, that the Bjorken sum rule result for $-\xi'_C(1)$ should be smaller than the one obtained from (3.39), and that the Voloshin sum rule result for Δ should be smaller than 0.5.[15] Unlike the case

[15]Imposing those constraints we would get $195\ MeV \leq -c \leq 545\ MeV$.

of SSEQ, where both bounds on c came from the Voloshin sum rule, in this case the Bjorken sum rule provides the upper bound on c, while the Voloshin sum rule gives the lower bound, so that we have

$$110\ MeV \leq -c \leq 555\ MeV\ . \tag{4.26}$$

This range of allowed values of c is twice as wide as the one we found for SSEQ. For the heavy quark masses this result implies $1442\ MeV \leq m_c \leq 1887\ MeV$, and $4778\ MeV \leq m_b \leq 5223\ MeV$. We emphasize again that (4.26) should be considered as a conservative estimate, since imposing the stronger constraints, and also including more P-wave states, would lead to a slightly narrower range for allowed values of c. As in the case of SSEQ, semileptonic $B_s \to D_s, D_s^*$ decays were found to be less restrictive than corresponding B decays from which the above results were obtained.

For the calculation of semileptonic B decays, which will be presented in Chapter 5, we choose parameters corresponding to $c = -200\ MeV$, so that

$$\begin{aligned} m_{u,d} &= 0.300\ GeV\ , \\ m_s &= 0.507\ GeV\ , \\ m_c &= 1.532\ GeV\ , \\ m_b &= 4.868\ GeV\ , \\ \alpha_s &= 0.390\ , \\ b &= 0.181\ GeV^2\ , \\ c &= -0.200\ GeV\ . \end{aligned} \tag{4.27}$$

It can be seen in Figures 4.4 and 4.5 that model with these parameters satisfies the stronger requirements for both sum rules, and also gives $-\xi_C' \simeq 0.70$. With

Table 4.3: SSEQ and RFTM predictions for the spin-averaged heavy-light meson masses. Model parameters are given in (4.17) for SSEQ, and in (4.27) for RFTM. We have assumed that the unknown D_0 and D_1 mesons ($0^+_{1/2}$ and $1^+_{1/2}$ states) have spin-averaged mass of 2350 MeV. Heavy quark symmetry arguments then lead to the spin-averaged mass of 2452 MeV for the corresponding D_{s0} and D_{s1} mesons. Errors for both models are shown in brackets.

Meson	State	Mass $[MeV]$	SSEQ $[MeV]$	RFTM $[MeV]$
$D(1867)$	$0^-_{1/2}$	$1S(1974)$	$1974(+0)$	$1976(+2)$
$D^*(2009)$	$1^-_{1/2}$			
$D_0(\sim 2350)$	$0^+_{1/2}$	$1P(2414)$	$2416(+2)$	$2413(-1)$
$D_1(\sim 2350)$	$1^+_{1/2}$			
$D_1(2425)$	$1^+_{3/2}$			
$D^*_2(2459)$	$2^+_{3/2}$			
$D_s(1969)$	$0^-_{1/2}$	$1S(2076)$	$2075(-1)$	$2074(-2)$
$D^*_s(2112)$	$1^-_{1/2}$			
$D_{s0}(\sim 2452)$	$0^+_{1/2}$	$1P(2523)$	$2521(-2)$	$2524(+1)$
$D_{s1}(\sim 2452)$	$1^+_{1/2}$			
$D_{s1}(2535)$	$1^+_{3/2}$			
$D^*_{s2}(2573)$	$2^+_{3/2}$			
$B(5279)$	$0^-_{1/2}$	$1S(5314)$	$5311(-3)$	$5313(-1)$
$B^*(5325)$	$1^-_{1/2}$			
$B_s(5374)$	$0^-_{1/2}$	$1S(5409)$	$5412(+3)$	$5410(+1)$
$B^*_s(5421)$	$1^-_{1/2}$			

this value of c the LDF energy in the S-wave heavy-light mesons is 445 MeV, which is about 100 MeV above the range obtained in [56]. RFTM results for the spin-averaged heavy-light states (obtained with parameters given above) are compared to experiment in Table 4.3.

4.4 Salpeter Equation with Vector Confinement (SEVC)

The instantaneous version of the Bethe-Salpeter equation [81,82] (usually referred to as the Salpeter equation [83]) is widely used for the discussion of bound state problems. It is also equivalent [84] to the so called "no-pair" equation [85], which was introduced in order to avoid the problem of mixing of positive and negative energy states that occurred in the Dirac equation for the helium atom. A similar problem also occurs for a single fermionic particle moving in the confining Lorentz vector potential. For a very long time [86] it has been known that there are no normalizable solutions to the Dirac equation in this case.

It has been shown analytically for the heavy-light case [53], and numerically for the case of fermion and antifermion with arbitrary mass [87,88], that in this type of model linear scalar confinement does not yield linear Regge trajectories. Because of that, in this section we investigate the time component vector confinement with short range Coulomb interaction, even though it is well known that this model gives the wrong sign of the spin-orbit coupling. The flux tube model based on the Salpeter equation (SFTM) will be discussed

in Section 4.5, while the Salpeter equation with a half-half mixture of vector and scalar confinement (SVSC) will be investigated in Section 4.6.

The Hamiltonian for the heavy-light Salpeter equation with vector confinement is given by [53]

$$H = m_Q + H_{\bar{q}} + \Lambda_+ V(r) \Lambda_+ \ . \tag{4.28}$$

In the above, $H_{\bar{q}}$ is the free particle Dirac Hamiltonian,

$$H_{\bar{q}} = \gamma^0 \boldsymbol{\gamma} \cdot \boldsymbol{p} + \gamma^0 m_{\bar{q}} \ , \tag{4.29}$$

while $V(r) = V_{oge}(r) + V_{conf}(r)$ is the time component vector interaction, with $V_{oge}(r)$ and $V_{conf}(r)$ being specified in (4.2) and (4.3), respectively. The positive energy projection operator Λ_+ is defined as ($E_{\bar{q}} = \sqrt{\boldsymbol{p}^2 + m_{\bar{q}}^2}$)

$$\Lambda_+ = \frac{E_{\bar{q}} + H_{\bar{q}}}{2E_{\bar{q}}} \ . \tag{4.30}$$

In [53] it was shown that this model exhibits linear Regge behavior with the slope

$$\alpha'_{HL} = \frac{1}{4b} \ , \tag{4.31}$$

which, together with (4.6), implies the same effective string tension as in the case of SSEQ, i.e.,

$$b = 0.142 \ GeV^2 \ . \tag{4.32}$$

For models based on the Dirac (or Salpeter) equation, the sum rule part of the analysis is slightly different from the one described in Section 4.2. As explained in Section 3.5, in these models the two P-wave doublets are not

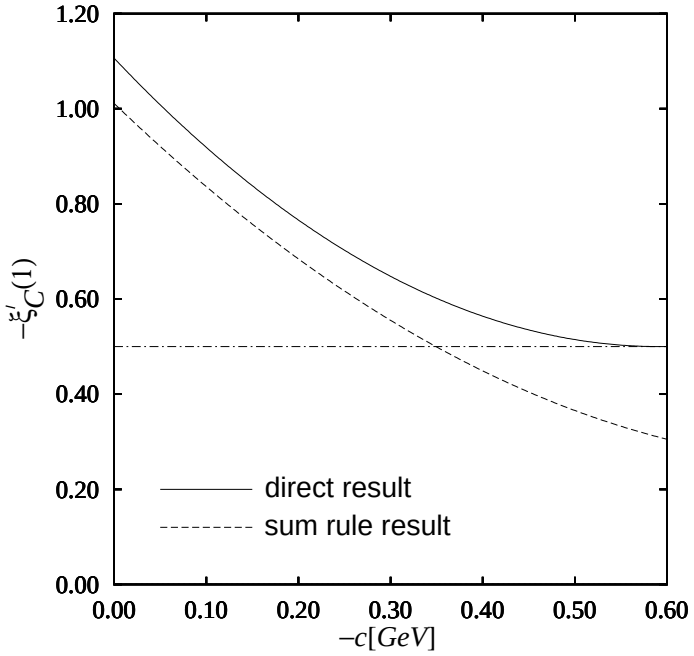

Figure 4.6: SEVC calculation of $-\xi'_C(1)$ (full line) for $B \to D, D^*$ semileptonic decays. The Bjorken sum rule result is shown with the dashed line. The dotted line is the bound $-\xi'_C(1) \geq \frac{1}{2}$ coming from (3.39).

degenerate. Instead of (4.10), by using (3.41) and (3.44), and neglecting continuum contributions to (2.49), we find

$$\begin{aligned} -\xi'_C(1) &\geq \frac{1}{4} + \frac{1}{36}\sum_i \left[(E_C + E_E^{(i)})\langle r\rangle^{(i)}_{\frac{1}{2}\frac{1}{2}}\right]^2 \\ &+ \frac{1}{18}\sum_j \left[(E_C + E_F^{(j)})\langle r\rangle^{(j)}_{\frac{3}{2}\frac{1}{2}}\right]^2 , \end{aligned} \tag{4.33}$$

while instead of (4.11) we obtain

$$\begin{aligned} \frac{1}{2} &\geq \frac{1}{36}\sum_i (\frac{E_E^{(i)}}{E_C} - 1)\left[(E_C + E_E^{(i)})\langle r\rangle^{(i)}_{\frac{1}{2}\frac{1}{2}}\right]^2 \\ &+ \frac{1}{18}\sum_j (\frac{E_F^{(j)}}{E_C} - 1)\left[(E_C + E_F^{(j)})\langle r\rangle^{(j)}_{\frac{3}{2}\frac{1}{2}}\right]^2 \equiv \Delta\ . \end{aligned} \tag{4.34}$$

Using the property $\Lambda_+\phi = \phi$ of the Salpeter wave function, it is not hard to

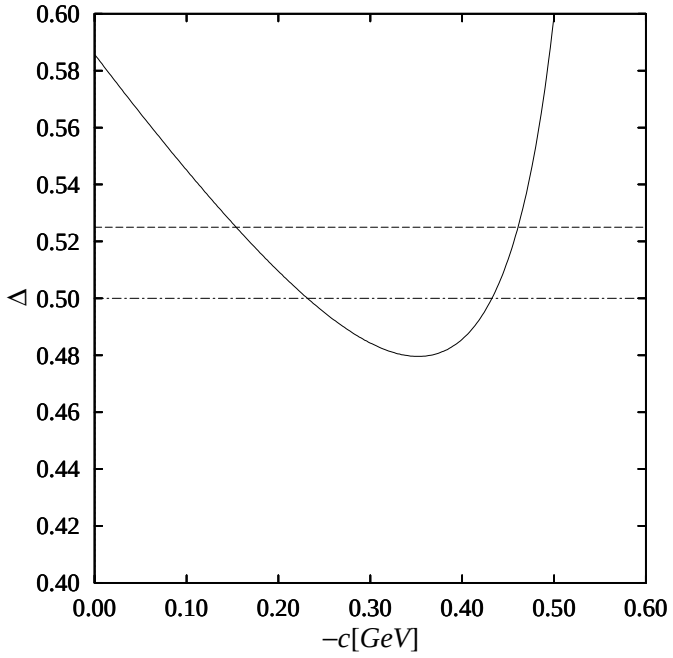

Figure 4.7: SEVC Voloshin sum rule calculation of Δ (full line) for $B \to D, D^*$ semileptonic decays. The expected upper bound of 0.5, and the 5% relaxed bound of 0.525 are shown with the dotted and dashed line, respectively.

show that in the SEVC model c again just renormalizes the heavy quark mass, as was the case with SSEQ and RFTM. Therefore, we can again choose $c = 0$, and determine other parameters of the model from the fit to the observed spin-averaged heavy-light meson states.[16] Fixing $m_{u,d} = 350\ MeV$ and $b = 0.142\ GeV^2$, from the heavy-light spectrum we find $m_s = 620\ MeV$, $m_c = 1387\ MeV$, $m_b = 4723\ MeV$, and $\alpha_s = 0.527$. We use these parameters for the sum rule analysis of the model.

[16]For models based on the Salpeter (or Dirac) equation we do not need additional assumptions for the mass of the unknown (E, E^*) doublet in the D-systems.

In Figure 4.6 we show comparison of the calculation of $-\xi'_C(1)$ (for semileptonic $B \to D, D^*$ decays) from (3.39), with the result obtained from the right-hand side of (4.33), using the five lowest P-wave states. There one can see that SEVC always satisfies the Bjorken sum rule. However, this is not the case with the Voloshin sum rule (Figure 4.7). Imposing 5% weaker requirements on sum rule calculations of Δ (i.e., $\Delta \leq 0.525$) yields[17]

$$155\ MeV \leq -c \leq 460\ MeV\ . \tag{4.35}$$

For the constituent heavy quark masses this result implies $1542\ MeV \leq m_c \leq 1847\ MeV$ and $4878\ MeV \leq m_b \leq 5183\ MeV$.

Following the same reasoning as before, we choose c so that model obeys the sum rule requirements. The choice of $-240\ MeV$ yields

$$\begin{aligned} m_{u,d} &= 0.350\ GeV\ , \\ m_s &= 0.620\ GeV\ , \\ m_c &= 1.627\ GeV\ , \\ m_b &= 4.963\ GeV\ , \\ \alpha_s &= 0.527\ , \\ b &= 0.142\ GeV^2\ , \\ c &= -0.240\ GeV\ . \end{aligned} \tag{4.36}$$

With these parameters we have the S-wave LDF energy of $350\ MeV$, and find $-\xi'_C(1) \simeq 0.71$, which is slightly above the range found in [56]. Model predictions for the spin-averaged heavy-light masses are given in Table 4.5.

[17] The uncertainties coming from spin-averaging of meson masses should be smaller for the Dirac-type models, since these distinguish between the E, E^* and F, F^* doublets. Nevertheless, in order to get a more conservative estimate on the value of c, we still impose a 5% weaker requirements on the sum rule calculations. Note that imposing the stronger requirements would, instead of (4.35), lead to $235\ MeV \leq -c \leq 430\ MeV$.

4.5 Flux Tube Model Based on the Salpeter Equation (SFTM)

The formalism for fermionic quark confinement in this model is unusual in that the confinement is introduced into the kinetic rather than the usual interaction term. The flux tube contributes to both energy and momentum, so it makes little sense to consider it as a potential-type interaction. By a covariant substitution [89] the tube is added to the quark momentum and energy. This may be viewed as a "minimal substitution" of a vector interaction field. The result nicely reduces to the Nambu string in the limit in which the quark moves ultra-relativistically. This physically motivated generalization of the potential model incorporates many aspects of QCD [54].

In [54] the flux tube four-momentum,

$$p_t^\mu = (H_t, \boldsymbol{p}_t) \ , \tag{4.37}$$

where $\boldsymbol{p}_t = (-\hat{\mathbf{r}} \times \hat{\mathbf{L}})p_t$ was quantized by symmetrization of the classical expressions [77,78], so that

$$H_t(r) = \frac{a}{2}\{r, \frac{\arcsin v_\perp}{v_\perp}\} \ , \tag{4.38}$$

$$p_t(r) = \frac{L_t}{r} = a\{r, f(v_\perp)\} \ . \tag{4.39}$$

Here, the function $f(v_\perp)$ is given in (4.23). These expressions were then introduced into the Salpeter equation by a "flux tube transformation" [89],

$$p^\mu \to p^\mu - p_t^\mu \ . \tag{4.40}$$

As in the case of RFTM, the short range interaction is not part of the flux tube configuration, and has to be added separately. The resulting Hamiltonian for the heavy-light systems can then be written in the form [54][18]

$$H = m_Q + H_{\bar{q}} + \Lambda_+[H_t(r) + c + V_{oge}(r) - \gamma^0 \boldsymbol{\gamma} \cdot \boldsymbol{p}_t]\Lambda_+ \ . \tag{4.41}$$

In the above $H_{\bar{q}}$ is the free Dirac Hamiltonian (4.29), and Λ_+ is defined in (4.30). We again take $V_{oge}(r) = -4\alpha_s/(3r)$. When (4.41) is reduced to the two radial equations, one ends up with the two unknown $v_\perp$ operators, one for each orbital angular momentum state in the Salpeter (or Dirac) wave function (3.51). These are determined from the corresponding orbital angular momentum equations, similar to (4.22) [54].

SFTM yields linear Regge trajectories with the heavy-light slope of [54]

$$\alpha'_{HL} = \frac{1}{\pi b} \ , \tag{4.42}$$

which is the same as in the case of spinless RFTM. This again implies

$$b = 0.181 \ GeV^2 \ . \tag{4.43}$$

Fixing $c = 0$ and $m_{u,d} = 350 \ MeV$, we determine other parameters of the model from the fit to the observed heavy-light spin-averaged states. This leads to $m_s = 604 \ MeV$, $m_c = 1331 \ MeV$, $m_b = 4667 \ MeV$, and $\alpha_s = 0.501$. With these parameters we perform the sum rule analysis of the model, using the five lowest P-wave states in (4.33) and (4.34). Results are shown in Figures 4.8 and 4.9, for the Bjorken and Voloshin sum rules, respectively. As in the case

[18] In [54] c was simply absorbed into the heavy quark mass. This can be done because Salpeter wave function satisfies $\Lambda_+\phi = \phi$.

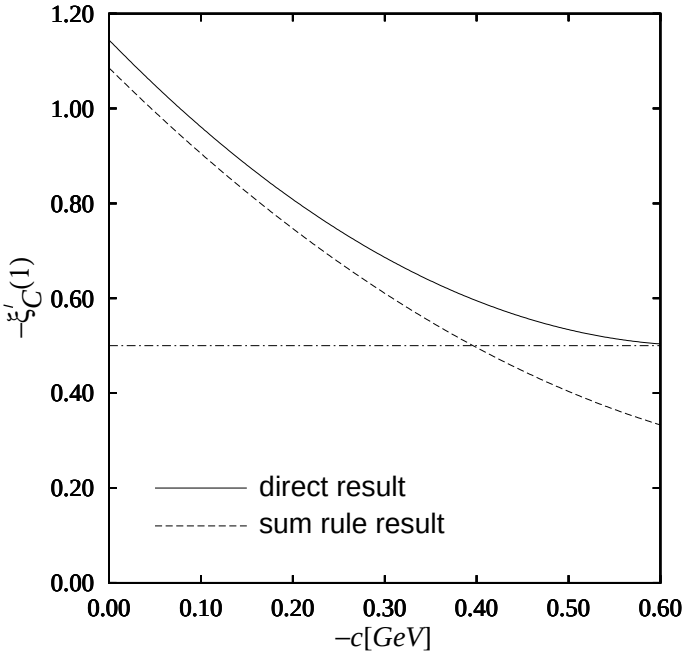

Figure 4.8: SFTM calculation of $-\xi'_C(1)$ (full line). Bjorken sum rule result is shown with dashed line. The dotted line is the bound $-\xi'_C(1) \geq \frac{1}{2}$ coming from (3.39). These results are for $B \to D, D^*$ semileptonic decays.

of SEVC, the Bjorken sum rule is satisfied for all values of c, but the Voloshin sum rule requirement yields[19]

$$155\ MeV \leq -c \leq 530\ MeV\ . \tag{4.44}$$

The above result implies $1486\ MeV \leq m_c \leq 1861\ MeV$ and $4822\ MeV \leq m_b \leq 5197\ MeV$ for the constituent heavy quark masses.

Choosing $c = -230\ MeV$, we find parameters of the SFTM which will be

[19]This result is also obtained using $\Delta \leq 0.525$. Stronger constraint ($\Delta \leq 0.5$) would lead to $225\ MeV \leq -c \leq 510\ MeV$.

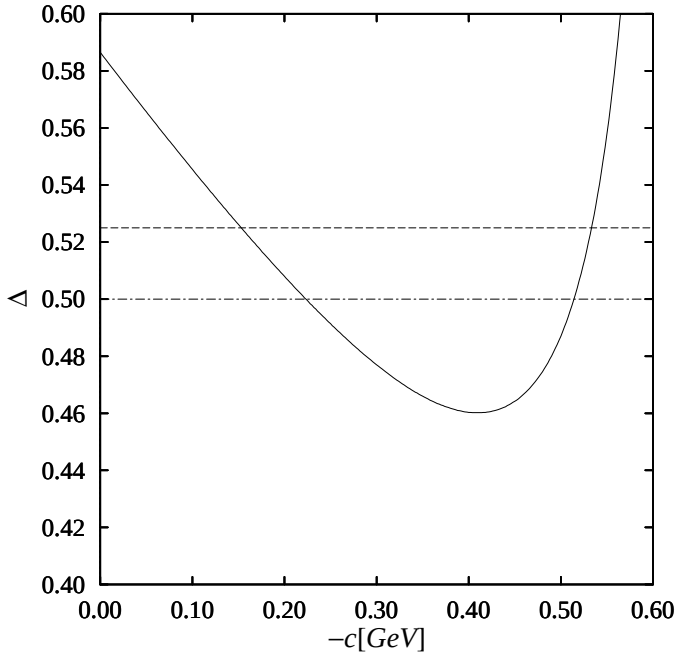

Figure 4.9: SFTM Voloshin sum rule calculation of Δ (full line). The expected upper bound of 0.5, and the 5% relaxed bound of 0.525 are shown with the dotted and dashed line, respectively. These results are for $B \to D, D^*$ semileptonic decays.

used in Chapter 5 for calculation of the semileptonic B decays:

$$\begin{aligned} m_{u,d} &= 0.350\ GeV\ , \\ m_s &= 0.604\ GeV\ , \\ m_c &= 1.561\ GeV\ , \\ m_b &= 4.897\ GeV\ , \\ \alpha_s &= 0.501\ , \\ b &= 0.181\ GeV^2\ , \\ c &= -0.230\ GeV\ . \end{aligned} \tag{4.45}$$

These parameters imply the S-wave LDF energy of about 415 MeV, and also $-\xi_C'(1) \simeq 0.77$. Model predictions for the spin-averaged heavy-light masses

are given in Table 4.5.

4.6 Salpeter Equation with a Mixed Vector and Scalar Confinement (SVSC)

In [88] it has been shown that the full Salpeter equation, with a pure scalar confinement and with arbitrary constituent quark masses, cannot be solved by a variational method. In fact, it seems that the only kernel which leads to a stable variational solution of the full Salpeter equation is the time component vector kernel ($\gamma^0 \times \gamma^0$). Because of that, the confining kernel has to contain at least one half of the $\gamma^0 \times \gamma^0$ kernel if one wants to use a full Salpeter equation in the description of meson states. Several authors have used this as a motivation for considering the full Salpeter equation with a half-half mixture of $\gamma^0 \times \gamma^0$ and 1×1 confining kernels [90–93]. In this way, a maximal possible cancelation of the unwanted spin-orbit splitting is achieved, while the stability of variational solutions to the full Salpeter equation is still retained. As can be seen from Table 4.4, in these papers a wide variety of confining parameters were used. In this section we investigate heavy-light limit of the Salpeter equation in order to determine the effective string tension b, and the allowed range for c which is consistent with the HQET sum rules.

The heavy-light Hamiltonian for the Salpeter equation with an equal mixture of vector and scalar confinement is similar to (4.28),

$$H = m_Q + H_{\bar{q}} + \Lambda_+ V(r) \Lambda_+ \ . \tag{4.46}$$

The only difference is that now $V(r) = V_{oge}(r) + \frac{1}{2}(1 + \gamma^0) V_{conf}(r)$, where

Table 4.4: Parameters of the confining interaction with an equal mixture of $\gamma^0 \times \gamma^0$ and 1×1 kernels used in several papers which employed the full Salpeter equation. Zöller et al. [90] employed two different sets of confining parameters for the heavy-heavy (HH) and the light-light (LL) mesons. Münz [93] used two different light quark masses, $m_{u,d} = 220\ MeV$ (SRM) and $m_{u,d} = 330\ MeV$ (NRM), and determined other parameters of the model from the fit to the light quarkonia. To obtain the universal Regge slope, Salpeter equation with this mixture of vector and scalar confinement requires $b = 0.284\ GeV^2$, while the range of values for c, for which SVSC satisfies the sum rule constraints, depends on other parameters of the model.

Author(s)	Reference	$b\ [GeV^2]$	$-c\ [GeV]$
Zöller et al. (1995)	[90]	0.335	1.027
Klempt et al. (1995)	[91]	0.410	1.751
Parramore et al. (1995)	[92] (HH)	0.257	0
Parramore et al. (1995)	[92] (LL)	0.374	1.427
Münz (1996)	[93] (SRM)	0.366	1.273
Münz (1996)	[93] (NRM)	0.386	1.418

$V_{oge}(r)$ and $V_{conf}(r)$ are again given in (4.2) and (4.3), respectively. As before, $H_{\bar{q}}$ is the free Dirac Hamiltonian given in (4.29), and Λ_+ is defined in (4.30).

While it would be quite difficult, if not impossible, to investigate analytically the Regge structure of the full Salpeter equation in the light-light limit, a similar analysis was done in the heavy-light limit [54]. There it was shown that scalar part of the interaction cancels in the ultra-relativistic limit, and that is precisely the reason why pure scalar confinement in the Salpeter equation does not exhibit linear Regge behavior. The heavy-light Regge slope for an equal mixture of vector and scalar confinement in (4.46) is

$$\alpha'_{HL} = \frac{1}{2b}\ , \tag{4.47}$$

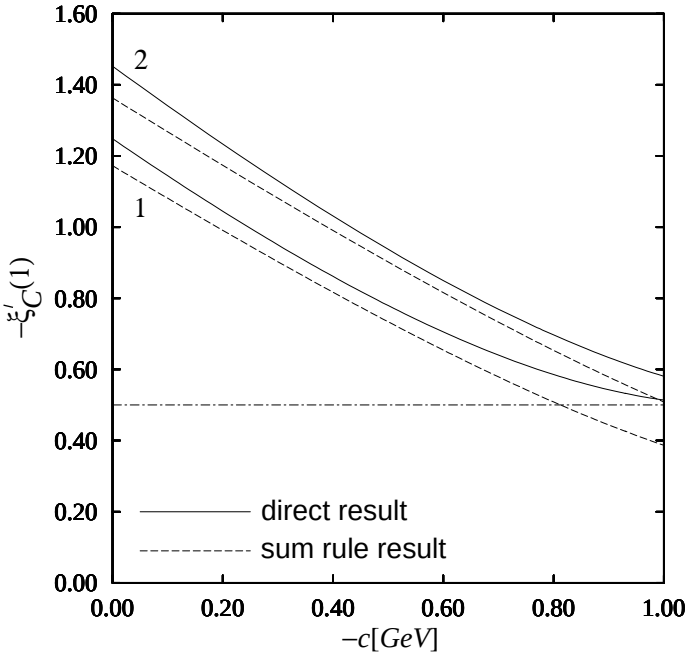

Figure 4.10: SVSC calculations of $-\xi'_C(1)$ (full lines) for $B \to D, D^*$ semileptonic decays. Bjorken sum rule results are shown with dashed lines. 1 and 2 denote calculations done with $b = 0.284\ GeV^2$ and $b = 0.335\ GeV^2$, respectively. The dotted line is the bound $-\xi'_C(1) \geq \frac{1}{2}$ coming from (3.39).

which, together with $\alpha'_{HL} = 2\alpha'_{LL}$ and (4.6), implies

$$b = 0.284\ GeV^2\ . \tag{4.48}$$

This value for the effective string tension is in general smaller than values used in the literature (see Table 4.4).

In SVSC constant c cannot be absorbed into the heavy quark mass in the heavy-light limit. Because of that, the sum rule part of the model analysis is not as simple as was the case for models investigated so far. We fix $b = 0.284\ GeV^2$ and $m_{u,d} = 350\ MeV$ (parameter set 1), and for each value of c we perform a new fit to the heavy-light spectrum in order to determine other parameters of the model, which then can be used for evaluation of $-\xi'_C(1)$

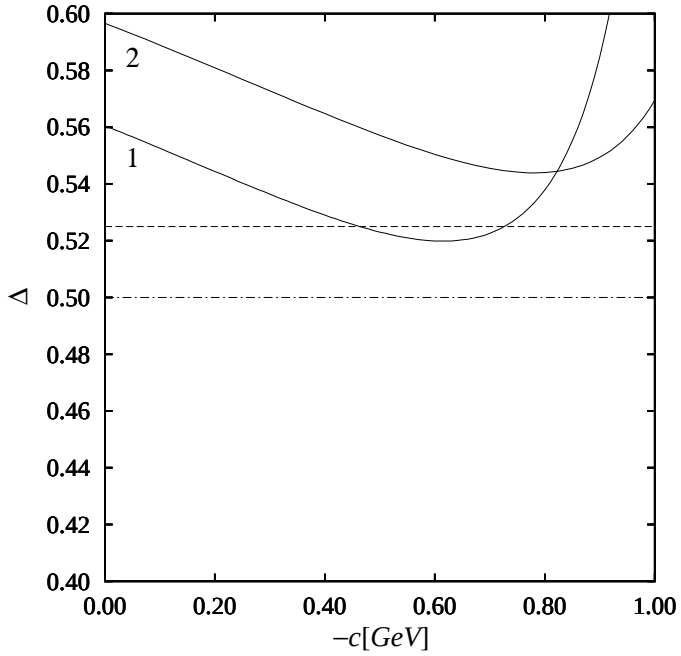

Figure 4.11: SVSC Voloshin sum rule calculations of Δ (full lines) for $B \to D, D^*$ semileptonic decays. 1 and 2 denote calculations done with $b = 0.284\ GeV^2$ and $b = 0.335\ GeV^2$, respectively. The expected upper bound of 0.5 is shown with the dotted line, while the 5% relaxed bound of 0.525 is shown with the dashed line.

and Δ. In Figures 4.10 and 4.11 we show results of our calculations with five lowest P-wave states. As one can see, the Bjorken sum rule is satisfied for all values of c (which is the same as in the case of other two models based on the Salpeter equation), while the requirement $\Delta \leq 0.525$ yields

$$470\ MeV \leq -c \leq 720\ MeV\ . \tag{4.49}$$

Range for the constituent heavy quark masses corresponding to (4.49) are $1529\ MeV \leq m_c \leq 1699\ MeV$ and $4865\ MeV \leq m_b \leq 5035\ MeV$. Note that we were unable to find parameters which would satisfy stronger constraint $\Delta \leq 0.5$.

Since values for b which can be found in the literature are mostly larger than 0.284 GeV^2, in order to see what are the effects of using larger b, we have chosen $b = 0.335\ GeV^2$ [90], and $m_{u,d} = 350\ MeV$ (parameter set 2), and repeated all calculations. Again, Bjorken sum rule was satisfied for all values of c (Figure 4.10), but this time we were unable to find parameters which would satisfy even the relaxed Voloshin sum rule constraint (Figure 4.11). The minimum of $\Delta(c)$ was 0.544 (the lowest P-wave contributed 0.513), and was obtained for $c = -0.775\ MeV$.

We next summarize parameters of the SVSC which will be used in Chapter 5 for calculation of the semileptonic B decays:

$$\begin{aligned} m_{u,d} &= 0.350\ GeV\ , \\ m_s &= 0.579\ GeV\ , \\ m_c &= 1.549\ GeV\ , \\ m_b &= 4.885\ GeV\ , \\ \alpha_s &= 0.423\ , \\ b &= 0.284\ GeV^2\ , \\ c &= -0.500\ GeV\ . \end{aligned} \tag{4.50}$$

The above parameters yield the S-wave LDF energy of 430 MeV, and also $-\xi_C'(1) \simeq 0.78$. Model predictions for the spin-averaged heavy-light masses are given in Table 4.5.

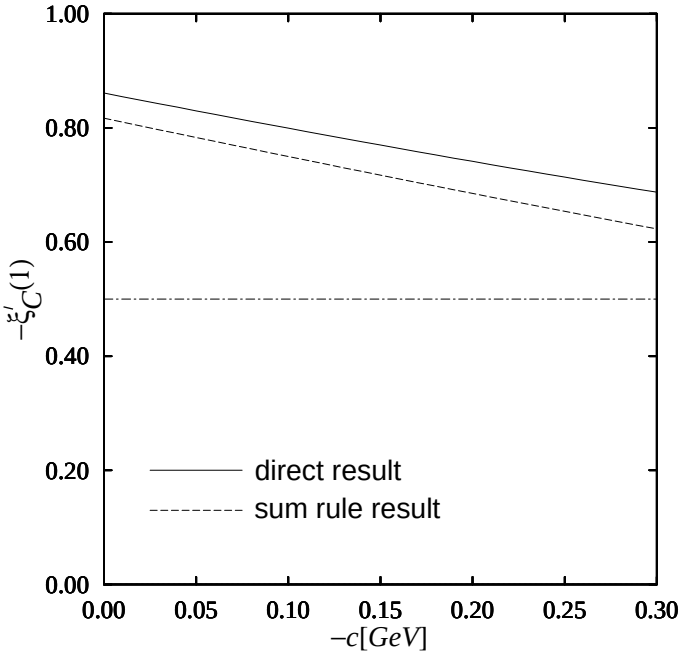

Figure 4.12: DESC calculation of $-\xi'_C(1)$ (full line). Bjorken sum rule result is shown with the dashed line. The dotted line is the bound $-\xi'_C(1) \geq \frac{1}{2}$ coming from (3.39). These results are for $B \to D, D^*$ semileptonic decays.

4.7 Dirac Equation with Scalar Confinement (DESC)

The last model we shall consider is the Dirac equation with pure scalar confinement, which is the only type of confinement potential that has the correct sign of the spin-orbit coupling. The Hamiltonian for DESC is given by

$$H = m_Q + \gamma^0 \boldsymbol{\gamma} \cdot \boldsymbol{p} + \gamma^0 (m_{\bar{q}} + V_{conf}(r)) + V_{oge}(r) \ , \tag{4.51}$$

with $V_{oge}(r)$ and $V_{conf}(r)$ given in (4.2) and (4.3), respectively.

The Regge structure of this model was investigated in [54], where it was

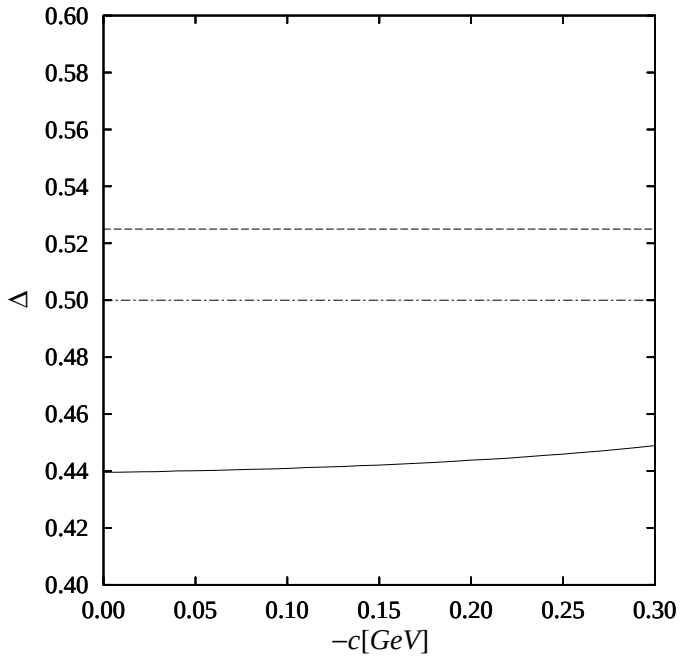

Figure 4.13: DESC Voloshin sum rule calculation of Δ (full line). The expected upper bound of 0.5 is shown with the dotted line, while the 5% relaxed bound of 0.525 is shown with the dashed line. These results are for $B \to D, D^*$ semileptonic decays.

found that

$$\alpha'_{HL} = \frac{1}{2b} \ . \tag{4.52}$$

Even though DESC yields the same slope as SVSC, the two models are qualitatively different. In the case of SVSC the Regge slope was due to the vector part of the potential, and it is only because we used an equal mixture of scalar and vector confinement that we find the same slope for DESC and SVSC. Same as before, (4.52) implies

$$b = 0.284 \ GeV^2 \ . \tag{4.53}$$

We now turn to the sum rule part of the model analysis. Unlike in the previous models which we considered, confining part of the potential here

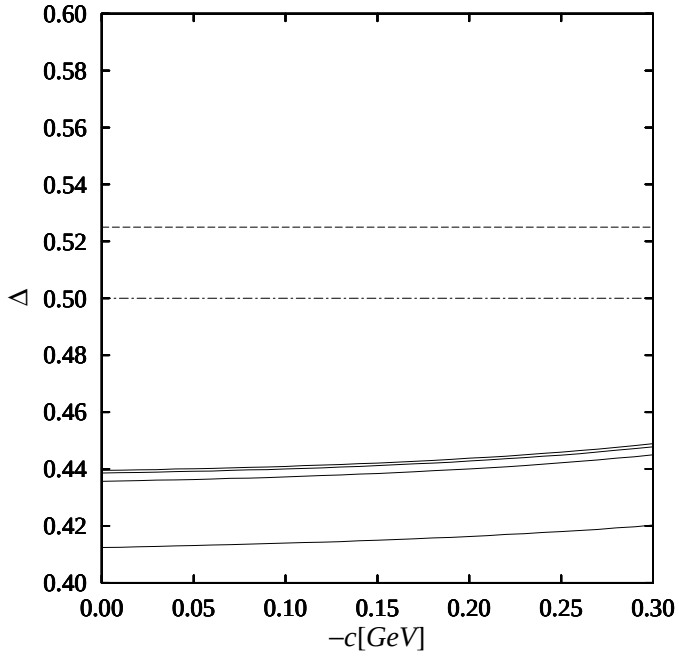

Figure 4.14: Convergence of the DESC Voloshin sum rule evaluation of Δ for $B \to D, D^*$ semileptonic decays. Plotted with full lines are calculations done with 1, 5, 10, and with 15 lowest P-wave states. The expected upper bound of 0.5, and the 5% relaxed bound of 0.525 are shown with the dotted and dashed line, respectively.

effectively just changes the constituent light quark mass. Therefore, with $m_{u,d}$ fixed, for each value of c one has to perform a separate fit to the observed heavy-light meson states in order to determine the other parameters of the model, and then use those parameters to calculate $-\xi'_C(1)$ and Δ from the Bjorken and Voloshin sum rules. Our results for the semileptonic $B \to D, D^*$ decays, obtained with the 15 lowest P-wave states and with $m_{u,d}$ fixed to 300 MeV, are shown in Figures 4.12 (Bjorken sum rule) and 4.13 (Voloshin sum rule). As one can see, DESC satisfies both sum rules for any value of $c \geq -300$ MeV (or constituent light quark mass $m_{u,d} \geq 0$). We also investigated convergence of the DESC sum rule calculations with respect to an increase in the number of

P-wave resonances included. The results for the Voloshin sum rule, obtained with 1, 5, 10 and 15 lowest P-wave doublets (i.e., 15 E, E^* and 15 F, F^* states), are shown in Figure 4.14.

Choosing $c = 0$, we have

$$\begin{aligned} m_{u,d} &= 0.300\ GeV\ , \\ m_s &= 0.465\ GeV\ , \\ m_c &= 1.357\ GeV\ , \\ m_b &= 4.693\ GeV\ , \\ \alpha_s &= 0.462\ , \\ b &= 0.284\ GeV^2\ , \\ c &= 0\ . \end{aligned} \tag{4.54}$$

The above parameters yield the S-wave LDF energy of 620 MeV and $-\xi_C'(1) \simeq 0.86$, and will be used for the calculation of the semileptonic B decays in Chapter 5. Model predictions for the spin-averaged heavy-light masses are given in Table 4.5. To make an easier comparison between different models investigated in this chapter, we summarized their parameters in Table 4.6.

4.8 Conclusion

In this chapter we have investigated several hadronic models in the heavy quark limit. For each model we have fixed the effective slope of the linear potential b by comparing the model prediction for the Regge slope to experiment. In order to constrain the constant c of the confining part of the potential, we have used the HQET sum rules. Other parameters of the model were determined from the spin-averaged heavy-light meson spectrum.

Table 4.5: SEVC, SFTM, SVSC and DESC results for the spin-averaged heavy-light meson masses. Parameters for different models are given in (4.36), (4.45), (4.50), and in (4.54) for SEVC, SFTM, SVSC, and DESC, respectively. Errors for all models are shown in brackets.

Meson	State	Mass $[MeV]$	SEVC $[MeV]$	SFTM $[MeV]$	SVSC $[MeV]$	DESC $[MeV]$
$D(1867)$	$0^-_{1/2}$	1974	1979(+5)	1980(+6)	1980(+6)	1977(+3)
$D^*(2009)$	$1^-_{1/2}$					
$D_1(2425)$	$1^+_{3/2}$	2446	2441(−5)	2440(−6)	2440(−6)	2444(−2)
$D^*_2(2459)$	$2^+_{3/2}$					
$D_s(1969)$	$0^-_{1/2}$	2076	2072(−4)	2072(−4)	2072(−4)	2074(−2)
$D^*_s(2112)$	$1^-_{1/2}$					
$D_{s1}(2535)$	$1^+_{3/2}$	2559	2563(+4)	2563(+4)	2563(+4)	2560(+1)
$D^*_{s2}(2573)$	$2^+_{3/2}$					
$B(5279)$	$0^-_{1/2}$	5314	5315(+1)	5315(+1)	5315(+1)	5313(−1)
$B^*(5325)$	$1^-_{1/2}$					
$B_s(5374)$	$0^-_{1/2}$	5409	5408(−1)	5408(−1)	5408(−1)	5410(+1)
$B^*_s(5421)$	$1^-_{1/2}$					

Table 4.6: Parameters of the six hadronic models which will be used for calculation of semileptonic B decays in Chapter 5.

Model	$m_{u,d}$ $[GeV]$	m_s $[GeV]$	m_c $[GeV]$	m_b $[GeV]$	α_s	b $[GeV^2]$	c $[GeV]$
SSEQ	0.350	0.542	1.696	5.033	0.390	0.142	-0.330
RFTM	0.300	0.507	1.532	4.868	0.390	0.181	-0.200
SEVC	0.350	0.620	1.627	4.963	0.527	0.142	-0.240
SFTM	0.350	0.604	1.561	4.897	0.501	0.181	-0.230
SVSC	0.350	0.579	1.549	4.885	0.423	0.284	-0.500
DESC	0.300	0.465	1.357	4.693	0.462	0.284	0

Once again, we emphasize that our goal here was not to show whether a given model is correct in terms of a particular equation, a type of confinement, or a specific potential it uses. Instead, our intention was to find several qualitatively different hadronic models, which not only yield a good description of the spin-averaged heavy-light meson states, but are also consistent with experiment in terms of their Regge structure, and self-consistent with respect to the sum rules of the heavy quark effective theory. These models, with parameters summarized in Table 4.6, will be used in the next chapter for calculation of semileptonic B decays into higher charmed resonances.

Chapter 5

Semileptonic B Decays

5.1 Introduction

Semileptonic B decays represent one of the most important and most reliable applications of heavy quark effective theory (HQET). In previous chapters we have emphasized many times the great significance of these decays, especially their role in determining the CKM matrix element V_{cb}.

As the number of measured B decays increases, other questions related to semileptonic $B \to D^{**}$ decays can be addressed.[1] Among these are, for example, the $B \to D, D^*$ spectrum shapes, and the ratio of $B \to D^*$ to $B \to D$ rates. Nevertheless, one of the most pressing questions concerns the large difference between the experimental result for the inclusive semileptonic rate, and the sum of the two exclusive elastic rates, $B \to D$ and $B \to D^*$. Namely, semileptonic decays into hadrons account for over 20% of all B decays. In the case of B^- meson decaying into electron, neutrino, and all hadrons the branching ratio is [94]

$$\mathcal{B}(B^- \to X e^- \bar{\nu}_e) = (10.49 \pm 0.46)\% \ . \tag{5.1}$$

[1] We use the symbol D^{**} to denote any charmed meson.

Slightly less than 70% of the inclusive rate is accounted for by $X = D^0$ and $X = D^{*0}$. The measured branching ratios for these final states are [52,95]

$$\mathcal{B}(B^- \to D^0 e^- \bar{\nu}_e) = (1.95 \pm 0.55)\% , \tag{5.2}$$

$$\mathcal{B}(B^- \to D^{*0} e^- \bar{\nu}_e) = (5.13 \pm 0.84)\% . \tag{5.3}$$

This leaves about 30% of all semileptonic B decays unaccounted for, and is one of the most important reasons for studying semileptonic B decays into higher charmed resonances. Interest in these decays also in part stems from the recent experimental data for the inelastic processes $B \to D^{**} X e \bar{\nu}_e$, where D^{**} could be D_1 or D_2^* (or their radial excitations), and X are any non-charmed hadrons [96–98].

Important ingredients in understanding semileptonic $B \to D^{**}$ decays are the unknown hadronic form factors, which survive after application of HQET. In Chapter 3 we have found precise definitions for these form factors (in the valence quark approximation), which are given in terms of the wave functions and energies of the light degrees of freedom (LDF) [42]. In Chapter 4 we used those definitions in the Bjorken [22,23] and Voloshin [24] sum rules, in order to extract information on several hadronic models in the heavy quark limit. Here we shall apply those models for the investigation of semileptonic B decays. The main advantage of using many qualitatively different models will be the ability to obtain reasonable estimates of model dependence for all of our results.

Calculations similar to the one presented in this chapter have already appeared in [99,100]. The main difference is that here we use models which not

only yield a good description of the spin-averaged heavy-light spectrum, but are also self-consistent with respect to the HQET sum rules.

5.2 Decays $B \to D^{**} e \bar{\nu}_e$ in the Heavy Quark Limit

Assuming that lepton masses are zero, momentum transfer for $B \to D^{**} e \bar{\nu}_e$ decays is given by

$$\begin{aligned} q^2 &= (m_B v - m_{D^{**}} v')^2 = (p_1 + p_2)^2 \\ &= m_B^2 + m_{D^{**}}^2 - 2 m_B m_{D^{**}} \omega \ . \end{aligned} \tag{5.4}$$

In the above v^μ and v'^μ are the four-velocities of B and D^{**} mesons, respectively, and $\omega = v \cdot v'$. Using (5.4), and denoting

$$x = (p_1 + m_{D^{**}} v')^2 = (m_B v - p_2)^2 \ , \tag{5.5}$$

the standard expression [31] for the width of the semileptonic decay of a B meson into any of the charmed meson states D^{**} can be written as

$$\frac{d\Gamma}{d\omega} = \frac{m_{D^{**}}}{128 \pi^3 m_B^2} \int_{x_-}^{x_+} dx \overline{|\mathcal{M}|^2} \ . \tag{5.6}$$

In (5.6) kinematical limits of integration are

$$x_\pm = m_B m_{D^{**}} (\omega \pm \sqrt{\omega^2 - 1}) \ . \tag{5.7}$$

The invariant amplitude,

$$\mathcal{M} = \frac{G_F V_{cb}}{\sqrt{2}} \bar{u}_e \gamma^\mu (1 - \gamma^5) v_{\bar{\nu}_e} \langle D^{**}(v', \varepsilon') | \bar{c} \gamma_\mu (1 - \gamma^5) b | B(v) \rangle \ , \tag{5.8}$$

after squaring and summing over e and $\bar{\nu}_e$ spins, and also over D^{**} polarization, yields

$$\overline{|\mathcal{M}|^2} = \frac{1}{2} G_F^2 |V_{cb}|^2 L_{\mu\nu} H^{\mu\nu} \ . \tag{5.9}$$

In (5.9) we defined leptonic and hadronic tensors as

$$L^{\mu\nu} = 8(p_1^\mu p_2^\nu - g^{\mu\nu} p_1 \cdot p_2 + p_1^\nu p_2^\mu + i\epsilon^{\mu\nu\alpha\beta} p_{1\alpha} p_{2\beta}) \ , \tag{5.10}$$

$$\begin{aligned} H^{\mu\nu} &= \sum_{\varepsilon'} \langle D^{**}(v', \varepsilon') | \bar{c} \gamma^\mu (1 - \gamma^5) b | B(v) \rangle \\ &\times \langle D^{**}(v', \varepsilon') | \bar{c} \gamma^\nu (1 - \gamma^5) b | B(v) \rangle^\dagger \ . \end{aligned} \tag{5.11}$$

We can calculate matrix elements needed in $H^{\mu\nu}$ from (2.41), using states given in (2.40), while the sum over D^{**} polarization states can be performed using expressions (2.46) and (2.47) for spin one and spin two particles, respectively. With the help of kinematical identities which can be derived from definitions (5.4) and (5.5), and also from momentum conservation, we can express $\overline{|\mathcal{M}|^2}$ in terms of ω and x. Performing a simple integration in (5.6), we find

$$\frac{d\Gamma^{**}}{d\omega} = \frac{G_F^2 |V_{cb}|^2}{48\pi^3} m_B^2 m_{D^{**}}^3 \sqrt{\omega^2 - 1} |\xi^{**}(\omega)|^2 f^{**}(\omega, r^{**}) \ , \tag{5.12}$$

where $r^{**} = m_{D^{**}}/m_B$, and the function f^{**} is given by

$$f_C(\omega, r) = (\omega^2 - 1)(1 + r)^2 \ , \tag{5.13}$$

$$f_{C^*}(\omega, r) = (\omega + 1)\left[(\omega + 1)(1 - r)^2 + 4\omega(1 - 2\omega r + r^2)\right] \ , \tag{5.14}$$

$$f_E(\omega, r) = (\omega^2 - 1)(1 - r)^2 \ , \tag{5.15}$$

$$f_{E^*}(\omega, r) = (\omega - 1)\left[(\omega - 1)(1 + r)^2 + 4\omega(1 - 2\omega r + r^2)\right] \ , \tag{5.16}$$

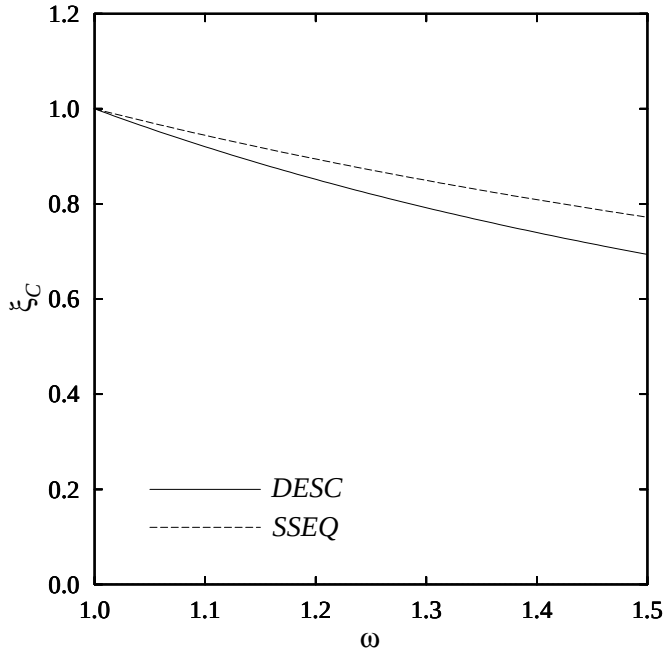

Figure 5.1: Form factor ξ_C for $C \to C, C^*$ transitions (B decays), obtained with DESC (full line) and SSEQ (dashed line). Kinematical limits for $C \to C$ transitions is $\omega \simeq 1.59$, while for $C \to C^*$ transitions it is $\omega \simeq 1.50$.

$$f_F(\omega, r) = \frac{2}{3}(\omega-1)(\omega+1)^2\left[(\omega-1)(1+r)^2+\omega(1-2\omega r+r^2)\right] , \quad (5.17)$$

$$f_{F^*}(\omega, r) = \frac{2}{3}(\omega-1)(\omega+1)^2\left[(\omega+1)(1-r)^2+3\omega(1-2\omega r+r^2)\right] , \quad (5.18)$$

$$f_G(\omega, r) = \frac{2}{3}(\omega-1)^2(\omega+1)\left[(\omega+1)(1-r)^2+\omega(1-2\omega r+r^2)\right] , \quad (5.19)$$

$$f_{G^*}(\omega, r) = \frac{2}{3}(\omega-1)^2(\omega+1)\left[(\omega-1)(1+r)^2+3\omega(1-2\omega r+r^2)\right] . \quad (5.20)$$

Here we used notation from previous chapters, i.e., $C, C^*, \ldots$ denote $D, D^*, \ldots$ mesons. These expressions can be found in [36,45,50,99]. In the following section we present our results for semileptonic $B \to D^{**}$ decays, obtained with six different hadronic models investigated in Chapter 4.

5.3 IW Form Factors, Branching Ratios and Comparison with Literature

We first show several results for the form factors and corresponding differential branching ratios. The elastic form factor ξ_C and differential branching ratios $d\mathcal{B}/d\omega$ for $C \to C, C^*$ decays, obtained with DESC and SSEQ, are shown in Figures 5.1 and 5.2, respectively. We have chosen DESC and SSEQ because ξ_C obtained from these two models yields the smallest (DESC) and the largest (SSEQ) $C \to C$ and $C \to C^*$ branching ratios. It is interesting to compare the zero-recoil point slope $\xi'_C(1)$ obtained from different models:

$$-\xi'_C(1) = \begin{cases} 0.59 & \text{(SSEQ)} \\ 0.70 & \text{(RFTM)} \\ 0.71 & \text{(SEVC)} \\ 0.77 & \text{(SFTM)} \\ 0.78 & \text{(SVSC)} \\ 0.86 & \text{(DESC)} \end{cases} . \tag{5.21}$$

Note that the experimental result is [52]

$$-\hat{\xi}'_C(1) = 0.84 \pm 0.14 \; . \tag{5.22}$$

Form factor $\hat{\xi}_C$ would be the Isgur-Wise function ξ_C in the absence of the symmetry breaking corrections.

Inelastic form factors ξ_E and ξ_F (which describe S to P-wave semileptonic B decays), and corresponding differential branching ratios are shown in Figures 5.3 through 5.6. For $C \to E, E^*$ transitions (Figures 5.3 and 5.4) the

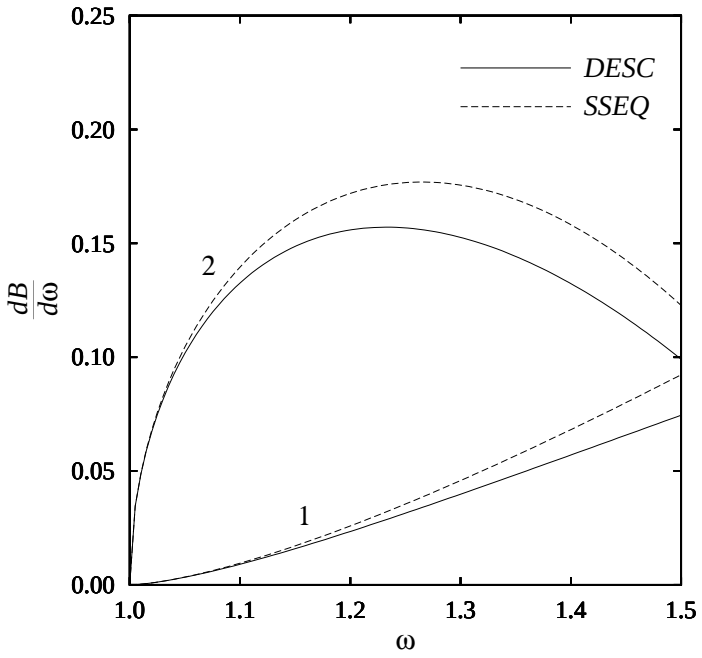

Figure 5.2: Differential branching ratios $\frac{d\mathcal{B}}{d\omega}$ for $C \to C$ (1) and $C \to C^*$ (2) transitions (B decays), obtained with DESC (full lines) and SSEQ (dashed lines). Kinematical limits for $C \to C$ transitions is $\omega \simeq 1.59$, while for $C \to C^*$ transitions it is $\omega \simeq 1.50$.

smallest branching ratios are obtained with SEVC, while the largest ones are found with RFTM. Note that ξ_E obtained from these two models differ considerably (Figure 5.3), which is not the case for ξ_C (Figure 5.1), where all models give similar results. Results for ξ_F and $d\mathcal{B}/d\omega$ (corresponding to $C \to F, F^*$ transitions and obtained with SSEQ and DESC) are shown in Figures 5.5 and 5.6, respectively.

Our results for branching ratios obtained from the six different models discussed in Chapter 4 are shown in Tables 5.1, 5.2 and 5.3. We have assumed $V_{cb} = 0.040$ and $\tau_B = 1.5ps$.[2] Table 5.4 contains a comparison of our results

[2]Experimental result is $V_{cb} = (37.7 \pm 2.0 \pm 2.1 \pm 1.2) \times 10^{-3}$ [52], while Neubert's analysis based on heavy quark symmetry yields $V_{cb} = 0.040 \pm 0.003$ [36].

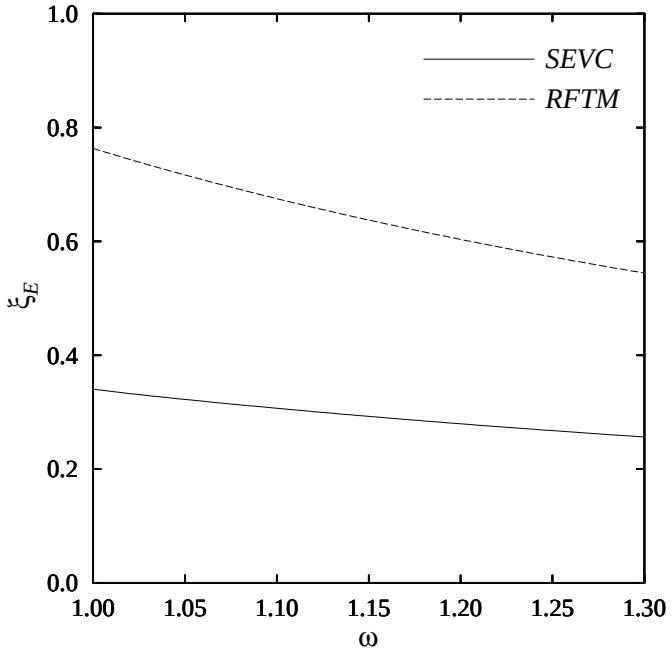

Figure 5.3: Form factor ξ_E for $C \to E, E^*$ transitions (B decays), obtained with SEVC (full line) and RFTM (dashed line). For both $C \to E$ and $C \to E^*$ transitions kinematical limits are $\omega \simeq 1.40$ (SEVC) and $\omega \simeq 1.32$ (RFTM).

with calculation of Suzuki et al. (SISM model) [50], the one of Scora and Isgur (ISGW2 model) [101], with the QCD sum rule approach of Colangelo et al. (CNP model) [102], and with the model of Sutherland et al. (SHJL model) [103]. It is worth noting that results quoted for SISM and CNP are also obtained in the heavy quark limit.[3] Table 5.5 contains our ratios of partial widths for B decays into members of the same D^{**} doublet, such as $\mathcal{B}(C \to C)/\mathcal{B}(C \to C^*)$, $\mathcal{B}(C \to E)/\mathcal{B}(C \to E^*)$, etc. The same ratios, but obtained in SISM, ISGW2, CNP, and SHJL models, are shown in Table 5.6.

For the calculation of branching ratios we used experimental meson masses

[3]Note that the calculation of [50] used form factor definitions which are not consistent with the covariant trace formalism.

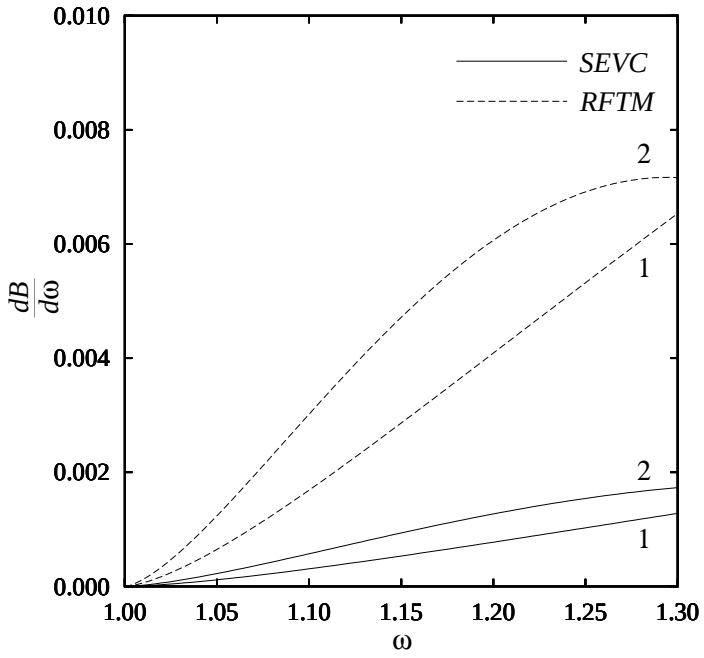

Figure 5.4: Differential branching ratios $\frac{d\mathcal{B}}{d\omega}$ for $C \to E$ (1) and $C \to E^*$ (2) transitions (B decays), obtained with SEVC (full lines) and RFTM (dashed lines). For both $C \to E$ and $C \to E^*$ transitions kinematical limits are $\omega \simeq 1.40$ (SEVC) and $\omega \simeq 1.32$ (RFTM).

wherever possible. In those cases the only model dependent inputs were the appropriate IW form factors. For decays where the D^{**} mass is unknown, we have used spin-averaged masses obtained in a specific model, which are also shown in Tables 5.1 through 5.3. Based on the available information on the splitting between D and D^* (or D_1 and D_2^*), one could estimate mass splitting in other excited doublets, and use that together with model dependent spin-averaged mass to obtain separate predictions for the masses of each member of that doublet. Meson masses obtained in this way could then be used in the calculation of the branching ratio for the corresponding decay. However, we have found that this procedure does not significantly affect results. For

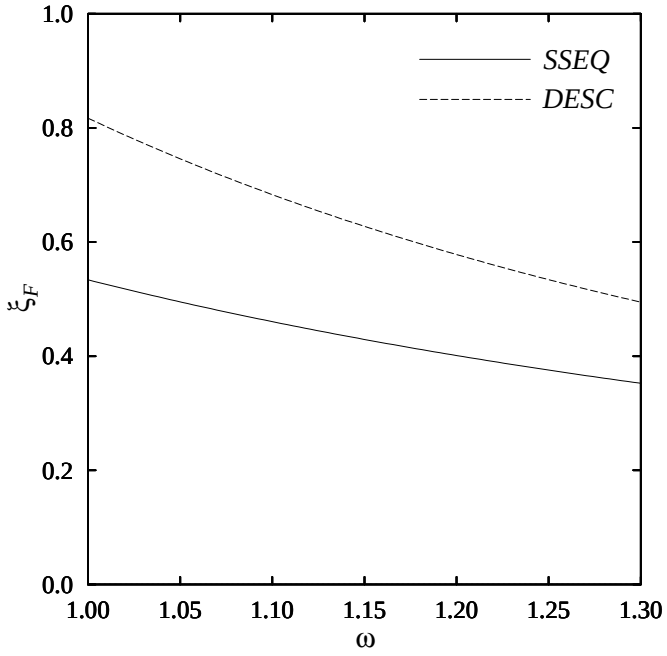

Figure 5.5: Form factor ξ_F for $C \to F, F^*$ transitions (B decays), obtained with SSEQ (full line) and DESC (dashed line). Kinematical limits for $C \to F$ transitions is $\omega \simeq 1.32$ and for $C \to F^*$ transitions it is $\omega \simeq 1.31$.

example, using a spin-averaged mass of 1974 MeV for $D(1867)$ and $D^*(2009)$, instead of their experimental masses, in the case of DESC yields branching ratios of 2.24% and 6.77% instead of 2.40% and 6.62%, which are given in Table 5.3. For higher states this effect is even less noticeable.

Let us first discuss $B \to D$ and $B \to D^*$ transitions. Recent results from CLEO [52,95], given in (5.2) and (5.3), and results given in Tables 5.1 through 5.4, imply that all models we used, as well as the ISGW2 and SHJL models, require a V_{cb} slightly lower than 0.040. In our models values range from about 0.033 for SSEQ and 0.034 for RFTM and SEVC, to about 0.035 for SFTM and SVSC and 0.036 for DESC. On the other hand, ISGW2 is consistent with 0.035, SHJL gives about 0.036, and SISM and CNP models agree with V_{cb} of

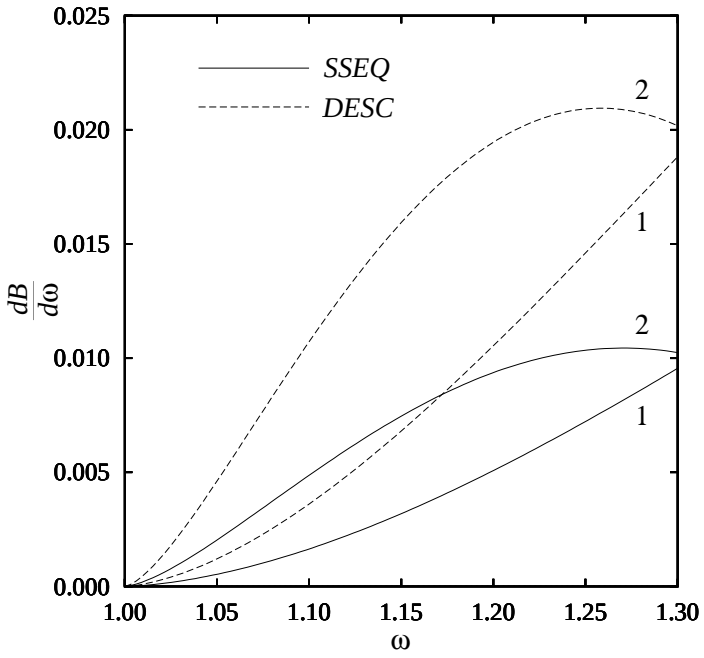

Figure 5.6: Differential branching ratios $\frac{d\mathcal{B}}{d\omega}$ for $C \to F$ (1) and $C \to F^*$ (2) transitions (B decays), obtained with SSEQ (full lines) and DESC (dashed lines). Kinematical limits for $C \to F$ transitions is $\omega \simeq 1.32$, and for $C \to F^*$ transitions it is $\omega \simeq 1.31$.

about 0.041. The experimental result is [52]

$$V_{cb} = 0.0377 \pm 0.0031 \ . \tag{5.23}$$

From Table 5.6 it can also be found that

$$\frac{\mathcal{B}(B \to De\bar{\nu}_e)}{\mathcal{B}(B \to D^* e\bar{\nu}_e)} = \begin{cases} 0.34 & \text{(SISM)} \\ 0.48 & \text{(ISGW2)} \\ 0.33 & \text{(CNP)} \\ 0.31 & \text{(SHJL)} \end{cases} \ . \tag{5.24}$$

For the same ratio our calculations with six different models (see Table 5.5) yield results in the range from 0.36 to 0.38. The results quoted in (5.2) and

(5.3) imply an experimental ratio of

$$\frac{\mathcal{B}(B \to De\bar{\nu}_e)}{\mathcal{B}(B \to D^* e\bar{\nu}_e)} = 0.38 \pm 0.17 \ . \tag{5.25}$$

Note that ratio of polarization states of D and D^* is 0.33.

Individual contributions of P-wave $j = 3/2$ states to the total semileptonic decay rate is another interesting point. From Table 5.1 it can be seen that the total semileptonic branching ratio for $B \to D_1$ and $B \to D_2^*$ in the two spinless models is expected to be

$$\begin{aligned} \mathcal{B}(B \to D_1 e\bar{\nu}_e) \ &+ \ \mathcal{B}(B \to D_2^* e\bar{\nu}_e) = \\ &= \begin{cases} 0.33\,|V_{cb}/0.040|^2\,(\tau_B/1.50ps)\% & \text{(SSEQ)} \\ 0.47\,|V_{cb}/0.040|^2\,(\tau_B/1.50ps)\% & \text{(RFTM)} \end{cases} . \end{aligned} \tag{5.26}$$

Models based on the Salpeter (or Dirac) equation give slightly larger results (see Tables 5.2 and 5.3), i.e.,

$$\begin{aligned} \mathcal{B}(B \to D_1 e\bar{\nu}_e) \ &+ \ \mathcal{B}(B \to D_2^* e\bar{\nu}_e) = \\ &= \begin{cases} 0.52\,|V_{cb}/0.040|^2\,(\tau_B/1.50ps)\% & \text{(SEVC)} \\ 0.60\,|V_{cb}/0.040|^2\,(\tau_B/1.50ps)\% & \text{(SFTM)} \\ 0.66\,|V_{cb}/0.040|^2\,(\tau_B/1.50ps)\% & \text{(SVSC)} \\ 0.69\,|V_{cb}/0.040|^2\,(\tau_B/1.50ps)\% & \text{(DESC)} \end{cases} . \end{aligned} \tag{5.27}$$

These results are in general larger than the SISM and CNP results of 0.20 and $0.37\ |V_{cb}/0.040|^2\,(\tau_B/1.50ps)\%$, and are comparable to the SHJL and ISGW2 models, which give 0.46 and $0.65\ |V_{cb}/0.040|^2\,(\tau_B/1.50ps)\%$, respectively. However, as one can see from Tables 5.5 and 5.6, our ratios of these two P-wave decays are qualitatively different from the ones obtained in ISGW2 and SHJL,

Table 5.1: Exclusive partial widths for decays $B \to D^{**} e\bar{\nu}_e$ obtained from SSEQ and RFTM. For the observed mesons we used experimental masses, otherwise we used model predictions for the spin-averaged meson masses. All masses are given in MeV. Γ is given in units of $[(V_{cb}/0.040)^2 10^{-15} GeV]$, $\mathcal{B}$ is in units of $\left[|V_{cb}/0.040|^2 (\tau_B/1.50ps)\%\right]$, while the ratio $R = \mathcal{B}(B \to D^{**} e\bar{\nu}_e)/\mathcal{B}(b \to ce\bar{\nu}_e)$ is given in [%]. Numerical values of $\mathcal{B}(b \to ce\bar{\nu}_e)$ for a particular model can be found in (5.35).

State		SSEQ				RFTM			
D^{**}	J_j^P	$Mass$	Γ	$\mathcal{B}$	R	$Mass$	Γ	$\mathcal{B}$	R
C	$0^-_{1/2}$	1867	12.62	2.876	24.32	1867	11.76	2.681	24.13
C^*	$1^-_{1/2}$	2009	32.78	7.470	63.15	2009	31.25	7.121	64.10
E	$0^+_{1/2}$	2416	0.326	0.074	0.629	2413	0.457	0.104	0.938
E^*	$1^+_{1/2}$	2416	0.448	0.102	0.863	2413	0.631	0.144	1.294
F	$1^+_{3/2}$	2425	0.568	0.129	1.094	2425	0.788	0.180	1.617
F^*	$2^+_{3/2}$	2459	0.891	0.203	1.716	2459	1.252	0.285	2.568
G	$1^-_{3/2}$	2673	0.028	0.006	0.053	2681	0.047	0.011	0.096
G^*	$2^-_{3/2}$	2673	0.028	0.007	0.055	2681	0.048	0.011	0.098
C_2	$0^-_{1/2}$	2436	0.040	0.009	0.077	2494	0.079	0.018	0.162
C_2^*	$1^-_{1/2}$	2436	0.077	0.018	0.148	2494	0.154	0.035	0.317
E_2	$0^+_{1/2}$	2750	0.010	0.002	0.020	2819	0.012	0.003	0.024
E_2^*	$1^+_{1/2}$	2750	0.013	0.003	0.026	2819	0.015	0.003	0.030
F_2	$1^+_{3/2}$	2750	0.019	0.004	0.036	2819	0.021	0.005	0.043
F_2^*	$2^+_{3/2}$	2750	0.029	0.007	0.055	2819	0.031	0.007	0.064
total			47.88	10.91	92.24		46.55	10.61	95.48

Table 5.2: Exclusive partial widths for decays $B \to D^{**} e\bar{\nu}_e$ obtained from SEVC and SFTM. For the observed mesons we used experimental masses, otherwise we used model predictions for the spin-averaged meson masses. All masses are given in MeV. Γ is given in units of $[(V_{cb}/0.040)^2 10^{-15} GeV]$, $\mathcal{B}$ is in units of $\left[|V_{cb}/0.040|^2 (\tau_B/1.50ps)\%\right]$, while the ratio $R = \mathcal{B}(B \to D^{**} e\bar{\nu}_e)/\mathcal{B}(b \to ce\bar{\nu}_e)$ is given in [%]. Numerical values of $\mathcal{B}(b \to ce\bar{\nu}_e)$ for a particular model can be found in (5.35).

State		SEVC				SFTM			
D^{**}	J_j^P	$Mass$	Γ	$\mathcal{B}$	R	$Mass$	Γ	$\mathcal{B}$	R
C	$0^-_{1/2}$	1867	11.79	2.687	23.33	1867	11.30	2.575	22.93
C^*	$1^-_{1/2}$	2009	31.29	7.132	61.92	2009	30.41	6.930	61.72
E	$0^+_{1/2}$	2216	0.143	0.033	0.282	2254	0.162	0.037	0.329
E^*	$1^+_{1/2}$	2216	0.199	0.045	0.393	2254	0.226	0.052	0.459
F	$1^+_{3/2}$	2425	0.882	0.201	1.746	2425	1.010	0.230	2.050
F^*	$2^+_{3/2}$	2459	1.408	0.321	2.787	2459	1.621	0.369	3.289
G	$1^-_{3/2}$	2569	0.009	0.002	0.017	2609	0.010	0.002	0.021
G^*	$2^-_{3/2}$	2569	0.009	0.002	0.018	2609	0.011	0.002	0.021
C_2	$0^-_{1/2}$	2437	0.075	0.017	0.149	2506	0.093	0.021	0.189
C_2^*	$1^-_{1/2}$	2437	0.148	0.034	0.293	2506	0.184	0.042	0.373
E_2	$0^+_{1/2}$	2608	0.004	0.001	0.008	2697	0.004	0.001	0.008
E_2^*	$1^+_{1/2}$	2608	0.005	0.001	0.010	2697	0.005	0.001	0.010
F_2	$1^+_{3/2}$	2763	0.031	0.007	0.061	2837	0.025	0.006	0.051
F_2^*	$2^+_{3/2}$	2763	0.046	0.011	0.092	2837	0.037	0.009	0.075
total			46.04	10.49	91.11		45.10	10.28	91.53

Table 5.3: Exclusive partial widths for decays $B \to D^{**} e\bar{\nu}_e$ obtained from SVSC and DESC. For the observed mesons we used experimental masses, otherwise we used model predictions for the spin-averaged meson masses. All masses are given in MeV. Γ is given in units of $[(V_{cb}/0.040)^2 10^{-15} GeV]$, $\mathcal{B}$ is in units of $\left[|V_{cb}/0.040|^2 (\tau_B/1.50ps)\%\right]$, while the ratio $R = \mathcal{B}(B \to D^{**} e\bar{\nu}_e)/\mathcal{B}(b \to ce\bar{\nu}_e)$ is given in [%]. Numerical values of $\mathcal{B}(b \to ce\bar{\nu}_e)$ for a particular model can be found in (5.35).

State		SVSC				DESC			
D^{**}	J_j^P	$Mass$	Γ	$\mathcal{B}$	R	$Mass$	Γ	$\mathcal{B}$	R
C	$0^-_{1/2}$	1867	11.14	2.540	22.72	1867	10.54	2.401	23.26
C^*	$1^-_{1/2}$	2009	30.14	6.868	61.45	2009	29.04	6.617	64.11
E	$0^+_{1/2}$	2323	0.176	0.040	0.360	2421	0.324	0.074	0.715
E^*	$1^+_{1/2}$	2323	0.245	0.056	0.499	2421	0.448	0.102	0.989
F	$1^+_{3/2}$	2425	1.105	0.252	2.254	2425	1.162	0.265	2.565
F^*	$2^+_{3/2}$	2425	1.766	0.403	3.601	2459	1.855	0.423	4.095
G	$1^-_{3/2}$	2684	0.009	0.002	0.018	2763	0.023	0.005	0.050
G^*	$2^-_{3/2}$	2684	0.009	0.002	0.019	2763	0.023	0.005	0.052
C_2	$0^-_{1/2}$	2545	0.080	0.018	0.163	2589	0.067	0.015	0.149
C_2^*	$1^-_{1/2}$	2545	0.158	0.036	0.321	2589	0.132	0.030	0.291
E_2	$0^+_{1/2}$	2780	0.007	0.002	0.015	2858	0.001	0.000	0.003
E_2^*	$1^+_{1/2}$	2780	0.009	0.002	0.019	2858	0.002	0.000	0.003
F_2	$1^+_{3/2}$	2857	0.018	0.004	0.036	2896	0.029	0.007	0.063
F_2^*	$2^+_{3/2}$	2857	0.026	0.006	0.053	2896	0.045	0.010	0.099
total			44.89	10.23	91.53		43.69	9.95	96.44

Table 5.4: Branching ratios ($\mathcal{B}$) for $B \to D^{**} e \bar{\nu}_e$ decays obtained by SISM [50], ISGW2 [101], CNP [102], and SHJL [103] models. All results are given in units of $\left[|V_{cb}/0.040|^2 (\tau_B/1.50ps)\%\right]$. Results for E_2, E_2^* and F_2, F_2^* doublets were not given in any of those papers. Our results with models based on the Salpeter (or Dirac) equation, and the ones including all models, are given in the last two columns.

D^{**}	SISM	ISGW2	CNP	SHJL	Salpeter/Dirac Models	All Models
C	1.778	2.860	1.736	2.160	2.401 - 2.687	2.401 - 2.876
C^*	5.279	5.950	5.331	6.980	6.617 - 7.132	6.617 - 7.470
E	0.027	0.072	0.062	0.067	0.033 - 0.074	0.033 - 0.104
E^*	0.035	0.072	0.087	0.096	0.045 - 0.102	0.045 - 0.144
F	0.083	0.432	0.124	0.281	0.201 - 0.265	0.129 - 0.265
F^*	0.118	0.216	0.248	0.182	0.321 - 0.423	0.203 - 0.423
G	0.000	-	-	0.005	0.002 - 0.005	0.002 - 0.011
G^*	0.000	-	-	0.001	0.002 - 0.005	0.002 - 0.011
C_2	0.016	0.000	-	0.132	0.015 - 0.021	0.009 - 0.021
C_2^*	0.039	0.144	-	-	0.030 - 0.042	0.018 - 0.042
E_2	-	-	-	-	0.000 - 0.002	0.000 - 0.003
E_2^*	-	-	-	-	0.000 - 0.002	0.000 - 0.003
F_2	-	-	-	-	0.004 - 0.007	0.004 - 0.007
F_2^*	-	-	-	-	0.006 - 0.011	0.006 - 0.011
total	7.38	9.74	7.59	9.91	9.95 - 10.49	9.95 - 10.91

Table 5.5: Ratios of partial widths for the B decays into the members of the same D^{**} doublet obtained using six different hadronic models discussed in the previous chapter.

Doublet	SSEQ	RFTM	SEVC	SFTM	SVSC	DESC
C/C^*	0.38	0.38	0.38	0.37	0.37	0.36
E/E^*	0.73	0.72	0.72	0.72	0.72	0.72
F/F^*	0.64	0.63	0.63	0.62	0.63	0.63
G/G^*	0.97	0.97	0.97	0.97	0.97	0.97
C_2/C_2^*	0.52	0.51	0.51	0.51	0.51	0.51
E_2/E_2^*	0.78	0.79	0.80	0.80	0.78	0.84
F_2/F_2^*	0.65	0.67	0.67	0.68	0.68	0.64

and agree with SISM and CNP models. We find that $\mathcal{B}(B \to D_1 e\bar{\nu}_e)/\mathcal{B}(B \to D_2^* e\bar{\nu}_e)$ ranges from 0.62 to 0.64, while the other models yield

$$\frac{\mathcal{B}(B \to D_1 e\bar{\nu}_e)}{\mathcal{B}(B \to D_2^* e\bar{\nu}_e)} = \begin{cases} 0.70 & \text{(SISM)} \\ 2.00 & \text{(ISGW2)} \\ 0.50 & \text{(CNP)} \\ 1.54 & \text{(SHJL)} \end{cases} . \tag{5.28}$$

Note that the ratio of number of polarization states of D_1 and D_2^* is 0.6. It remains to be seen whether this discrepancy between our results (which are obtained in the heavy-light limit) and ISGW2 and SHJL[4] models can be explained with large $1/m_c$ effects [104].

The last issue that we want to consider in this section is the question whether in any of the models we considered, semileptonic B decays into higher

[4]In [103] one can also find results obtained in the heavy quark limit. These are in general much smaller than our results, but the ratios of partial widths for the B decays into the members of the same D^{**} doublet agree much better with our predictions.

Table 5.6: Ratios of partial widths for the B decays into the members of the same D^{**} doublet obtained by SISM [50], ISGW2 [101], CNP [102], and SHJL [103] models. Results for E_2, E_2^* and F_2, F_2^* doublets were not given in any of those papers. In the last column we show our results which include all models.

Doublet	SISM	ISGW2	CNP	SHJL	This Work
C/C^*	0.34	0.48	0.33	0.31	0.36 - 0.38
E/E^*	0.76	1.00	0.71	0.70	0.72 - 0.73
F/F^*	0.70	2.00	0.50	1.54	0.62 - 0.64
G/G^*	0.98	-	-	7.00	0.97
C_2/C_2^*	0.41	0.00	-	-	0.51 - 0.52
E_2/E_2^*	-	-	-	-	0.78 - 0.84
F_2/F_2^*	-	-	-	-	0.64 - 0.68

charmed resonances can saturate the inclusive semileptonic rate. Of course, at the same time model results for $B \to D$ and $B \to D^*$ decays should agree with experiment. To answer this question we rescale our results, given in Tables 5.1 through 5.3, by changing V_{cb} in such a way that rates for $B \to D$ and $B \to D^*$ decays are consistent with experimental numbers, i.e., with the central values of (5.2) and (5.3). Then for the total resonant contribution to the inclusive semileptonic rate we find

$$\sum_{D^{**}} \mathcal{B}(B \to D^{**} e \bar{\nu}_e) = \begin{cases} 7.43\,|V_{cb}/0.033|^2\,(\tau_B/1.50ps)\% & \text{(SSEQ)} \\ 7.67\,|V_{cb}/0.034|^2\,(\tau_B/1.50ps)\% & \text{(RFTM)} \\ 7.58\,|V_{cb}/0.034|^2\,(\tau_B/1.50ps)\% & \text{(SEVC)} \\ 7.87\,|V_{cb}/0.035|^2\,(\tau_B/1.50ps)\% & \text{(SFTM)} \\ 7.83\,|V_{cb}/0.035|^2\,(\tau_B/1.50ps)\% & \text{(SVSC)} \\ 8.06\,|V_{cb}/0.036|^2\,(\tau_B/1.50ps)\% & \text{(DESC)} \end{cases} . \quad (5.29)$$

Similarly, rescaling results obtained in other models (Table 5.4), we obtain

$$\sum_{D^{**}} \mathcal{B}(B \to D^{**} e \bar{\nu}_e) = \begin{cases} 7.75\,|V_{cb}/0.041|^2\,(\tau_B/1.50ps)\% & \text{(SISM)} \\ 7.46\,|V_{cb}/0.035|^2\,(\tau_B/1.50ps)\% & \text{(ISGW2)} \\ 7.97\,|V_{cb}/0.041|^2\,(\tau_B/1.50ps)\% & \text{(CNP)} \\ 8.03\,|V_{cb}/0.036|^2\,(\tau_B/1.50ps)\% & \text{(SHJL)} \end{cases} . \quad (5.30)$$

Recalling that the experimental inclusive semileptonic rate is $(10.49 \pm 0.46)\%$ [94], it seems that more than 20% of all semileptonic B decays cannot be accounted for with decays into charmed resonances, no matter which model one uses. One may seek the possible explanation of the difference between theory and experiment in the continuum contributions to the inclusive semileptonic rate.[5] In fact, the most recent measurement of V_{cb} from $B^0 \to D^{*-} e^+ \nu_e$ decays by DELPHI [105] supports that conclusion.[6] This measurement determined the ratio of the branching fractions

$$\frac{\mathcal{B}(B^+ \to D^{*-} l^+ \nu_l X)}{\mathcal{B}(B^+ \to D^{*-} l^+ \nu_l X) + \mathcal{B}(B^0 \to D^{*-} l^+ \nu_l)} = 0.19 \pm 0.12 \ , \quad (5.31)$$

and also the total branching ratio for $B^0 \to D^{*-} l^+ \nu_l$ decays,

$$\mathcal{B}(B^0 \to D^{*-} l^+ \nu_l) = (5.47 \pm 0.69)\% \ . \quad (5.32)$$

In the above, X represents the additional non-charmed hadrons, such as π^+. Even though the errors given in (5.31) are large, the central value of 0.19, which corresponds to the branching fraction for $B^+ \to D^{*-} l^+ \nu_l X$ decays of about

[5] By continuum contributions we mean decays which also involve other non-charmed particles.

[6] In [105] it was found $V_{cb} = (38.5 \pm 2.1 \pm 2.5 \pm 1.7) \times 10^{-3}$.

1.2%, suggests that the non-resonant contributions to the inclusive semileptonic B rate may be large, and that decays involving additional pions could account for the missing semileptonic B decays. If this turns out to be true, then there is no disagreement between theory and experiment. If, on the other hand, the non-resonant contributions to the inclusive semileptonic rate turn out to be small, then it remains an open question whether inconsistency between theoretical predictions and measurement can be explained with inadequacy of hadronic models we used here (or the ones that can be found in the literature).

As already mentioned, within the HQET framework the only model dependent input for the decays $C \to C, C^*$ and $C \to F, F^*$ are the unknown IW functions. For these decays the relative uncertainty introduced by using a particular model should be smaller than for the decays where D^{**} mass is not known, and we had to use model predictions. From the last two columns of Table 5.4 one can see that this is indeed the case. Nevertheless, all results obtained from the six hadronic models are comparable. The uncertainty by using a specific model is even smaller if only models with spin are considered.[7] Also note that ratios of the two exclusive decay widths for members of the same doublet are all consistent (Table 5.5), which is a consequence of application of HQET.

[7]One of the reasons why spinless models we considered in most cases give either the smallest or the largest branching ratio for a particular decay, is that these models do not distinguish between the two different doublets with the same $L \neq 0$.

5.4 Fractional Semileptonic Decay Rates

The exclusive decay rates discussed earlier suffer from a variety of theoretical oversimplifications. Some of the things which were not taken into account are QCD corrections, spectator effects, and deviations from exact heavy quark symmetry. In addition, there are several parameters which need to be specified before definite predictions can be made. Among these are the CKM parameter V_{cb}, the b-quark lifetime, and the quark masses.

Many of the above problems can be reduced by considering fractions of the inclusive $b \to ce\bar{\nu}_e$ rate. In particular, V_{cb} exactly cancels. Also, since the sum of the exclusive rates equals the inclusive rate, and since the inclusive calculation is structurally similar to the exclusive ones, there should be some cancellation of the QCD, spectator corrections, and heavy quark mass dependence. Since the inclusive rate has been measured, one can directly compare these fractional predictions with experiment in several cases.

The inclusive spectator model decay rate for $b \to ce\bar{\nu}_e$ is [106–108]

$$\Gamma(b \to ce\bar{\nu}_e) = \frac{G_F^2 m_b^5 |V_{cb}|^2}{192\pi^3} I(\frac{m_c^2}{m_b^2}, 0, 0) \ , \tag{5.33}$$

where

$$I(x,0,0) = (1-x^2)(1-8x+x^2) - 12x^2 \ln x \ . \tag{5.34}$$

If for the moment we ignore the oversimplifications of the above inclusive model and assume $V_{cb} = 0.040$, the b-quark lifetime of $\tau_b = 1.5 \times 10^{-12} s$, and the quark masses of the six models from Chapter 4, we find the total branching

ratios

$$\mathcal{B}(b \to ce\bar{\nu}_e) = \begin{cases} 11.83\,|V_{cb}/0.040|^2\,(\tau_B/1.50ps)\% & \text{(SSEQ)} \\ 11.11\,|V_{cb}/0.040|^2\,(\tau_B/1.50ps)\% & \text{(RFTM)} \\ 11.52\,|V_{cb}/0.040|^2\,(\tau_B/1.50ps)\% & \text{(SEVC)} \\ 11.23\,|V_{cb}/0.040|^2\,(\tau_B/1.50ps)\% & \text{(SFTM)} \\ 11.18\,|V_{cb}/0.040|^2\,(\tau_B/1.50ps)\% & \text{(SVSC)} \\ 10.32\,|V_{cb}/0.040|^2\,(\tau_B/1.50ps)\% & \text{(DESC)} \end{cases} . \qquad (5.35)$$

The above numbers are in general (except for DESC) slightly larger than the experimental branching ratio of $(10.49 \pm 0.46)\%$ [94]. However, one should keep in mind that the predicted value is very sensitive to the choice of V_{cb}, τ_b, and quark masses.

One plausibly assumes that ratio of the exclusive branching ratios to the inclusive one,

$$R^{**} = \frac{\mathcal{B}(B \to D^{**}e\bar{\nu}_e)}{\mathcal{B}(b \to ce\bar{\nu}_e)} , \qquad (5.36)$$

will be more accurate than either of these separately. We first apply this idea to $B \to D$ and $B \to D^*$ decays. From (5.1), (5.2) and (5.3) we find experimental fractions,

$$R_D = 0.19 \pm 0.06 , \qquad (5.37)$$

$$R_{D^*} = 0.49 \pm 0.10 . \qquad (5.38)$$

From Tables 5.1, 5.2 and 5.3 one can see that our models predict R_D in the range from 0.23 to 0.24, and R_{D^*} in the range of 0.61 to 0.64. These values are slightly higher than the measured ones.

The fraction of semileptonic decay into final states other than D or D^* is by (5.37) and (5.38)

$$\begin{aligned} R(D^{**} \text{ other than } D \text{ and } D^*) &= 1 - (R_D + R_{D^*}) \\ &= 0.32 \pm 0.16 \, . \end{aligned} \tag{5.39}$$

Again, from Tables 5.1 through 5.3 we find that our models for this fraction imply range from 0.12 to 0.15, which is a factor of two smaller than the experimental number.

It is also interesting to observe that single excited charmed states alone are nearly consistent with accounting for the entire inclusive semileptonic decay fraction, regardless of the model we used. As a more direct way of seeing this note the total fractional percentage in Tables 5.1 through 5.3. The predicted fraction into all D^{**} states is larger than 90% for all models we considered.

5.5 Conclusion

In this chapter we have investigated semileptonic B decay into higher charmed mesons. Within a HQET framework we have evaluated branching ratios for $B \to D^{**} e \bar{\nu}_e$, where the D^{**} are all S and P-wave mesons, D-wave mesons with $j = 3/2$, and some of their radial excitations.

Our numerical calculations are based upon six hadronic models, which not only yield a good description of the known spin-averaged heavy-light mesons, but are also self-consistent in terms of the HQET sum rules. This is in fact the main difference between this calculation and the one presented in [100]. There, SEVC, SFTM and DESC models were also used, although with different

parameters for SEVC and SFTM.[8] Because of that, SEVC and SFTM results obtained here are different than the ones given in [100].[9] The numbers for $C \to C$ and $C \to C^*$ transitions we obtained in this work are about 25% higher than the ones given in [100]. On the other hand, for the inelastic decays we found branching ratios somewhat smaller than the ones quoted in [100].

We have also compared our results with experiment and with other calculations available in the literature. We found significant disagreements with [101] and [103] in ratios of decay widths for B decays into the members of the same D^{**} doublet, and our results are in general significantly larger than the ones obtained in [50] and [102]. If we rescale all our predictions by changing V_{cb} in such a way that results for $C \to C$ and $C \to C^*$ transitions are brought in agreement with experiment, we find that more than 20% of all semileptonic B decays cannot be accounted for with decays into charmed resonances, no matter which model one uses. It remains an open question whether this difference between theory and experiment can be explained with the non-resonant contributions to the inclusive semileptonic rate, which is suggested by the recent experimental data. If this turns out not to be the case, a possible explanation would be inadequacy of hadronic models we used here (or the ones that can be found in the literature). Nevertheless, it is also interesting to note that we find that more than 90% of the inclusive spectator model $b \to ce\bar{\nu}_e$ rate can

[8] In [100] constant c was absorbed into the heavy quark mass for both SEVC and SFTM, which led to inconsistency of these two models with the Voloshin sum rule.

[9] Because of the higher accuracy of numerical calculations performed in this work, results with DESC given here may also differ slightly (in the last decimal place) from the ones given in [100].

be accounted by B meson semileptonic decays into a single excited charmed resonance.

In this chapter we considered only the helicity averaged decay rates for semileptonic B decays. However, the same Isgur-Wise form factors calculated here also appear in the calculation of partial rates into polarized current components, and in the angular decay distributions [109,110]. These angular correlation measurements would provide additional information on the decay dynamics, which would be useful in determining the validity of various theoretical models.

Chapter 6

Radiative Rare B Decays

6.1 Introduction

Flavor changing neutral current transitions involving the B meson provide a unique opportunity to study the electroweak theory at higher orders. Although transitions like $b \to s\gamma$, $b \to se^+e^-$, and $b \to sg$ vanish at the tree level, they can be described by one loop ("penguin") diagrams, in which a W^- is emitted and reabsorbed [111–113]. These processes occur at a rate small enough to be sensitive to physics beyond the Standard Model [114]. Similar flavor violating processes in the K meson system have the disadvantage that nonperturbative long distance effects are quite large, and it is difficult to extract the quark level physics from the well-known processes like $K^+ \to \pi^+e^+e^-$.

Among all rare B decays, radiative processes $B \to X_s\gamma$ (especially decay $B \to K^*(892)\gamma$) have received an increasing attention, because of the experimental measurement of the $B \to K^*(892)\gamma$ exclusive branching ratio [115],

$$\mathcal{B}(B \to K^*(892)\gamma) = (4.5 \pm 1.5 \pm 0.9) \times 10^{-5} \ , \tag{6.1}$$

which has been recently updated [116] to

$$\mathcal{B}(B \to K^*(892)\gamma) = (4.3^{+1.1}_{-1.0} \pm 0.6) \times 10^{-5} \ , \tag{6.2}$$

and also of the inclusive rate [117],

$$\mathcal{B}(B \to X_s\gamma) = (2.32 \pm 0.57 \pm 0.35) \times 10^{-4} \ . \tag{6.3}$$

Several methods have been employed to predict exclusive $B \to K^*(892)\gamma$ decay rate: HQET [47,118], QCD sum rules [119–124], quark models [125–135], bound state resonances [136], and Lattice QCD [137–140]. The theoretical uncertainty, which was originally of two orders of magnitude, has been greatly reduced in the more recent studies. However, there is still a large spread between different results.

In this chapter we reexamine contributions of higher K resonances[1] to the radiative rare decays $b \to s\gamma$ in the limit where both b and s quark are considered heavy [58]. Even though there is no doubt that s quark is not heavy in the sense that its mass is much larger than Λ_{QCD}, it is still heavier than u and d quarks. Considering K^{**} resonances as heavy-light mesons considerably simplifies the analysis of the radiative rare B decays, and is useful for organizing phenomenology.

In Chapter 3 we showed that form factor definitions used in [47] are inconsistent with the covariant trace formalism [16,32–34]. Because of that, our results, which are obtained with form factors given in Chapter 3, are in significant disagreement with those of Ali et al. [47], and in excellent agreement with experimental results. In order to clearly identify the differences implied by correct form factor definitions, we have also used nonrelativistic quark model for the wave functions of the light degrees of freedom. Our results show that the ratio of the exclusive $B \to K^{**}\gamma$ to the inclusive decay rate

[1] Generic K resonance is denoted as K^{**}.

$B \to X_s\gamma$ was underestimated for the channel $B \to K^*(892)\gamma$ ($(16.8 \pm 6.4)\%$ as opposed to (3.5-12.2)% from [47]), and significantly overestimated for the decay $B \to K_2^*(1430)\gamma$ ($(6.2 \pm 2.9)\%$ as opposed to (17.3-37.1)% from [47]). We emphasize that our prediction for the decay $B \to K^*(892)\gamma$ is in agreement with experimental result of $(19 \pm 5)\%$. Although other exclusive decays have not yet been identified, we have compared with experiment the contribution from the eight $B \to K^{**}\gamma$ decays to the inclusive $B \to X_s\gamma$ mass distribution.

6.2 Theory of $B \to K^{**}\gamma$ Decays

The effective Hamiltonian for the decays $B \to X_s\gamma$ can be found in many places, e.g., [141–143]. It is derived by integrating out the top quark and W boson at the same scale $\mu \approx M_W$. An appropriate operator basis for the effective Hamiltonian consists of four-quark operators and the magnetic moment type operators of dimension six ($\mathcal{O}_1$-$\mathcal{O}_8$). Higher dimensional operators are suppressed by powers of the masses of the heavy particles. For the $B \to K^{**}\gamma$ decays only the operator $\mathcal{O}_7$ contributes, so that

$$H_{eff} = -\frac{4G_F}{\sqrt{2}} V_{tb}V_{ts}^* C_7(m_b)\mathcal{O}_7(m_b) \ . \tag{6.4}$$

Here, $\mathcal{O}_7$ is given by

$$\mathcal{O}_7 = \frac{e}{32\pi^2} F_{\mu\nu}[m_b \bar{s}\sigma^{\mu\nu}(1+\gamma_5)b + m_s \bar{s}\sigma^{\mu\nu}(1-\gamma_5)b] \ , \tag{6.5}$$

with $\sigma^{\mu\nu} = \frac{i}{2}[\gamma^\mu, \gamma^\nu]$. The explicit expression for the Wilson coefficient $C_7(m_b)$ as a function of m_t^2/M_W^2 can be found in [143,144]. The value of C_7 can be calculated perturbatively at the mass scale $\mu = M_W$. The evolution from

M_W down to a mass scale $\mu = m_b$ introduces large QCD corrections. This procedure also introduces large theoretical uncertainties, primarily due to the choice of the renormalization scale μ (taken above as m_b), which can be as large as 25% [143].

As proposed in [47], we evaluate the hadronic matrix element of $\mathcal{O}_7$ between a B meson in the initial state, and a generic K^{**} meson in the final state, in the heavy quark limit for the b and s quarks. In Chapter 3 we have seen that matrix elements of bilinear currents of two heavy quarks can be conveniently calculated by taking traces of matrices describing meson states. Using (2.41), we can write

$$\langle K^{**}(v',\varepsilon')\gamma|\mathcal{O}_7(m_b)|B(v)\rangle = \frac{e}{16\pi^2}\eta_\mu q_\nu \mathrm{Tr}[\bar{M}'(v',\varepsilon')\Omega^{\mu\nu}M(v)]\mathcal{M}_l(\omega) \ , \quad (6.6)$$

where the factor $q_\nu = m_B v_\nu - m_{K^{**}} v'_\nu$ came from the derivative in the field strength $F_{\mu\nu}$ of (6.5). Matrices M' and M are given in (2.40), function $\mathcal{M}_l$ is defined in (2.42), η_μ is the photon polarization vector, and

$$\Omega^{\mu\nu} = m_B \sigma^{\mu\nu}(1+\gamma_5) + m_{K^{**}}\sigma^{\mu\nu}(1-\gamma_5) \ . \quad (6.7)$$

Expression (6.6) can be further simplified using $\not{v} M(v,\varepsilon) = M(v,\varepsilon)$.

Now, using the mass shell condition of the photon ($q^2 = 0$), and polarization sums for spin one and spin two particles given in (2.46) and (2.47), we obtain the following decay rates [47]:

$$\Gamma(B \to K^*(892)\gamma) = \Omega|\xi_C(\omega)|^2 \frac{1}{r}[(1-r)^3(1+r)^5(1+r^2)] \ , \quad (6.8)$$

$$\Gamma(B \to K_1(1270)\gamma) = \Omega|\xi_E(\omega)|^2 \frac{1}{r}[(1-r)^5(1+r)^3(1+r^2)] \ , \quad (6.9)$$

$$\Gamma(B \to K_1(1400)\gamma) = \Omega|\xi_F(\omega)|^2 \frac{1}{24r^3}[(1-r)^5(1+r)^7(1+r^2)] \ , \quad (6.10)$$

$$\Gamma(B \to K_2^*(1430)\gamma) = \Omega|\xi_F(\omega)|^2 \frac{1}{8r^3}[(1-r)^5(1+r)^7(1+r^2)] \ , \quad (6.11)$$

$$\Gamma(B \to K^*(1680)\gamma) = \Omega|\xi_G(\omega)|^2 \frac{1}{24r^3}[(1-r)^7(1+r)^5(1+r^2)] \ , \quad (6.12)$$

$$\Gamma(B \to K_2(1580)\gamma) = \Omega|\xi_G(\omega)|^2 \frac{1}{8r^3}[(1-r)^7(1+r)^5(1+r^2)] \ , \quad (6.13)$$

$$\Gamma(B \to K^*(1410)\gamma) = \Omega|\xi_{C_2}(\omega)|^2 \frac{1}{r}[(1-r)^3(1+r)^5(1+r^2)] \ , \quad (6.14)$$

$$\Gamma(B \to K_1(1650)\gamma) = \Omega|\xi_{E_2}(\omega)|^2 \frac{1}{r}[(1-r)^5(1+r)^3(1+r^2)] \ . \quad (6.15)$$

In the above we used abbreviations

$$r = \frac{m_{K^{**}}}{m_B} \ , \quad (6.16)$$

$$\Omega = \frac{\alpha}{128\pi^4} G_F^2 m_b^5 |V_{tb}|^2 |V_{ts}|^2 |C_7(m_b)|^2 \ . \quad (6.17)$$

The argument of the IW functions is fixed by the mass shell condition of the photon ($q^2 = 0$),

$$\omega = \frac{1+r^2}{2r} \ . \quad (6.18)$$

Note that in the expressions for the decay rates (6.8)-(6.15) given in [47], a factor of $(1-r^2)$ was omitted. Also, as observed in [47], since decays into the states belonging to the same spin symmetry doublet are described by the same IW function, and since in the heavy quark limit the two members of a spin doublet are degenerate in mass, from (6.10) and (6.11), and from (6.12) and (6.13), one has

$$\Gamma(B \to K_2^*(1430)\gamma) \approx 3\Gamma(B \to K_1(1400)\gamma) \ , \quad (6.19)$$

$$\Gamma(B \to K_2(1580)\gamma) \approx 3\Gamma(B \to K_1(1680)\gamma) \ . \quad (6.20)$$

These relations are only approximate due to a large breaking of the spin symmetry for the s quark.

6.3 Model for the IW Functions

Even though we also use nonrelativistic quark model for numerical estimates, our calculation differs significantly from [47] in evaluation of the IW form factors needed for the decay rates. In Chapter 3 we have found that correct form factor definitions should include a Lorentz invariant factor in front of the overlap of the two wave functions describing the initial and the final states of the LDF. Relevant expressions for the IW functions are given in (3.37), (3.40), (3.43), and (3.46).

Nonrelativistic quark model for calculations of the unknown form factors was advocated in [17] within the ISGW model. It is basically the Schrödinger equation with

$$V(r) = -\frac{4}{3}\frac{\alpha_s}{r} + br + c \; . \tag{6.21}$$

With a sensible choice of parameters, this simple model gives reasonable spin-averaged spectra of $b\bar{d}$ and $s\bar{d}$ mesons up to $L = 2$. However, instead of just using a single harmonic oscillator wave function for the radial wave function of the LDF (as was done in [47]), we numerically solve the Schrödinger equation. To determine the parameters of the model, we fix $b = 0.18\ GeV^2$ (which was also used in [17]), and vary α_s and c for a given value of $m_{u,d}$ (in the range 0.30-0.35 GeV), and m_s (in the range 0.5-0.6 GeV), until a reasonably good description of the spin-averaged spectra of K meson states is obtained.

Following this procedure, we find that α_s ranges from 0.37 to 0.48, while c takes values from $-0.83\ GeV$ to $-0.90\ GeV$. These parameters are in good agreement with the original ISGW values [17] ($\alpha_s = 0.50$ and $c = -0.84\ GeV$ for $m_{u,d} = 0.33\ GeV$ and $m_s = 0.55$). We emphasize that the original ISGW parameters give results that are well inside the ranges quoted here for all decays. By varying the c and b quark masses we could also obtain good spin-averaged description of the B and D mesons. However, to be consistent with heavy quark symmetry, the wave function for the B meson was chosen to be the same as the one obtained for the spin-averaged (ground state for $L = 0$) K and $K^*(892)$ mesons.

To completely define our procedure, we have to specify how we determine the LDF energy E_M in a meson M. In [47] for a given K^{**} meson the LDF energy was defined as

$$E_{K^{**}} = \frac{m_{K^{**}} * m_{u,d}}{m_s + m_{u,d}} \ . \tag{6.22}$$

This definition was proposed to account for the fact that s quark is not particularly heavy. On the other hand, a definition that is consistent with HQS is

$$E_{K^{**}} = m_{K^{**}} - m_s \ . \tag{6.23}$$

It should be noted that these two expressions are not equivalent in the heavy quark limit. In order to explore the sensitivity of our results on the choice of $E_{K^{**}}$, we have repeated all calculations employing both of these two definitions, and in the final results we have quoted the broadest possible range obtained for the form factors (and for all other results). The LDF energy for the B meson has been taken to be the same as the one for the $K^*(892)$ meson, which

is consistent with HQS. It turns out that this is actually a very reasonable assumption. The range of E_M that was used here for B and $K^*(892)$ meson was from 0.296 GeV to 0.396 GeV. On the other hand, from the CLEO data on semileptonic B decays [52], and the LQCD heavy-light wave function [57], it was estimated that in B systems E_M ranges from 0.266 GeV to 0.346 GeV [56].

We believe that the procedure outlined above enables us to estimate a reasonable range for the unknown IW form factors in a physically more acceptable way than it was done in [47], by simply varying the scale parameter of the single harmonic oscillator wave function.

6.4 Our Results and Comparison with Previous Investigations

In Table 6.1 we present our results [58] for the range of (absolute) values of the form factors at the indicated value of ω, for the ratio $R = \Gamma(B \to K^{**}\gamma)/\Gamma(B \to X_s\gamma)$, and for the branching ratio $\mathcal{B}(B \to K^{**}\gamma)$, for the various K^{**} mesons. The inclusive branching ratio $B \to X_s\gamma$ is usually taken to be QCD improved quark decay rate for $b \to s\gamma$, which can be written as [141,143,144]

$$\Gamma(B \to X_s\gamma) = 4\Omega(1 - \frac{m_s^2}{m_b^2})^3(1 + \frac{m_s^2}{m_b^2}) \ . \tag{6.24}$$

The leading log prediction for $\mathcal{B}(b \to s\gamma)$ is $(2.8 \pm 0.8) \times 10^{-4}$ [143,144], where the uncertainty is due to the choice of the QCD scale. The next-to-leading order terms that have been calculated tend to reduce the prediction to about

Table 6.1: Results [58] for the range of absolute values of the form factors at indicated value of ω, for the ratio $R = \Gamma(B \to K^{**}\gamma)/\Gamma(B \to X_s\gamma)$, and for the branching ratio $\mathcal{B}(B \to K^{**}\gamma)$, for the various K^{**} mesons. For the calculation of branching ratios we used the value $\Gamma(B \to X_s\gamma) = 2.8 \times 10^{-4}$ [143].

Meson	State	J_j^P	ω	ξ	$R[\%]$	$\mathcal{B} \times 10^5$
K	C	$0^-_{1/2}$		forbidden		
$K^*(892)$	C^*	$1^-_{1/2}$	3.031	0.289 ± 0.057	16.8 ± 6.4	4.71 ± 1.79
$K^*(1430)$	E	$0^+_{1/2}$		forbidden		
$K_1(1270)$	E^*	$1^+_{1/2}$	2.194	0.277 ± 0.053	4.3 ± 1.6	1.20 ± 0.44
$K_1(1400)$	F	$1^+_{3/2}$	2.016	0.171 ± 0.040	2.1 ± 0.9	0.58 ± 0.26
$K_2^*(1430)$	F^*	$2^+_{3/2}$	1.987	0.175 ± 0.043	6.2 ± 2.9	1.73 ± 0.80
$K^*(1680)$	G	$1^-_{3/2}$	1.702	0.241 ± 0.035	0.5 ± 0.2	0.15 ± 0.04
$K_2(1580)$	G^*	$2^-_{3/2}$	1.820	0.203 ± 0.024	1.7 ± 0.4	0.46 ± 0.11
$K(1460)$	C_2	$0^-_{1/2}$		forbidden		
$K^*(1410)$	C_2^*	$1^-_{1/2}$	2.003	0.175 ± 0.014	4.1 ± 0.6	1.14 ± 0.18
$K_0^*(1950)$	E_2	$0^+_{1/2}$		forbidden		
$K_1(1650)$	E_2^*	$1^+_{1/2}$	1.756	0.229 ± 0.040	1.7 ± 0.6	0.47 ± 0.16
				total	37.4 ± 13.6	10.44 ± 3.78

1.9×10^{-4} [138]. Both of these predictions are in excellent agreement with the recent experimental result of $\mathcal{B}(b \to s\gamma) = (2.32 \pm 0.57 \pm 0.35) \times 10^{-4}$ [117]. For the numerical values of the $B \to K^{**}\gamma$ branching ratios given in Table 6.1 we used the leading log result of $\mathcal{B}(b \to s\gamma) = 2.8 \times 10^{-4}$.

In order to make comparison of our calculation with previous investigations easier, we have tabulated our results together with results of [47] and [127] in Table 6.2. As far as we know, except for [58] these two papers are the only

Table 6.2: Our results [58] for the ratios $R = \Gamma(B \to K^{**}\gamma)/\Gamma(B \to X_s\gamma)$, compared with the previous work done in [47] and [127]. Note that in the quark model calculations with the L-S coupling scheme, decay into the $^1P_1$ state is forbidden, because $\mathcal{O}_7$ is a spin-flip operator, and $K_1(1270)$ and $K_1(1400)$ are mixtures of $^1P_1$ and $^3P_1$ states. In [127] $^3P_1$ state had $R = 6\%$.

Meson	State	J_j^P	R[%] (This Work [58])	R[%] (Ref. [47])	R[%] (Ref. [127])
K	C	$0^-_{1/2}$		forbidden	
$K^*(892)$	C^*	$1^-_{1/2}$	16.8 ± 6.4	3.5 - 12.2	4.5
$K^*(1430)$	E	$0^+_{1/2}$		forbidden	
$K_1(1270)$	E^*	$1^+_{1/2}$	4.3 ± 1.6	4.5 - 10.1	forbidden/6.0
$K_1(1400)$	F	$1^+_{3/2}$	2.1 ± 0.9	6.0 - 13.0	forbidden/6.0
$K_2^*(1430)$	F^*	$2^+_{3/2}$	6.2 ± 2.9	17.3 - 37.1	6.0
$K^*(1680)$	G	$1^-_{3/2}$	0.5 ± 0.2	1.0 - 1.5	0.9
$K_2(1580)$	G^*	$2^-_{3/2}$	1.7 ± 0.4	4.5 - 6.4	4.4
$K(1460)$	C_2	$0^-_{1/2}$		forbidden	
$K^*(1410)$	C_2^*	$1^-_{1/2}$	4.1 ± 0.6	7.2 - 10.6	7.3
$K_0^*(1950)$	E_2	$0^+_{1/2}$		forbidden	
$K_1(1650)$	E_2^*	$1^+_{1/2}$	1.7 ± 0.6	-	-
		total	37.4 ± 13.6	44.1 - 90.9	29.1

ones that have dealt with radiative rare B decays into higher K-resonances. There has been much more work done on the decay $B \to K^*(892)\gamma$. We have tabulated some of those results in Table 6.3, where one can see that predictions for this particular ratio range from a 0.7% [133] to 97.0% [125]. The data suggest a value of $(19 \pm 5)\%$. Note that our result of $(16.8 \pm 6.4)\%$ is consistent with the data, unlike the values quoted in [47] and [127]. As far as decays into higher K resonances are concerned, our results are in general in

Table 6.3: Our result [58] for the ratio $R = \Gamma(B \to K^*\gamma)/\Gamma(B \to X_s\gamma)$, compared with several previous calculations.

Author(s)	Reference	R[%]
O'Donnell (1986)	[125]	97.0
Deshpande et al. (1988)	[126]	6.0
Dominguez et al. (1988)	[119]	28.0 ± 11.0
Altomari (1988)	[127]	4.5
Deshpande and Trampetić (1989)	[130]	6.0 - 14.0
Aliev et al. (1990)	[120]	39.0
Ali and Mannel (1991)	[118]	28.0 - 40.0
Du and Liu (1992)	[131]	69.0
Faustov and Galkin (1992)	[132]	6.5
El-Hassan and Riazuddin (1992)	[133]	0.7 - 12.0
O'Donnell and Tung (1993)	[128]	10.0
Colangelo et al. (1993)	[121]	17.0 ± 5.0
Ali et al. (1993)	[47]	3.5 - 12.2
Ali and Greub (1993)	[129]	13.0 ± 3.0
Ali et al. (1994)	[123]	16.0 ± 5.0
Ball (1994)	[122]	20.0 ± 6.0
Narison (1994)	[124]	16.0 ± 4.0
Holdom and Sutherland (1994)	[134]	17.0 ± 4.0
Atwood and Soni (1994)	[136]	1.6 - 2.5
Bernard et al. (1994)	[137]	$6.0 \pm 1.2 \pm 3.4$
Ciuchini et al. (1994)	[138]	23.0 ± 9.0
Bowler et al. (1994)	[139]	$9.0 \pm 3.0 \pm 1.0$
Burford et al. (1995)	[140]	15.0 - 35.0
Tang et al. (1995)	[135]	10.0 - 12.0
Veseli and Olsson (1996)	[58]	16.8 ± 6.4

much better agreement with [127] than with [47]. In particular, the authors of [47] emphasized a large branching ratio for the decay $B \to K_2^*(1430)\gamma$ ((17.3-37.1)% of the inclusive rate $\Gamma(B \to X_s\gamma)$), while our results indicate a 3-6 times smaller value of $(6.2 \pm 2.9)\%$, a result which agrees with the one quoted in [127] (6.0%). Also note that our numerical results from Table 6.2 support relations (6.19) and (6.20).

With the exception of the $K^*(892)\gamma$ channel, no other exclusive radiative processes have been identified so far. However, the inclusive radiative $B \to X_s\gamma$ mass distribution has been measured by CLEO [117], and is shown in Figure 6.1. We have normalized experimental data so that the integrated distribution gives unity. The $K^*(892)$ peak is evident, but the higher mass contribution are not resolved. We have attempted to model this inclusive distribution by considering the contributions from each of the exclusive $K^{**}\gamma$ channels considered here (and given in Table 6.2).

In order to compare our results to experiment, we replace a given $R_{K^{**}}$ by a mass distribution reflecting the finite total width $\Gamma_{K^{**}}$ of the K^{**} resonance [31],

$$\frac{dR(m_{X_s})}{dm_{X_s}} = \sum_{K^{**}} \frac{R_{K^{**}}}{\pi} \frac{\Gamma_{K^{**}}/2}{(m_{X_s} - m_{K^{**}})^2 + (\Gamma_{K^{**}}/2)^2} \ . \tag{6.25}$$

The integrated distribution gives

$$\int \frac{dR(m_{X_s})}{dm_{X_s}} dm_{X_s} = \sum_{K^{**}} R_{K^{**}} \ . \tag{6.26}$$

The total resonance contribution is shown in Figure 6.1 with the solid line, and can be compared to the experimental inclusive $B \to X_s\gamma$ mass distribution. The area of the resonance curve is 37.4% of the total inclusive rate (see Table

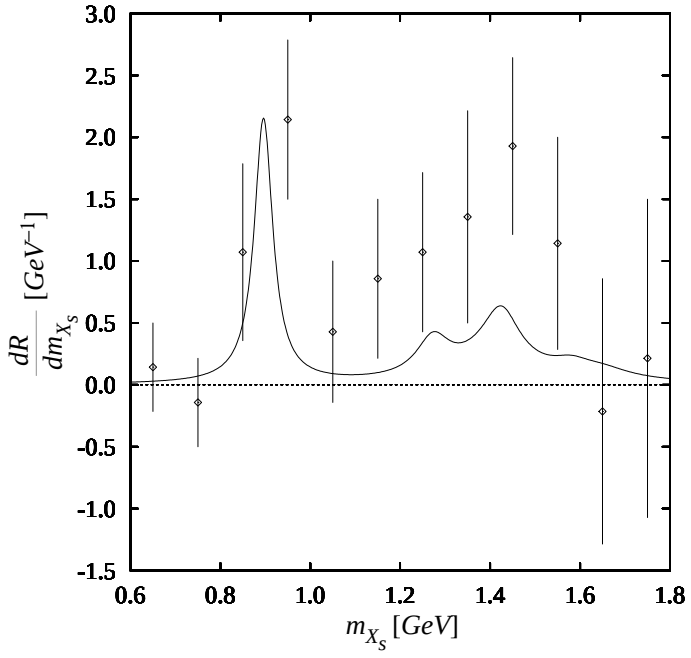

Figure 6.1: The experimental inclusive $B \to X_s\gamma$ mass distribution measured at CLEO [117]. The data have been normalized to unity. The curve [58] is the sum of the exclusive $K^{**}\gamma$ channels from Table 6.1 as calculated by (6.25).

6.1 or 6.2). We see that the general shape is correct, but it is difficult to make more quantitative statements due to the large errors involved.

6.5 Conclusion

In this chapter we have reexamined predictions of heavy quark symmetry for the radiative rare decays of B mesons into higher K resonances [58]. An earlier calculation [47] suggested a substantial fraction ((17.3-37.1)%) of the inclusive $b \to s\gamma$ branching ratio going into the $K_2^*(1430)$ channel, and only (3.5-12.2)% going into the $K^*(892)$ channel. Even though we also used nonrelativistic quark model, our calculation yields fractions of $(16.8 \pm 6.4)\%$ and $(6.2 \pm 2.9)\%$

for $K^*(892)$ and $K_2^*(1430)$ channels, respectively. Note that experimental results favor the value of $(19 \pm 5)\%$ for the $K^*(892)$ channel. Besides a more careful treatment of the uncertainty in the wave functions of the light degrees of freedom, our calculation differs from [47] only in employing form factor definitions [42] that are consistent with the covariant trace formalism, and are given in Chapter 3. As a consequence of that, our results for all decay channels significantly differ from [47]. The contribution of the eight $K^{**}\gamma$ channels to the inclusive $B \to X_s\gamma$ mass distribution was compared with experiment. We find the general shape of the mass spectrum to be correct, but due to the large errors involved one cannot reach more quantitative conclusions.

Despite the fact that one cannot argue that s quark is heavy, in the sense that its mass is much larger than the QCD scale, it is still heavier than u and d quarks. Therefore, it is not completely unjustified to perform the analysis of the radiative rare B decays into K^{**} resonances in the limit where K^{**} are considered as heavy-light mesons, even though one should not take numerical results too seriously. Nevertheless, this limit simplifies the analysis considerably and, if nothing else, it is useful in organizing phenomenology of radiative rare B decays.

Chapter 7

Conclusions

There is no doubt that heavy quark symmetry (HQS) and corresponding effective theory (HQET) represent a large step forward in our understanding of QCD. Nevertheless, there is only so much one can learn from symmetry arguments. For example, in the heavy quark limit HQS reduces six unknown form factors describing semileptonic $B \to D$ and $B \to D^*$ decays to a single form factor, the famous Isgur-Wise function. Even though some of the properties of this function can be deduced, it still cannot be calculated from first principles. Instead, one has to rely on some model of strong interactions. Therefore, the discovery of HQS has not eliminated the need for reliable and self-consistent hadronic models. This is in fact the principal motivation for this work.

There were two main areas which were investigated in this thesis. The first one concerns the problem of extraction of the unknown form factors, describing decays of heavy-light mesons, from a given model of strong interactions. It is reasonable to assume that these form factors will be related to the overlap of the wave functions of the light degrees of freedom (LDF) in the mesons before and after the decay. However, in defining form factors one has to be very careful, since definitions for different form factors may involve different

kinematical factors, which must be taken into account. By comparing the matrix elements of heavy quark currents calculated from the HQET covariant trace formalism (CTF), with the ones calculated in the ordinary wave function approach, we managed to find form factor definitions consistent with CTF. In order to extract form factors from a given bound state model (in the valence quark approximation), we expressed the LDF overlaps in terms of their rest frame wave functions and energies. Our results, especially the ones for the inelastic form factors, considerably differ from the expressions that can be found in the literature.

The second area investigated here was the question of self-consistency of several hadronic models in the heavy quark limit. We used the linear Regge structure of a given model, together with model calculations of the Bjorken and Voloshin sum rules, in order to find parameters which give results consistent with HQET sum rule expectations. We emphasize that the aim of our analysis was not to determine whether a particular model is right or wrong in terms of a particular equation, type of confinement, or specific potential it employs. Instead, our goal was to show how one can construct a model which not only yields a good description of the spin-averaged heavy-light spectrum, but is also consistent with experimental data on the light hadron spectroscopy, and self-consistent with respect to HQET sum rules. In this way, we were able not only to use various hadronic models in order to get information which cannot be obtained from HQET, but also to use HQET to extract information on a specific bound state model.

Putting all of those pieces together, we have used our form factor definitions, together with several hadronic models constructed to be self-consistent with respect to HQET sum rules, for the calculation of semileptonic B decays into higher charmed resonances, within the HQET framework. Our results obtained with six qualitatively different models are comparable for all decays considered. However, we found significant disagreement with existing literature, especially in the magnitude of branching ratios for some decays, and in the ratios of B decays into the members of the same heavy-light doublet. We also compared our results with experiment, and it turned out that our models, as well as none of the ones that can be found in the literature, cannot account for more than 20% of all semileptonic B decays. It remains an open question whether this difference between theory and experiment can be explained with the non-resonant contributions to the inclusive semileptonic rate, which is suggested by the recent experimental data. Otherwise, one possible explanation would be inadequacy of hadronic models we used here (or the ones that can be found in the literature).

As another application of our method of extracting form factors from a given bound state model, we reexamined HQS predictions for the radiative rare decays of B meson into higher K resonances. Even though one cannot argue that s quark is heavy, in the sense that its mass is much larger than the QCD scale, it is still heavier than u and d quarks. Therefore, it is not completely unjustified to perform the analysis of the radiative rare B decays into K^{**} resonances in the limit where K^{**} are considered as heavy-light mesons, even though the numerical results should not be taken too seriously. Nevertheless,

this limit simplifies the analysis considerably and, if nothing else, it is useful in organizing phenomenology of radiative rare B decays. An earlier calculation of $B \to K^{**}\gamma$ decays within HQET framework suggested a substantial fraction of the inclusive $b \to s\gamma$ branching ratio going into the $K_2^*(1430)$ channel, and much smaller fraction going into the $K^*(892)$ channel. Those results were obtained by employing the form factor definitions which are not consistent with CTF. As a consequence of that, our results significantly differ for all decay channels.

There are many directions in which one may proceed further. For example, in this thesis we have considered only the helicity averaged decay rates for semileptonic B decays. However, the same Isgur-Wise form factors we calculated here also appear in the calculation of partial rates into polarized current components, and in the angular decay distributions. These angular correlation measurements would provide additional information on the decay dynamics, which would be useful in determining the validity of various theoretical models. Theoretical study of the non-resonant contributions to the inclusive semileptonic B meson decay rate would probably shed some light on the problem of the missing semileptonic B decays. Another obvious possibility is to perform calculations for B_s semileptonic decays, similar to the one we did for semileptonic B decays. Finally, all results given in this work were obtained in the heavy quark limit. Since the theory of power and radiative corrections in HQET is to a large extent already developed, it would be worth the effort studying symmetry breaking corrections (such as $1/m_Q$ effects), from the point of view of hadronic models.

Appendix A

Numerical Methods

In this Appendix we briefly describe numerical methods used to deal with different hadronic models. For a state with a given angular momentum, all models we considered can be reduced to a set of radial equations involving the radial wave function(s) [53,54,78]. For the sake of simplicity we shall discuss here spinless models, which involve only one radial wave function R_{nL}, although the same method can be generalized to a heavy-light Salpeter and Dirac equations (which involve two radial wave functions) [53], and has also been successfully used for variational solution of the full and the reduced Salpeter equations with arbitrary quark masses [88,146].[1]

The radial equation in a spinless model has the form

$$HR_{nL} = MR_{nL} \ , \tag{A.1}$$

where H and M are the model Hamiltonian and the state mass, respectively. The easiest way to solve (A.1) is to expand radial wave function in terms of some complete set of basis functions $\{e_{iL}\}$, and truncate the expansion to the

[1] The full Salpeter equation with arbitrary quark masses involves as many as four radial wave functions.

first N basis states, i.e.,

$$R_{nL} \simeq \sum_{i=0}^{N-1} c_i e_{iL} \ . \tag{A.2}$$

Multiplying (A.1) from the left by $\int_0^\infty r^2 dr e^*_{jL}(\beta, r)$ (or by $\int_0^\infty p^2 dp e^*_{jL}(\beta, p)$, depending on whether we are working in coordinate or momentum space), we get the $N \times N$ matrix equation

$$\mathcal{H}\psi = M\psi \ , \tag{A.3}$$

where $\mathcal{H} = \langle H \rangle_{ji}$ is the Hamiltonian matrix, and ψ is an N dimensional vector,

$$\psi = \begin{pmatrix} c_0 \\ c_1 \\ \vdots \\ c_{N-1} \end{pmatrix} \ . \tag{A.4}$$

The matrix $\mathcal{H}$ and its eigenvalues depend on the variational parameter β characterizing the basis functions. However, if the calculation is stable, dependence of the eigenvalues on β should reduce as N increases. This is manifested by the development of plateaus in β having the same eigenvalues. As an example, in Figure A.1 we show our SSEQ calculations for the three lowest S-wave D^{**} resonances, which used 5, 15 and 25 basis states.[2]

A basis set that was shown to be very successful in calculations of this sort is given by [145]

$$e_{iL}(\beta, r) = N_{iL} \beta^{\frac{3}{2}} (2\beta r)^L e^{-\beta r} L_i^{(2L+2)}(2\beta r) \ . \tag{A.5}$$

[2]In order to ensure the desired accuracy, all results quoted in this thesis are obtained using 50 basis states.

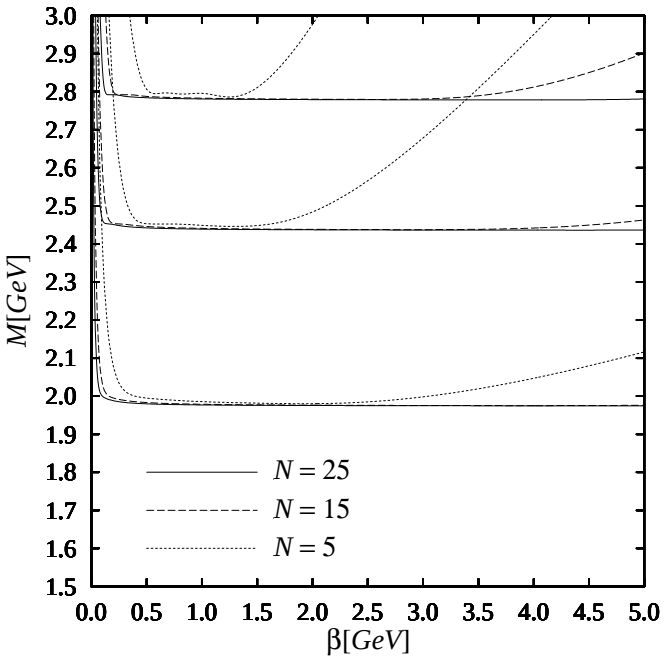

Figure A.1: Variational calculation for the three lowest S-wave D^{**} resonances. Results are obtained with SSEQ (constituent quark masses, $m_{u,d}$ and m_c, as well as the other parameters of the model, are given in (4.17)). We used $N = 5$ (dotted lines), 15 (dashed lines), and 25 (full lines) basis states.

Here, $L_i^{(a)}(x)$ are the generalized Laguerre polynomials, and

$$N_{iL} = \left[\frac{8(i!)}{(i+2L+2)!}\right]^{\frac{1}{2}} . \tag{A.6}$$

These basis states are normalized so that

$$\int_0^\infty r^2 dr e^*_{iL}(\beta, r) e_{jL}(\beta, r) = \delta_{i,j} . \tag{A.7}$$

The Fourier transform of (A.5) is known analytically,

$$e_{iL}(\beta, p) = (-i)^L \tilde{N}_{iL} \beta^{\frac{1}{2}} \left(\frac{\beta}{\beta^2+p^2}\right)^{L+2} p^L P_i^{(L+\frac{3}{2}, L+\frac{1}{2})}\left(\frac{p^2-\beta^2}{p^2+\beta^2}\right) , \tag{A.8}$$

where $P_i^{(a,b)}(x)$ are Jacobi polynomials, and

$$\tilde{N}_{iL} = \frac{2\Gamma(\frac{1}{2})}{\Gamma(i+L+\frac{3}{2})} \left[\frac{i!(i+2L+2)!}{\pi}\right]^{\frac{1}{2}} . \tag{A.9}$$

For computational precision and efficiency, whenever possible the matrix representation of operators has been calculated analytically. For $p_r^2 = -\frac{1}{r}\frac{\partial^2}{\partial r^2} r$ we have

$$\langle p_r^2 \rangle_{ij} = \beta^2 \left[-\delta_{i,j} + 2\frac{N_{jL}}{N_{iL}} \frac{(L+1)(2i+2L+3) - L(2L+3)(j-i)}{(2L+1)(2L+3)} \right] , \quad \text{(A.10)}$$

while the expression for $p^2 = p_r^2 + L(L+1)/r^2$ is

$$\langle p^2 \rangle_{ij} = \beta^2 \left[-\delta_{i,j} + 2\frac{N_{jL}}{N_{iL}} \frac{2i+2L+3}{2L+3} \right] . \quad \text{(A.11)}$$

Matrix element for r is given by

$$\begin{aligned} \langle r \rangle_{ij} &= \frac{1}{2\beta} \Big[(2i+2L+3)\delta_{i,j} - \sqrt{j(j+2L+2)}\,\delta_{i,j-1} \\ &- \sqrt{i(i+2L+2)}\,\delta_{i,j+1} \Big] , \end{aligned} \quad \text{(A.12)}$$

the one for $1/r$ is

$$\langle \frac{1}{r} \rangle_{ij} = \frac{\beta}{L+1} \frac{N_{jL}}{N_{iL}} , \quad \text{(A.13)}$$

while for $1/r^2$ we have

$$\langle \frac{1}{r^2} \rangle_{ij} = \frac{2\beta^2}{(L+1)(2L+1)(2L+3)} \frac{N_{jL}}{N_{iL}} \Big[(2L+1)(j-i) + 2j + 2L + 3 \Big] . \quad \text{(A.14)}$$

For the above expressions we assumed $i \leq j$. Results for $i > j$ can be obtained by simple reflection due to the symmetry of operators. Another useful matrix element is the one for $\frac{\partial}{\partial r}$,

$$\langle \frac{\partial}{\partial r} \rangle_{ij} = -\frac{\beta}{L+1} \times \begin{cases} (L+2)N_{jL}/N_{iL} & , \quad i < j \\ 1 & , \quad i = j \\ (-LN_{iL}/N_{jL}) & , \quad i > j \end{cases} . \quad \text{(A.15)}$$

This matrix element appears in models based on the Salpeter or Dirac equation.

In some models, such as SSEQ, for the constituent quark mass m the kinetic energy term of the $\mathcal{H}$ matrix has the form

$$\int_0^\infty p^2 dp e^*_{iL}(p)\sqrt{p^2+m^2}e_{jL}(p) \ , \tag{A.16}$$

where we dropped the dependence of the basis states on β. Matrix element such as this one can be very efficiently calculated using Gauss-Jacobi quadrature formula, after performing a change of integration variable from p to $x = (p^2 - \beta^2)/(p^2 + \beta^2)$.

For the flux tube models (RFTM and SFTM) the additional complication are the unknown matrix representations for the $v_\perp$ operators which appear in the Hamiltonian. These are obtained from the quantized orbital angular momentum equations such as (4.22). This involves solving non-linear transcendental matrix equation using the matrix iteration method developed in [78].

References

1. F. Gross, *Relativistic Quantum Mechanics and Field Theory*, John Wiley & Sons, New York, 1993.

2. J. Gasser and H. Leutwyler, Ann. Phys. **158**, 142 (1984).

3. N. Isgur and M. B. Wise, Phys. Lett. B **232**, 113 (1989); Phys. Lett. B **237**, 527 (1990).

4. A. De Rújula, H. Georgi, and S. L. Glashow, Phys. Rev. D **12**, 147 (1975).

5. E. V. Shuryak, Phys. Lett. B **93**, 134 (1980).

6. E. V. Shuryak, Nucl. Phys. B **198**, 83 (1982).

7. E. Eichten and F. L. Feinberg, Phys. Rev. Lett. **43**, 1205 (1979); Phys. Rev. D **23**, 2724 (1981).

8. E. Eichten, Nucl. Phys. B (Proc. Suppl.) **4**, 170 (1988).

9. G. Lepage and B. A. Thacker, Nucl. Phys. B (Proc. Suppl.) **4**, 190 (1988).

10. G. Altarelli, N. Cabibbo, G. Corbo, L. Maiani, and G. Martinelli, Nucl. Phys. B **208**, 365 (1982).

11. M. Suzuki, Nucl. Phys. B **258**, 533 (1985).

12. M. Bauer, B. Stech, and M. Wirbel, Z. Phys. C **29**, 637 (1985).

13. B. Grinstein, M. B. Wise, and N. Isgur, Phys. Rev. Lett. **56**, 298 (1986).

14. S. Nussinov and W. Wetzel, Phys. Rev. D **36**, 130 (1987).

15. T. Altomari and L. Wolfenstein, Phys. Rev. Lett. **58**, 1583 (1987).

16. J. G. Körner and G. A. Schuler, Z. Phys. C **38**, 511 (1988); erratum Z. Phys. C **41**, 690 (1989).

17. N. Isgur, D. Scora, B. Grinstein, and M. B. Wise, Phys. Rev. D **39**, 799 (1989).

18. M. B. Voloshin and M. A. Shifman, Sov. J. Nucl. Phys. **47**, 511 (1988).

19. M. B. Voloshin and M. A. Shifman, Sov. J. Nucl. Phys. **45**, 292 (1987).

20. H. D. Politzer and M. B. Wise, Phys. Lett. B **206**, 681 (1988).

21. H. D. Politzer and M. B. Wise, Phys. Lett. B **208**, 504 (1988).

22. J. D. Bjorken, *New Symmetries in Heavy Flavor Physics*, in *Results and Perspectives in Particle Physics*, Proceedings of the 4^{th} Recontres de Physique de la Vallée D'Aoste, La Thuile, Italy, 1990, edited by A. Greco, Editions Frontières, Gif-sur-Yvette, France, 1990.

23. N. Isgur and M. B. Wise, Phys. Rev. D **43**, 819 (1991).

24. M. B. Voloshin, Phys. Rev. D **46**, 3062 (1992).

25. H. Georgi, *Heavy Quark Effective Field Theory*, in *Perspectives in the Standard Model*, Proceedings of the Theoretical Advanced Study Institute, Boulder, Colorado, 1991, edited by R. K. Ellis et al., World

Scientific, Singapore, 1991.

26. N. Isgur and M. B. Wise, *Heavy Quark Symmetry*, in *Heavy Flavors*, edited by A. J. Buras and M. Lindner, World Scientific, Singapore, 1992.

27. B. Grinstein, Annu. Rev. Nucl. Part. Sci. **42**, 101 (1992).

28. M. Neubert, Phys. Rept. **245**, 259 (1994).

29. H. Georgi, Phys. Lett. B **240**, 447 (1990).

30. N. Isgur and M. B. Wise, Phys. Rev. Lett. **66**, 1130 (1991).

31. L. Montanet et al., Particle Data Group, Phys. Rev. D **50**, 1173 (1994).

32. A. F. Falk, H. Georgi, B. Grinstein, and M. B. Wise, Nucl. Phys. B **343**, 1 (1990).

33. H. Georgi, Nucl. Phys. B **348**, 293 (1991).

34. A. F. Falk, Nucl. Phys. B **378**, 79 (1992).

35. H. Umezawa, *Quantum Field Theory*, North-Holland, Amsterdam, 1956.

36. M. Neubert, Phys. Lett. B **264**, 455 (1991); Phys. Lett. B **338**, 84 (1994).

37. G. Preparata and W. I. Weisberger, Phys. Rev. **175**, 1965 (1968).

38. G. P. Koochemsky and A. V. Radyushkin, Nucl. Phys. B **283**, 342 (1987).

39. E. Eichten and B. Hill, Phys. Lett. B **243**, 427 (1990).

40. A. F. Falk, B. Grinstein, and M. E. Luke, Nucl. Phys. B **357**, 185 (1991).

41. K. Zalewski, Phys. Lett. B **264**, 432 (1991).

42. S. Veseli and M. G. Olsson, Phys. Lett. B **367**, 302 (1996).

43. H. D. Politzer, Phys. Lett. B **250**, 128 (1990).

44. M. Neubert and V. Rickert, Nucl. Phys. B **382**, 97 (1992).

45. M. Sadzikowski and K. Zalewski, Z. Phys. C **59**, 677 (1993).

46. H. H$\not{\text{o}}$gaasen and M. Sadzikowski, Z. Phys. C **64**, 427 (1994).

47. A. Ali, T. Ohl, and T. Mannel, Phys. Lett. B **298**, 195 (1993).

48. M. R. Ahmady, D. Liu, and Z. Tao, *Long Distance Contributions to B Decays into Higher K Resonances*, hep-ph/9302209.

49. M. R. Ahmady and D. Liu, Phys. Lett. B **324**, 231 (1994).

50. T. B. Suzuki, T. Ito, S. Sawada, and M. Matsuda, Prog. Theor. Phys. **91**, 757 (1994).

51. M. R. Ahmady, D. Liu, and A. H. Fariborz, *Estimates of B Decays into K Resonances and Dileptons*, hep-ph/9506235.

52. B. Barish et al., CLEO Collaboration, Phys. Rev. D **51**, 1014 (1995).

53. M. G. Olsson, S. Veseli, and K. Williams, Phys. Rev. D **51**, 5079 (1995).

54. M. G. Olsson, S. Veseli, and K. Williams, Phys. Rev. D **53**, 4006 (1996).

55. M. G. Olsson and S. Veseli, Phys. Rev. D **51**, 2224 (1995).

56. M. G. Olsson and S. Veseli, Phys. Lett. B **353**, 96 (1995).

57. A. Duncan, E. Eichten, and H. Thacker, Phys. Lett. B **303**, 109 (1993).

58. S. Veseli and M. G. Olsson, Phys. Lett. B **367**, 309 (1996).

59. J. S. Kang and H. Schnitzer, Phys. Rev. D **12**, 841 (1975).

60. J. Dias de Deus and J. Pulido, Z. Phys. C **28**, 413 (1985).

61. P. Cea, P. Colangelo, G. Nardulli, G. Paiano, and G. Preparata, Phys. Rev. D **26**, 1157 (1982).

62. P. Cea, G. Nardulli, and G. Paiano, Phys. Rev. D **28**, 2291 (1983).

63. A. Martin, Z. Phys. C **32**, 359 (1986).

64. C. Goebel, D. LaCourse, and M. G. Olsson, Phys. Rev. D **41**, 2917 (1990).

65. B. Durand and L. Durand, Phys. Rev. D **25**, 2312 (1982).

66. D. B. Lichtenberg, W. Namgung, E. Predazzi, and J. G. Wills, Phys. Rev. Lett. **48**, 1653 (1982).

67. B. Durand and L. Durand, Phys. Rev. D **30**, 1904 (1984).

68. S. Godfrey and N. Isgur, Phys. Rev. D **32**, 189 (1985).

69. S. Jacobs, M. G. Olsson, and C. J. Suchyta III, Phys. Rev. D **33**, 3338 (1986).

70. D. Gromes, Z. Phys. C **11**, 147 (1981).

71. W. Lucha, H. Rupprecht, and F. Schöberl, Phys. Rev. D **46**, 1088 (1992).

72. L. P. Fulcher, Z. Chen, and K. C. Yeong, Phys. Rev. D **47**, 4122 (1993).

73. L. P. Fulcher, *Matrix Approach to Solution of the Spinless Salpeter Equation*, in Proceedings of the International Conference on Quark Confinement and the Hadron Spectrum, Como, Italy, 1994, edited by N. Brambilla and G. M. Prosperi, World Scientific, Singapore, 1994.

74. D. S. Hwang and G.-H. Kim, Phys. Rev. D **53**, 3659 (1996).

75. V. D. Barger and D. B. Cline, *Phenomenological Theories of High Energy Scattering*, W. A. Benjamin Inc., New York, 1969.

76. M. Ida, Prog. Theor. Phys. **59**, 1661 (1978).

77. D. LaCourse and M. G. Olsson, Phys. Rev. D **39**, 2751 (1989).

78. M. G. Olsson and S. Veseli, Phys. Rev. D **51**, 3578 (1995).

79. A. Yu. Dubin, A. B. Kaidalov, and Yu. A. Simonov, Phys. Lett. B **323**, 41 (1994).

80. E. L. Gubankova and A. Yu. Dubin, Phys. Lett. B **334**, 180 (1994).

81. E. E. Salpeter and H. A. Bethe, Phys. Rev. **76**, 1232 (1949).

82. M. Gell-Mann and F. Low, Phys. Rev. **84**, 350 (1951).

83. E. E. Salpeter, Phys. Rev. **87**, 328 (1952).

84. C. Long and D. Robson, Phys. Rev. D **27**, 644 (1983).

85. G. Hardekopf and J. Sucher, Phys. Rev. A **30**, 703 (1984); Phys. Rev. A **31**, 2020 (1985).

86. M. S. Plesset, Phys. Rev. **41**, 278 (1932).

87. J.-F. Lagaë, Phys. Rev. D **45**, 317 (1992).

88. M. G. Olsson, S. Veseli, and K. Williams, Phys. Rev. D **52**, 5141 (1995).

89. M. G. Olsson and K. Williams, Phys. Rev. D **48**, 417 (1993).

90. G. Zöller, S. Hainzl, C. R. Münz, and M. Beyer, Z. Phys. C **68**, 103 (1995).

91. E. Klempt, B. C. Metsch, C. R. Münz, and H. R. Petry, Phys. Lett. B **361**, 160 (1995).

92. J. Parramore, H.-C. Jean, and J. Piekarewicz, *Stability Analysis of the Instantaneous Bethe-Salpeter Equation and the Consequences for Meson Spectroscopy*, report FSU-SCRI-95-105, nucl-th/9510024.

93. C. R. Münz, *Two Photon Decays of Mesons in a Relativistic Quark Model*, report BONN-TK-96-01, hep-ph/9601206.

94. J. Gronberg et al., CLEO Collaboration, *Measurement of the Branching Ratio $B \to Xe\bar{\nu}_e$ with Lepton Tags*, report CLEO-CONF-94-6.

95. Y. Kubota et al., CLEO Collaboration, *Measurement of the* $\mathcal{B}(B^- \to D^0 e^- \bar{\nu}_e)$ *Using Neutrino Reconstruction Techniques*, report CLEO-CONF-95-10.

96. J. P. Alexander et al., CLEO Collaboration, *Semileptonic B Meson Decay to P-Wave Charm Mesons*, report CLEO-CONF-95-30.

97. D. Buskulic et al., ALEPH Collaboration, Phys. Lett. B **345**, 103 (1995).

98. R. Akers et al., OPAL Collaboration, Z. Phys. C **67**, 57 (1995).

99. S. Veseli and M. G. Olsson, *S to P-Wave From Factors in Semileptonic B Decays*, report MADPH-95-907, hep-ph/9509230, to appear in Z. Phys. C.

100. S. Veseli and M. G. Olsson, Phys. Rev. D **54**, 886 (1996).

101. D. Scora and N. Isgur, Phys. Rev. D **52**, 2783 (1995).

102. P. Colangelo, G. Nardulli, and N. Paver, Phys. Lett. B **293**, 207 (1992); report BARI TH/93-132, UTS-UFT-93-3, hep-ph/9303220.

103. M. Sutherland, B. Holdom, S. Jaimungal, and R. Lewis, Phys. Rev. D **51**, 5053 (1995).

104. N. Isgur, private communication.

105. P. Abreu et al., DELPHI Collaboration, *Determination of* $|V_{cb}|$ *from the Semileptonic Decay* $B^0 \to \bar{D}^{*-} l^+ \nu$, report CERN-PPE-96-011.

106. G. Altarelli and S. Petrarca, Phys. Lett. B **261**, 303 (1991).

107. I. Bigi, R. Blok, M. Shifman, and A. Vainshtein, Phys. Lett. B **323**, 408 (1994).

108. J. L. Cortes, X. Y. Pham, and A. Tounsi, Phys. Rev. D **25**, 188 (1982).

109. P. Bialas, J. G. Körner, and K. Zalewski, Z. Phys. C **59**, 117 (1993).

110. S. Balk, J. G. Körner, G. Thompson, and F. Hussain, Z. Phys. C **59**, 283 (1993).

111. A. I. Vainshtein, V. I. Zakharov, and M. A. Shifman, JETP Lett. **22**, 55 (1975).

112. J. Ellis, M. K. Gaillard, and D. V. Nanopoulos, Nucl. Phys. B **100**, 313 (1975).

113. M. Bander, D. Silverman, and A. Soni, Phys. Rev. Lett. **43**, 242 (1979).

114. J. L. Hewett, *Top Ten Models Constrained by* $b \to s\gamma$, report SLAC-PUB-6521, hep-ph/9406302.

115. R. Ammar et al., CLEO Collaboration, Phys. Rev. Lett. **71**, 674 (1993).

116. K. W. Edwards et. al., CLEO Colaboration, *Update on Exclusive* $B^0 \to K^{*0}(892)\gamma$ *Measurement at CLEO*, report CLEO-CONF-95-6.

117. M. S. Alam et al., CLEO Collaboration, Phys. Rev. Lett. **74**, 2885 (1995).

118. A. Ali and T. Mannel, Phys. Lett. B **264**, 447 (1991); erratum Phys. Lett. B **274**, 526 (1992).

119. C. A. Dominguez, N. Paver, and Riazuddin, Phys. Lett. B **214**, 459 (1988).

120. T. M. Aliev, A. A. Ovchinnikov, and V. A. Slobodenyuk, Phys. Lett. B **237**, 569 (1990).

121. P. Colangelo, C. A. Dominguez, G. Nardulli, and N. Paver, Phys. Lett. B **317**, (1993).

122. P. Ball, *The Decay $B \to K^*\gamma$ from QCD Sum Rules*, report TUM-T31-43/93, hep-ph/9308244.

123. A. Ali, V. M. Braun, and H. Simma, Z. Phys. C **63**, 437 (1994).

124. S. Narison, Phys. Lett. B **327**, 354 (1994).

125. P. J. O'Donnell, Phys. Lett. B **175**, 369 (1986).

126. N. G. Deshpande, P. Lo, J. Trampetić, G. Eilam, and P. Singer, Phys. Rev. Lett. **59**, 183 (1987).

127. T. Altomari, Phys. Rev. D **37**, 677 (1988).

128. P. J. O'Donnell and H. K. Tung, Phys. Rev. D **48**, 2145 (1993).

129. A. Ali and C. Greub, Z. Phys. C **60**, 433 (1993).

130. N. G. Deshpande and J. Trampetić, Mod. Phys. Lett. A **4**, 2095 (1989).

131. D. Du and C. Liu, *The $1/m_s$ Corrections to the Exclusive Rare B Meson Decays*, report BIHEP-TH-92-41.

132. R. N. Faustov and V. O. Galkin, Mod. Phys. Lett. A **7**, 2111 (1992).

133. E. El-Hassan and Riazuddin, Phys. Rev. D **47**, 1026 (1993).

134. B. Holdom and M. Sutherland, Phys. Rev. D **49**, 2356 (1994).

135. J. Tang, J. Liu, and K. Chao, Phys. Rev. D **51**, 3501 (1995).

136. D. Atwood and A. Soni, Z. Phys. C **64**, 241 (1994).

137. C. Bernard, P. Hsieh, and A. Soni, Phys. Rev. Lett. **72**, 1402 (1994).

138. M. Ciuchini, E. Franco, G. Martinelli, L. Reina, and L. Silvestrini, Phys. Lett. B **334**, 137 (1994).

139. K. C. Bowler et al., *A Lattice Calculation of the Branching Ratio for Some of the Exclusive Modes of $b \to s\gamma$*, report EDINBURGH-94-544, hep-lat/9407013.

140. D. R. Burford et al., *Form Factors for $B \to \pi l \bar{\nu}_l$ and $B \to K^* \gamma$ Decays on the Lattice*, report FERMILAB-PUB-95/023-T, hep-lat/9503002.

141. B. Grinstein, R. Springer, and M. B. Wise, Nucl. Phys. B **339**, 269 (1990).

142. A. Ali and C. Greub, Z. Phys. C **49**, 431 (1991).

143. A. J. Buras, M. Misiak, M. Münz, and S. Pokorski, Nucl. Phys. B **424**, 374 (1994).

144. N. G. Deshpande, *Theory of Penguins in B Decay*, in *B Decays*, 2nd edition, edited by S. Stone, World Scientific, Singapore, 1994.

145. E. J. Weniger, J. Math. Phys. **26**, 276 (1985).

146. M. G. Olsson, S. Veseli, and K. Williams, Phys. Rev. D **53**, 504 (1996).